

## INFORMATION TO USERS

This reproduction was made from a copy of a document sent to us for microfilming. While the most advanced technology has been used to photograph and reproduce this document, the quality of the reproduction is heavily dependent upon the quality of the material submitted.

The following explanation of techniques is provided to help clarify markings or notations which may appear on this reproduction.

1. The sign or "target" for pages apparently lacking from the document photographed is "Missing Page(s)". If it was possible to obtain the missing page(s) or section, they are spliced into the film along with adjacent pages. This may have necessitated cutting through an image and duplicating adjacent pages to assure complete continuity.
2. When an image on the film is obliterated with a round black mark, it is an indication of either blurred copy because of movement during exposure, duplicate copy, or copyrighted materials that should not have been filmed. For blurred pages, a good image of the page can be found in the adjacent frame. If copyrighted materials were deleted, a target note will appear listing the pages in the adjacent frame.
3. When a map, drawing or chart, etc., is part of the material being photographed, a definite method of "sectioning" the material has been followed. It is customary to begin filming at the upper left hand corner of a large sheet and to continue from left to right in equal sections with small overlaps. If necessary, sectioning is continued again—beginning below the first row and continuing on until complete.
4. For illustrations that cannot be satisfactorily reproduced by xerographic means, photographic prints can be purchased at additional cost and inserted into your xerographic copy. These prints are available upon request from the Dissertations Customer Services Department.
5. Some pages in any document may have indistinct print. In all cases the best available copy has been filmed.

University  
Microfilms  
International

300 N. Zeeb Road  
Ann Arbor, MI 48106



8416225

**Raatz, Wolfgang Eduard**

ARCTIC HAZE: METEOROLOGICAL ASPECTS OF LONG-RANGE  
TRANSPORT

*University of Alaska*

Ph.D. 1983

University  
Microfilms  
International 300 N. Zeeb Road, Ann Arbor, MI 48106



PLEASE NOTE:

In all cases this material has been filmed in the best possible way from the available copy. Problems encountered with this document have been identified here with a check mark .

1. Glossy photographs or pages \_\_\_\_\_
2. Colored illustrations, paper or print \_\_\_\_\_
3. Photographs with dark background \_\_\_\_\_
4. Illustrations are poor copy \_\_\_\_\_
5. Pages with black marks, not original copy \_\_\_\_\_
6. Print shows through as there is text on both sides of page \_\_\_\_\_
7. Indistinct, broken or small print on several pages
8. Print exceeds margin requirements \_\_\_\_\_
9. Tightly bound copy with print lost in spine \_\_\_\_\_
10. Computer printout pages with indistinct print \_\_\_\_\_
11. Page(s) \_\_\_\_\_ lacking when material received, and not available from school or author.
12. Page(s) \_\_\_\_\_ seem to be missing in numbering only as text follows.
13. Two pages numbered \_\_\_\_\_. Text follows.
14. Curling and wrinkled pages \_\_\_\_\_
15. Other \_\_\_\_\_

University  
Microfilms  
International



ARCTIC HAZE: METEOROLOGICAL ASPECTS OF  
LONG-RANGE TRANSPORT

A  
THESIS

Presented to the Faculty of the University of Alaska  
in Partial Fulfillment of the Requirements  
for the Degree of

DOCTOR OF PHILOSOPHY

By  
Wolfgang E. Raatz, Dipl. Met.

Fairbanks, Alaska

MAY 1983

ARCTIC HAZE: METEOROLOGICAL ASPECTS  
OF LONG-RANGE TRANSPORT

RECOMMENDED:

W. D. Harrison

J. Keith Chilton

Sue Ann Brown

G. Wong

Glen E. Shaw  
Chairman, Advisory Committee

John V. Allen  
Head, Space Physics and  
Atmospheric Sciences Program

APPROVED:

William D. Beer  
for Vice Chancellor for Research and Advanced Study

6 May 1983  
Date

## ABSTRACT

A time series of concentrations of pollution aerosols collected over a period of four years in the near-surface air at Barrow, Alaska, was used to investigate tropospheric long-range transport of anthropogenic pollution from mid-latitudes into the Arctic. This transport takes place when the mid-latitudinal and arctic atmospheric circulations remain in a quasi-persistent mode. Sudden changes in the circulation pattern explain the episodic character of the arctic pollution aerosol. Transport of aerosols is accomplished by quasi-stationary anticyclones and takes place along their peripheries where pressure gradients are relatively strong. The seasonal variation in concentration of the arctic pollution aerosol is explained by the seasonal variation in the occurrence and position of mid-latitude blocking anticyclones, of the arctic anticyclone, and of the Asiatic anticyclone. The positions of the major anticyclonic centers are responsible for the fact that Soviet industrial sources contribute to the arctic pollution aerosol predominantly during winter, European sources during spring, and that North American and Far Eastern industrial sources contribute little to the arctic pollution aerosols.

Air masses carrying pollutants can be traced by their chemical characteristics obtained over the source regions, however, the original meteorological characteristics are lost during the transport which lasts for about 8-9 days.

A second data set, collected during the "Ptarmigan" weather reconnaissance flights, was investigated for observations of Arctic Haze over the Alaskan Arctic. A connection between Arctic Haze and the arctic pollution aerosols is suggested, for the occurrence of Arctic Haze undergoes a similar seasonal variation as that of the pollution aerosols, and similar circulation modes leading to the Soviet Union and Europe can be found during the presence of Arctic Haze. In addition, the data seem to suggest that besides a probable pollution-derived component during winter/spring Arctic Haze might be desert dust-derived during summer.

Dedicated to my friends in Alaska

TABLE OF CONTENTS

	page
LIST OF FIGURES.....	ix
LIST OF TABLES.....	xii
ACKNOWLEDGEMENTS.....	xiv
I INTRODUCTION.....	1
1.1 Introduction.....	1
1.2 Objective of Dissertation.....	4
1.3 Relevance of Dissertation.....	5
1.4 Limitations of Dissertation.....	7
1.5 Outline And Summary of Major Results.....	7
II SOME CHARACTERISTICS OF THE POLLUTION AEROSOL AT BARROW, ALASKA.....	11
2.1 The Chemical Data Bank.....	11
2.2 Sampling Method And Analysis.....	13
2.3 Definition of Excess Vanadium and Excess Manganese.....	15
2.4 The XMn/XV Ratio As a Tracer.....	24
2.5 Seasonal And Episodic Variations of XV and XMn.....	25
2.6 Seasonal Variation of the XMn/XV Ratio.....	31
III METEOROLOGICAL CHARACTERISTICS OF POLLUTED AIR MASSES AT BARROW, ALASKA.....	36
3.1 The Climate of Barrow.....	36
3.1.1 Introduction.....	36
3.1.2 Winter Circulation Patterns.....	37

3.1.3	Seasonal Variation of Monthly Mean Meteorological Elements.....	41
3.2	Occurrence and Characteristics of Polluted Air Masses.....	56
3.2.1	On the Origin of the Polluted Air Masses.....	56
3.2.2	Meteorological Characteristics of the Polluted Air Masses.....	63
3.2.3	Spectrum and Cross Spectrum Analysis.....	79
IV	TRANSPORT PATHWAYS OF MID-LATITUDE AEROSOLS.....	88
4.1	Industrial Mid-Latitude Source Areas of Pollutants.....	88
4.2	Method for Identifying Transport Pathways of Pollutants.....	91
4.3	Transport Pathway Types of Pollution Aerosol.....	94
4.3.1	Introduction.....	94
4.3.2	Transport Pathway Types From North American Source Regions.....	96
4.3.3	Transport Pathway Types From European Source Regions.....	101
4.3.4	Transport Pathway Types From Soviet Source Regions.....	108
4.3.5	Quasi-Persistent Modes of the Atmospheric Circulation in the Arctic and Mid-Latitudes.....	114
4.4	Characteristics of Transport Pathway Types.....	121
4.4.1	Synoptic Conditions over The Mid-Latitude Source Areas.....	121
4.4.2	Synoptic Conditions Along the Transport Pathway and Associated Travel Times.....	131
4.4.3	Meteorological Characteristics of Transport Pathway Types Reaching Barrow.....	135
4.4.4	On the Seasonal Variation of Transport Pathway Types.....	138

V	OBSERVATIONS OF "ARCTIC HAZE" DURING THE "PTARMIGAN" WEATHER RECONNAISSANCE FLIGHTS, 1948-1961.....	146
5.1	Introduction.....	146
5.2	The "Ptarmigan" Data Set.....	147
5.3	On the Occurrence of Arctic Haze.....	150
5.4	Synoptic Conditions During Observations of Arctic Haze.....	160
5.5	On the Possible Origin of Arctic Haze.....	166
VI	DISCUSSION AND CONCLUSION.....	171
	REFERENCES.....	189
	APPENDIX.....	201

LIST OF FIGURES

	page
Fig. 1: Monthly mean total and crustal components of a) vanadium, b) manganese.....	20
Fig. 2: Mean monthly concentration of excess vanadium and excess manganese (1976-1980).....	26
Fig. 3: Monthly mean concentration of a) excess vanadium b) excess manganese.....	28
Fig. 4: Time series of concentrations of excess vanadium for the four winter seasons.....	29
Fig. 5: Time series of concentrations of excess manganese for the four winter seasons.....	30
Fig. 6: Frequency distribution of XMn/XV ratios: a) October-April b) October-January, c) February-April.....	32
Fig. 7: Excess (noncrustal) manganese, excess (noncrustal) vanadium and the XMn/XV ratio in daily samples during winter 1979/80 (after N. Lewis, personal communication)....	34
Fig. 8: Characteristic winter circulation patterns (after Moritz, 1979).....	38
Fig. 9: Seasonal variation of frequency of occurrence of winter circulation patterns (after Moritz, 1979).....	40
Fig. 10: Seasonal variation of monthly mean surface air temperature.....	43
Fig. 11: Seasonal variation of monthly mean height of surface temperature inversion.....	44
Fig. 12: Seasonal variation of monthly mean intensity of surface temperature inversion.....	46
Fig. 13: Seasonal variation of monthly mean surface pressure.....	47
Fig. 14: Monthly wind roses for the winter seasons 1976/77, 1977/78, 1978/79 (after Harris et al., 1980).....	48
Fig. 15: Seasonal variation of monthly mean total cloud amount.....	52
Fig. 16: Seasonal variation of monthly mean precipitation amount.....	54

Fig. 17: Frequency distribution of wind directions for different XV and XMn concentrations.....	61
Fig. 18: Height/time cross section of potential temperature.....	65
Fig. 19: Height/time cross section of mixing ratio.....	67
Fig. 20: Height/time cross section of wind direction and speed.....	69
Fig. 21: Frequency of deviations from the monthly mean value (surface data), a) temperature, b) pressure.....	73
Fig. 22: Frequency of deviations from the monthly mean value (surface data), a) wind speed, b) cloud cover.....	74
Fig. 23: Seasonal variation of frequency of positive and negative deviations, a) temperature, b) pressure, c) sky cover....	76
Fig. 24: Frequency of deviations from the monthly mean value (850 mb), a) temperature, b) wind speed.....	77
Fig. 25: Frequency of surface temperature inversions.....	78
Fig. 26: Power spectrum for a) excess vanadium, b) excess manganese...	82
Fig. 27: Power spectrum for a) temperature, b) pressure.....	84
Fig. 28: Transport pathway type Ia.....	99
Fig. 29: Transport pathway type Ib.....	100
Fig. 30: Transport pathway type IIa.....	103
Fig. 31: Transport pathway type IIb.....	105
Fig. 32: Transport pathway type IIc.....	107
Fig. 33: Transport pathway type IIIa.....	109
Fig. 34: Transport pathway type IIIb.....	111
Fig. 35: Transport pathway type IIIc.....	113
Fig. 36: Transport pathway type IIId.....	115
Fig. 37: Synoptic conditions over Europe during a surge.....	123
Fig. 38: Mean monthly intensity of the arctic anticyclone when located over the Pacific Arctic.....	144

Fig. 39: Number of days with yellow sand over Nagasaki, Japan (after Arao et al., 1979).....	154
Fig. 40: Spatial frequency distribution of Arctic Haze reports.....	157
Fig. 41: Frequency distribution of altitude of occurrence of Arctic Haze.....	159
Fig. 42: Frequency of weather conditions during haze reports a) November-April, b) May-October.....	161
Fig. 43: Frequency of wind direction during haze reports a) November-April, b) May-October.....	163
Fig. 44: Singularities over central Europe a) frequency of anticyclonic Grosswetterlagen, b) mean surface pressure (after Schulz, 1963).....	186

## LIST OF TABLES

	page
Table 1: Frequency distribution of samples and sampling periods.....	12
Table 2: Occurrence of extreme values of concentration of pollution aerosol and other meteorological parameters.....	55
Table 3: Daily meteorological surface data at Barrow, December 28, 1976 - January 6, 1977.....	58
Table 4: Characteristics of samples with homogeneous meteorological conditions.....	59
Table 5: Frequency distribution of wind directions for the ten highest and smallest XV and XMn concentrations.....	62
Table 6: Correlation coefficients between daily chemical and meteorological data.....	83
Table 7: Samples with XMn/XV ratio less than 0.7.....	97
Table 8: Mean XMn/XV ratio for each transport pathway type.....	125
Table 9: Mean travel times for different transport pathway types...	134
Table 10: Mean values of meteorological parameters for different transport pathway types.....	137
Table 11: Seasonal variation of frequency of occurrence of transport pathway types.....	139
Table 12: Seasonal variation of mean XMn/XV ratios for each transport pathway type.....	140
Table 13: Monthly frequency of "Ptarmigan" weather reconnaissance flights.....	148
Table 14: Monthly frequency of "Ptarmigan" weather reconnaissance flights with haze reports.....	151
Table 15: Monthly frequency distribution of frequency of haze observations during one flight.....	155
Table 16: Frequency of visibility range during haze reports and different weather conditions.....	164

Table 17:	Monthly frequency of occurrence of transport pathways leading to different source regions.....	168
Table 18:	Monthly frequency of occurrence of transport pathway types IIb and IIIb.....	180
Table 19:	Possible correlation between the occurrence of pressure singularities over central Europe and the occurrence of high concentration of pollution aerosol at Barrow, Alaska.....	187

## ACKNOWLEDGEMENTS

I would like to thank my advisor, Professor Glenn E. Shaw, for his constant encouragement and support in my research efforts. His enthusiasm in my work always inspired me to thoughts and to new beginnings whenever I found myself lost in the maze of questions to be answered.

Similar thanks has to be expressed to Professor Kenneth A. Rahn, University of Rhode Island, who shared his chemical data set with me and who provided plenty of helpful comments during my two visits at his laboratory.

I appreciate the help of all persons who collected the chemical and meteorological data out in the field and analyzed them in their laboratories. Special thanks to Thomas Conway and Doug Lowenthal.

John Miller kindly provided the ARL-GMCC back-trajectories and Gary Herbert the new GMCC back-trajectory set.

Special thanks to Angelika Ambs who typed several versions of the manuscript. Without her help I would have never been able to complete it.

This research has been done under sponsorship of the Office of Naval Research (ONR: N-00014-C-0435) and the National Science Foundation (Grant DPP79-19816).

## I INTRODUCTION

### 1.1 Introduction

The term "Arctic Haze" was introduced by Mitchell (1956) to describe the haze found over the Arctic during the "Ptarmigan" weather reconnaissance flights. In subsequent years the phenomenon of Arctic Haze was forgotten, because ground observers in the Arctic can rarely detect the haze.

In 1972, it was observed that measurements of atmospheric turbidity were higher during the spring than during the summer (Shaw and Wendler, 1972) leading to the rediscovery of Arctic Haze. Flights in the vicinity of Barrow during March 1974 led to the detection of haze bands showing colors similar to polluted air over industrial areas (Holmgren et al., 1974). These observations caused interest in determining the chemical composition of the haze. Research flights were made again during April and May of 1976 and particles collected on filters were analyzed. It was found that haze bands consisted of crustal particles indicating a desert dust origin (Rahn et al., 1977; Rahn et al., 1981). Thus, it was initially assumed that Arctic Haze was a natural phenomenon.

Surface air aerosols have been collected at Barrow since September 1976. The aerosol has both coarse-particle ( $r > 1\mu\text{m}$ ) and fine-particle ( $r < 1\mu\text{m}$ ) components (Rahn, 1980; Bigg, 1980; Shaw, 1982a). The coarse

particles consist mainly of natural materials such as sea salt and soil dust, which tend to be locally derived, and are of little interest to this study. The fine particles, on the other hand, have a much more complex chemistry in their composition, and show evidence of a distant origin. In addition, they account for 75-80% of the mass of the near-surface arctic aerosol, and produce more than 90% of the optical effects (Rahn, 1980). The absolute concentration of the submicron arctic aerosol is about  $4 \mu\text{g m}^{-3}$  for the dry fraction, and probably another 25-50% of associated water (Rahn, 1980). The major constituents of the dry aerosol are sulfate ( $\sim 2 \mu\text{g m}^{-3}$ ) (Rahn and McCaffrey, 1980), organic matter ( $\sim 1 \mu\text{g m}^{-3}$ ) (Daisey et al., 1981; Weschler, 1981), black carbon ( $\sim 0.3-0.5 \mu\text{g m}^{-3}$ ) (Rosen et al., 1981) and probably nitrate. In addition, there is a great variety of minor constituents, including compounds containing the elements V, Mn, Pb, Cd, Fe, As, Sb, Se, and others.

The submicron aerosol is to a large extent secondary, that is, a large fraction of its material has been added to it from the gas phase during transport. In other words, the aerosol has spent several days in the atmosphere and, therefore, is highly aged (Rahn and McCaffrey, 1980; Shaw, 1982). The chemical composition of the aerosol shows evidence that this aerosol is largely pollution-derived as indicated by high aerosol-crust enrichment factors for pollution elements such as V, Mn etc.. Also, concentrations of sulfate are too high to have come from natural sources (Rahn, 1978), and silicones are present (Weschler, 1981). Sources of the pollution aerosols are suspected to be mid-

latitude industrial areas (Rahn and McCaffrey, 1980).

It has been observed that during times of high pollution concentrations at the ground, haze bands aloft were also present (Shaw, 1982b). For this reason episodes of high pollution concentrations were also referred to as Arctic Haze episodes. Rahn et al. (1981) define Arctic Haze as an anomalously abundant tropospheric aerosol found north of 70°N during many otherwise clear periods of the year. It should be noted, however, that since May 1976 no measurements of chemical composition have been made to confirm that the haze bands aloft also carry pollution aerosols. To avoid confusion we will use the term "Arctic Haze" only when referring to the "Ptarmigan" data or to observed haze bands, and we will use the term "pollution aerosol" when referring to the submicron pollution-derived aerosol sampled at the surface.

It is a characteristic feature of the pollution aerosol that it undergoes a pronounced seasonal variation: from a minimum in summer concentrations it rises gradually during fall and winter before reaching a maximum in spring. After March there is usually a dramatic drop in concentrations (Rahn and McCaffrey, 1980). Similar results have been reported from other arctic sites (Barrie et al., 1981; Larssen and Hanssen, 1979; Heidam, 1981; Heintzenberg, 1980; 1981). Thus, it appears that the arctic region as a whole contains significant amounts of pollution aerosols, at least during the winter and spring. A similar phenomenon has not yet been reported from Antarctica.

In the Arctic, energy transformations are very susceptible to changes of the radiation budget and Shaw and Stamnes (1978) estimated

that the pollution aerosol may cause a heating of the earth-atmosphere system. In the Arctic this heating is comparable to the heating caused by all atmospheric trace gases combined (Eiden, 1979). Rey et al. (1983) cautioned that the sensitive arctic ecosystems can easily be damaged by further industrial development of the North.

It is therefore of importance to identify the source regions of Arctic Haze and the pollution aerosol, to find the transport mechanisms which allow long-range transport and to explain the seasonal variation of Arctic Haze and the pollution aerosols.

## 1.2 Objective of Dissertation

Substantial amounts of information on the chemical, physical and optical properties of the arctic pollution aerosol have been collected. It has been recognized that the meteorological aspects are of extreme importance, and attempts have been made to explain the seasonal variation of the pollution aerosols and the formation of possible transport pathways created by the synoptic conditions in the Arctic (e.g. Rahn, 1981a; Reiter, 1981; Carlson, 1981; Shaw, 1981). However, these attempts have been of a sporadic nature, including scattered case studies or climatological arguments. It is the objective of this dissertation to investigate the meteorological conditions in a more systematic manner. In particular, we will determine the meteorological characteristics of polluted air masses at Barrow; we will

attempt to identify transport pathways from possible source areas to Barrow and describe the meteorological conditions along such a path; and we will investigate if the seasonal variations of the concentration of the pollution aerosol are caused by seasonal variations of the atmospheric circulations in mid-latitudes and the Arctic which create the transport pathways.

### 1.3 Relevance of Dissertation

We are describing tropospheric long-range transport of aerosols on a scale up to 10,000 km and associated travel times of possibly 4-20 days, neither of which has been adequately documented in the past. The largest known transport distances, on the order of hemispheric scales, have been found in the stratosphere with residence times of one year and more (e.g. Reiter, 1971). Long-range transport of desert soils has been reported for several desert areas of the world (e.g. Schuetz, 1980). For example, Carlson and Prospero (1972) documented Saharan dust reaching Barbados over a distance of 6,000 km and after a travel time of 5-6 days. Rahn et al. (1981) showed that aerosols from Asian deserts travelled a distance of 12,000-15,000 km to Barrow, Alaska, within 4-8 days. Transport of anthropogenic pollution by cyclones is well known in that it produces acid rain (Likens et al., 1979; Pearce, 1982; Wolff, 1980). Due to the precipitation within the cyclonic system, transport distances of pollutants are of the order of 500-1,000 km before they are

rained out. Transport of anthropogenic pollutants, especially ozone, by anticyclones has been documented as well (Hall et al., 1973; Samson and Ragland, 1977; Lyons et al., 1978; Wolff et al., 1981; Guicherit and van Dop, 1977). Interestingly, all these cases of transport by anticyclones have been documented for the summer and Rahn (1981b) questioned whether a haze blob, defined as an area of decreased visibility due to the presence of elevated sulfate and ozone levels (Lyons and Husar, 1976), can be used as a tracer. The summer atmospheric circulation in general is weak, especially during stagnant anticyclonic influence, and it is possible that the haze blob has renewed itself during transport by picking up more pollutants.

In contrast, Selezneva (1979) represents the traditional opinion that a transport of pollutants beyond 400 km is unlikely. Transport over a larger scale would be possible only if the transport were to proceed without dispersion of the aerosol, directly via a "corridor" or in other words via a laterally bounded transport pathway as we will propose. Selezneva (1979) pointed out that trajectories of particles are extremely complex and, especially in the presence of a turbulent atmosphere and intense diffusion, they will spread out over a large area. Clouds and precipitation will inevitably occur along such a long path and particles will be removed. Our work suggests that the arctic atmosphere during winter/spring is indeed capable of providing such unlikely conditions, necessary for low-level tropospheric transport.

#### 1.4 Limitations

We are attacking a problem which is rather difficult since numerous meteorological factors are involved characterizing the conditions at the source, along the path, and at the receptor site. The problem becomes even more difficult due to the sparcity of meteorological data, especially in the Arctic where there are only a few stations. Our chemical data set is taken at Barrow only, and we do not have "checkpoints" along the path to trace the pollution aerosol. Also, we do not have any chemical data on the characteristics of the pollution aerosols in their source area.

Thus, with these limitations imposed, this dissertation can only attempt to give a qualitative and coherent description on how long-range transport is possible and why there is a seasonal variation of the concentration of the arctic pollution aerosol.

#### 1.5 Outline and Summary of Major Results

We have two independent basic data sets: 1) chemical data from Barrow, Alaska and 2) flight records from the "Ptarmigan" weather reconnaissance flights. The first data set will be investigated in Chapters II-IV, the second in Chapter V. In addition, Northern Hemispheric weather maps and surface and upper air data will be used in order to describe the meteorological/synoptic conditions.

In Chapter II we will describe data on the chemical composition of the surface aerosol collected at Barrow (Section 2.1) and the way it was collected and analyzed (Section 2.2). It is important to determine the excess component of vanadium and manganese (abbreviated as XV and XMn, respectively) in order to describe the pollution-derived aerosol (Section 2.3). In addition, the possibility exists of using the XMn/XV ratio as a tracer for polluted air masses from different emission sources (Section 2.4). It is shown that XV and XMn undergo a pronounced and repeatable seasonal variation in concentration and that smaller fluctuations are superimposed on it (Section 2.5). The XMn/XV ratio seems to undergo a seasonal variation as well, implying that the pollution-derived aerosols come from different source regions during different times of the winter season (Section 2.6).

In Chapter III we will describe the meteorological/synoptic conditions which prevail at Barrow during times when high pollution concentrations are measured. We present climatological data on winter circulation patterns (Section 3.1.2) and on the seasonal variation of monthly mean meteorological elements (Section 3.1.3). Highest concentrations of XV and XMn occur during the months when it is dark, cold, dry, clear and stable. But highest concentrations of XV and XMn are not necessarily correlated with the extreme values of the meteorological elements. In Section 3.2 we identify polluted air masses and describe their meteorological characteristics. Polluted air masses always come from the north under anticyclonic conditions as an arctic air mass (Section 3.2.1) and therefore bear the characteristics of

arctic air masses (Section 3.2.2). Interestingly, higher than normal wind speeds are always associated with the arrival of polluted air masses. Spectral analysis (Section 3.2.3) seems to indicate characteristics of the pollution aerosol not reflected in the meteorological data.

In Chapter IV we will identify and describe possible transport pathway types to Barrow from mid-latitude industrial sources which will be considered as point sources (Section 4.1). The method employed to subjectively identify individual transport pathways and associated "pollution episodes" is similar to an iteration process, with the intent of gaining a coherent (admittedly not complete) picture of long-range transport through the Arctic. This approach describes the "signal" part of the arctic pollution aerosol, whereas diffusion models, for example, which average over space and time, describe the "noise" or background aerosol. Different types of transport pathways from possible North American (Section 4.3.2), European (Section 4.3.3) and Soviet source regions (4.3.4) will be presented. It appears that North American sources contribute little to the arctic pollution aerosol. It is pointed out that these transport pathways represent stable modes of the arctic and mid-latitude atmospheric circulation due to quasi-stationary anticyclonic pressure systems (Section 4.3.5). Synoptic conditions over the source area seem to be characterized by stagnation followed by a surge of pollutants northward (Section 4.4.1). Along the path synoptic conditions remain anticyclonic, but transport seems to take place along the peripheries of anticyclones associated with high wind speeds.

Travel times are on the order of 10 days and travel times for pollutants from European source regions are about 1 day shorter than from Soviet source regions (Section 4.4.2). Once the polluted air mass reaches Barrow its original meteorological characteristics seem to have been lost (Section 4.4.3). It will be shown that the seasonal variation of the transport pathway types can be explained by the seasonal variation of occurrence and position of the major anticyclonic systems, especially the Asiatic anticyclone (Section 4.4.4), and that the seasonal variation of the pressure systems can explain the seasonal variation of the XMn/XV ratio as well.

In Chapter V we will present the "Ptarmigan" weather reconnaissance data set which will yield information on the seasonal, spatial and vertical occurrence of Arctic Haze (Section 5.3) and information on the synoptic conditions during the observations of Arctic Haze (Section 5.4). In Section 5.5 we will speculate on the origin of Arctic Haze based on possible transport pathways. The data seem to suggest that Arctic Haze is probably pollution-derived during winter/early spring and may have a desert dust-derived component during late spring/summer.

## II SOME CHARACTERISTICS OF THE POLLUTION AEROSOL AT BARROW, ALASKA

### 2.1 The Chemical Data Bank

Since September 1976, aerosols have been collected continuously at Barrow, Alaska, except for summer 1977 and a few other days. For this dissertation four years of data were available, but the analysis was restricted to the winter data (October-April) only, because there is little pollution aerosol present during the summer (Rahn and McCaffrey, 1980). During the four winter seasons only 46 days of data are missing. Thus, the data set represents a unique time series of chemical data describing the seasonal variation of the arctic aerosols.

At the beginning of 1976, sampling times were relatively long, but during the years when the episodic nature of the pollution aerosols became better recognized, sampling times were shortened. During winter 1979/80 almost only daily samples were collected. The periods of long sampling times are very difficult to analyze from a meteorological point of view because meteorological conditions usually were not persistent enough (Section 3.2).

Table 1 represents the total number of samples available for this dissertation. With the decreasing sampling time the number of total samples during a season increased. Table 1 also represents a frequency distribution of the sampling times. Except for the daily samples taken during 1979/80, samples of four days duration are the most numerous.

Table 1: Frequency distribution of samples and sampling periods

	sampling period (in days)																	total
	1	2	3	4	5	6	7	8	9	10	11	12	13	14	15	16	17	
1976/77					2	6	4	5	2	3	2	3	1				1	29
1977/78				5	14	10	3	5	1	1								39
1978/79				4	39	3												46
1979/80	118	15																148
total	118	15	11	71	20	8	7	4	2	4		1					1	262

## 2.2 SAMPLING METHOD AND ANALYSIS

At the GMCC (Geophysical Monitoring for Climatic Change) site in Barrow, operated by the U.S. Department of Commerce, a ground-based high volume ( $100 \text{ m}^3 \text{ hr}^{-1}$ ) sampler collects aerosols on a Whatman No. 41 (size: 20x25 cm) cellulose filter. The filter is housed in a wooden shelter designed for use in the Arctic which accepts aerosols up to a radius of  $10 \text{ }\mu\text{m}$  but excludes snow crystals. To minimize the effects of those few crystals that do reach the filter, one or two 250-watt infrared heat lamps shine on the filter at all times. The Rotron pump is nearly contamination-free, but to avoid any chance of contamination, it is separated vertically from the filter shelter (Rahn, personal communication). The advantages of using Whatman filters in Neutron Activation Analysis were discussed by Dams et al. (1972).

During most of the time aerosol samples were "sector controlled", which means the pump was only operated when the wind was blowing out of the "clean" sector (5-125 degrees) as defined by Bodhaine et al. (1981) who presented a compass rose with possible local pollution sources relative to the sampling site. Even if the filter picked up local contamination this does not effect our analysis significantly because the tracers of pollution aerosol we are using in this study are not of local origin (Section 2.3).

The chemical analysis of the composition of the aerosols was done by Neutron Activation Analysis (NAA) at the 2-megawatt nuclear reactor of the Rhode Island Nuclear Science Center by Kenneth Rahn. The NAA

technique is described by Ragaini (1978), for example.

The filter with the collected aerosols is exposed to a high neutron flux. Radioactive species produced by neutron-induced reactions emit  $\gamma$ -rays which are detected or "counted". In the nondestructive procedure separation of the various elements is effected by taking advantage of the differences in  $\gamma$ -ray energy and half-lives, and using high-resolution Ge(Li) energy spectrometers to resolve the  $\gamma$ -ray photopeaks. The radioisotopes are identified by their half-lives and the energies of the  $\gamma$ -rays. The disintegration rate is then computed from the area of the  $\gamma$ -ray peaks, and the elemental concentration is calculated by comparing the activity of the sample to the activities of known elemental standards.

In NAA studies two different irradiations are routinely used: a) a short irradiation (seconds to minutes) is used to produce radionuclides with half-lives between 2 minutes and several hours, and b) a long irradiation (several hours) to produce radionuclides of long half-lives. For the present study only the data from the short irradiation were available which included the following elements: Al, Mg, Ti, V, Cr, Cl, Na, Mn, Br, I, Ba, Tl. Reliable (10-15%) analytical results, however, were only available for Al, Na, V and Mn (Rahn, personal communication). Therefore, it was decided to use Al as the crustal reference element and V and Mn as indicator for a pollution aerosol (Section 2.3). Neutron activation analysis has the capability of detecting a large number of the inorganic constituents of the aerosols. However, NAA does not have the ability to distinguish the

molecular composition.

### 2.3 Definition of Excess Vanadium and Excess Manganese

Solid and liquid particulate matter suspended in the air are collectively referred to as atmospheric aerosol. The particles can range in size from Aitken nuclei ( $10^{-3}$   $\mu\text{m}$  diameter) to the "giant" aerosol ( $10^2$   $\mu\text{m}$  diameter). Particles larger or smaller than this range have extremely short residence times in the free atmosphere. Pollution-derived and natural aerosol particles are found throughout the troposphere all over the world. Antarctica is the cleanest region on the planet with the lowest natural aerosol background (Shaw, 1979). Aerosols originate (as primary or secondary aerosols) from a wide variety of sources and source types, are continually modified (i.e. coagulation, coalescence, selective removal etc.) while in the atmosphere, and are eventually removed (dry deposition, rain out, washout, etc.) onto the land and the sea (e.g. Bach, 1976).

The atmospheric aerosol is composed of three major components: a carbonaceous fraction (sooty carbon plus organics), a water soluble ionic fraction (sulfate, nitrate, ammonium ions), and a mostly insoluble inorganic fraction (elements, oxides, etc.). In addition, water is a small but highly variable component (Rahn, 1976). For this study information is available only on the inorganic fraction (elements) because, as mentioned above, only this part of the aerosol can be

analyzed by NAA.

Elements detected in the aerosol can come from a variety of sources. Soils contribute primarily O, Si, Al, Fe to the atmospheric aerosol. But O and Si cannot be detected by NAA, and Fe has, in contrast to Al, a significant pollution source. Therefore, Al is almost universally used as a good indicator for crustal sources (Rahn, 1976). We refer to Al as a crustal reference element.

Atmospheric vanadium (V) has two major sources: a crustal and a pollution source (Zoller et al., 1973; Duce and Hoffman, 1976). Vanadium is found in mineral ores, coal and oil. The pollution component of vanadium is primarily due to the combustion of oil, whereas much of the vanadium from coal combustion is contained in large silicate particles that never leave the stack. Iron-ore processing and steel making are not important contributors to the world-wide atmospheric vanadium concentrations (Athanassiadis, 1969). The pollution component of V can be used as a good indicator for mid-latitude aerosol at Barrow, because it originates mainly from the combustion of heavy residual oil (Zoller et al., 1973) whereas the lighter fuels used at high latitudes contain insignificant amounts of vanadium (Hofstader et al., 1976).

Manganese (Mn) also has a crustal and a pollution source (Sullivan, 1969). Concentrations of Mn in soil are several times higher than V, and Mn is not quite as good a pollution indicator as V, because Mn is emitted from more and different sources. A principal source of man-made Mn pollution to the atmosphere has been the ferromanganese blast furnace. Other sources include the use of organic manganese fuel

additives, welding rods, and incineration of manganese-containing products.

It is desirable to separate the pollution and crustal components of V and Mn, respectively. We will explain the separation procedure for V; a corresponding procedure is used for Mn.

The total measured V (TV) can be represented as the sum of the crustal V (CV) and the excess or pollution V (XV):

$$TV = CV + XV.$$

The contribution of CV is estimated by using the  $Al_{aer}$  concentration measured in the same aerosol, as the crustal reference element. With the Al measured and a ratio of  $(V/Al)_{crust}$  for the average bulk crustal rock one is able to estimate how much of the vanadium is expected to be derived from the crustal material of the aerosol:

$$CV = Al_{aer} \times (V/Al)_{crust}.$$

The excess (=noncrustal) or pollution vanadium is derived as a residue from the measured total concentration and the estimated crustal concentration,

$$XV = TV - CV.$$

A detailed description of the procedure and its limitations is given by

Rahn (1976).

The  $(V/Al)_{\text{crust}}$  ratio is based on Mason's (1966) average crustal rock. Several objections can be made against the use of such a ratio: a) soil is a better reference material for the aerosol than rock, b) if rock is used as a reference then one should use local rock instead of "average" rock, c) there is strong physical fractionation during the production of crustal aerosol, with the aerosol appearing in a size range where only negligible soil mass exists. It thus follows that to the extent that soils have a size-dependent composition, their bulk composition may not truly reflect the 1-10 $\mu$ m precursor of soil-derived aerosol.

At the present time, the composition of average rock is better known than that of average soil, especially for the rarer trace elements, favoring the use of average rock as a reference material. Average rather than local rock was chosen because most aerosol analyses are not accompanied by corresponding analyses of local rock (soil) and the use of a constant reference material makes analyses at different sites comparable. Schuetz and Rahn (1982) found that elemental compositions of desert soils are nearly constant over the aerosol size range and that soils from different deserts are similar in composition, thus, the use of an average crustal reference material is reasonable. The only exception has been reported by Borys and Rahn (1981), when the ratio had to be based on local rock.

Another concept quite frequently used in air chemistry is the enrichment factor (Rahn, 1976). The enrichment factor for vanadium is

defined as

$$EF_V = \frac{(V/Al)_{\text{aerosol}}}{(V/Al)_{\text{rock}}},$$

i.e., the ratio of (V/Al) measured in the aerosol to (V/Al) present in average rock. Elements with enrichment factors significantly greater than unity are called "enriched" and probably have another major source other than the crust.

Fig. 1a presents the monthly mean total concentrations and the corresponding estimated crustal component of vanadium at Barrow for the period October 1976 through June 1978. No samples were taken during June/July 1977. During January-March the crustal component represents less than 10% of the total vanadium, that is, the vanadium measured is dominated by its pollution component. During the summer the situation is reversed, the crustal component now represents up to 71% of the total vanadium. Conditions for manganese are different (Fig. 1b). Contributions of the crustal component range from a minimum of 17% to 110% in June of 1977. In this case our estimate of crustal Mn predicts more than is actually present. Thus, we note that during the winter season, and especially during spring, the crustal contribution is usually at its minimum. The aerosol collected during this period is dominated by the pollution components.

At this point we would like to summarize some pieces of evidence that XMn and XV, in particular, are truly derived from mid-latitude pollution sources and not local sources.

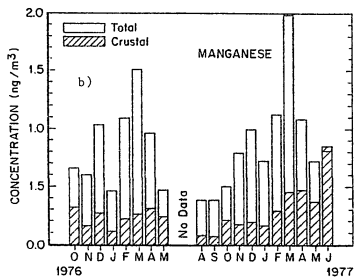
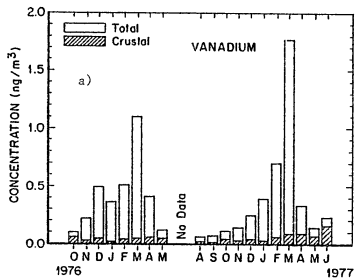


Fig. 1: Monthly mean total and crustal components of  
a) vanadium, b) manganese.

1. No vanadium is emitted by the village of Barrow (Rahn, unpublished). As mentioned above, vanadium originates from heavy oils. At Barrow, the fuels used are primarily natural gas (which is free of trace elements like V and Mn) and highly refined jet fuels, which are also extremely low in impurities.

2. The samples were sector-controlled, that is, air was sampled only from directions other than Barrow (Section 2.2).

3. As a test some samples were taken deliberately out-of-sector, i.e. from the direction of Barrow. No significant differences with the in-sector samples were seen (Rahn, unpublished).

4. During spring 1979 simultaneous daily aerosol samples were taken at Barrow and Narwhal Island, 30 km north of Prudhoe Bay, under clean-air conditions (N/NE winds) at both sides. The result showed conclusively that Barrow air from the clean sector truly represents the Alaskan Arctic as a whole. Concentrations of the pollutants V and  $SO_4$  were nearly the same at Barrow and Narwhal, also excluding Prudhoe Bay as a possible source (Conway and Rahn, unpublished).

5. The aerosol collected is well aged as inferred from sulfate/V ratios (Rahn and McCaffrey, 1980),  $^{210}Pb$  concentrations (Rahn and McCaffrey, 1980), carbon data (Rahn et al., 1980), size distributions (Shaw, 1982a) and from optical properties (DeLuisi, 1981).

6. The seasonal variations of XV and XMn (Section 2.5) are similar at several arctic sites (e.g. Barrie et al., 1981; Larssen and Hanssen, 1979).

Volcanic particles in the upper troposphere/lower stratosphere and

stratospheric particles present another possible source of the aerosol collected at Barrow. On March 5 and 6, 1980 Noelle Lewis (unpublished) was able to detect the signatures of volcanic particles at Barrow following the eruption of Klyuchevskaya on Kamchatka ( $56.06^{\circ}\text{N}$ ,  $160.64^{\circ}\text{E}$ ). No other evidence of volcanic particles has been detected (Rahn, unpublished). Stratospheric/tropospheric exchange takes place near the core of jet streams which are located below breaks or gaps in the tropopause. Stratospheric air enters the convergent left-rear quadrant of the jet maximum, subsides and slips underneath the jet axis and leaves the jet maximum on the equator side under anticyclonic flow (Reiter, 1963). The stratospheric air is now contained within a stable layer in the anticyclone, and this layer bears all the characteristics of a subsidence inversion. As soon as this inversion is tapped by convective motions caused by diurnal heating of the ground, its stratospheric aerosol will be transported to the ground by dry mixing, washout or both. The process by which stratospheric air intrudes through the jet-stream into the troposphere is also known as tropopause folding. The polar-front jet has been investigated extensively, but is of little interest to us because its position during winter/spring is too far to the south to create a source of aerosols within the arctic air mass. A stratospheric-tropospheric exchange is also expected to occur along the arctic front, but no investigations have been made.

We are not aware of any seasonal variation of the occurrence of tropopause folding. However, the occurrence of the spring maximum of stratospheric ozone and other radioactive fallout at the surface in mid-

latitudes can be explained by seasonal changes in the large-scale stratospheric circulation patterns which lead to a maximum of ozone during middle and late winter in the stratosphere. The breakdown of the stratospheric vortex and the occurrence of "sudden warming" cause meridional transport of aerosols into the polar stratosphere. These large-scale turbulent exchange processes increase the radioactivity burden and the ozone content of the lower stratosphere by spring. These layers, however, are continuously "tapped" by cyclogenetic processes associated with jet streams, causing a transfer of low-stratospheric air into the troposphere as described above. The maximum of surface stratospheric-derived ozone lags about two months behind the maximum of the stratospheric ozone and reaches its maximum in May, two months after the maximum of the arctic pollution aerosol. According to Reiter (1971) one can assume residence times of 1-2 years in the stratosphere. This would produce a homogeneous aerosol and different  $X_{Mn}/X_V$  ratios would not be detected (Section 2.6).

Feely (1979) determined  $^7\text{Be}$  concentrations from high volume filter samples of the four GMCC sites (Barrow, Mauna Loa, Samoa, and South Pole station). Samples from the arctic sites show a summer minimum and a winter maximum in  $^7\text{Be}$  concentration.  $^7\text{Be}$  is produced predominantly in the upper troposphere and lower stratosphere, and reaches the surface layer preferentially at mid-latitudes. He concludes that evidently  $^7\text{Be}$  is transported at low tropospheric levels into the Arctic from mid-latitudes at the same time of formation of the Arctic Haze layer. If Feely's (1979) conclusion is correct, stratospheric-derived air will

have to be transported along the same low-level transport pathways as the pollution-derived aerosol from mid-latitudes to Barrow.

#### 2.4 The XMn/XV Ratio as a Tracer

Rahn (1981c) suggested the use of the XMn/XV ratio as a tracer of air masses from different mid-latitudinal source regions. He showed that neither the enrichment factor of V nor the enrichment factor of Mn can be used separately to distinguish North American from Eurasian aerosol. Although the enrichment factors are initially different, during aging and selective removal of the larger particles the enrichment factor will change and completely obscure any distinction between North American and Eurasian air masses.

Aerosols are best traced by using elements with the same mass-size function, so that their ratio will remain nearly the same during transport. A possible, but not the best, choice for us is the XMn/XV ratio because no other elements were available. Tabulating available data Rahn (1981c) found that the XMn/XV ratio is greater than unity in Eurasia and less than unity in the northeast USA. Mean ratios for the two areas are  $2.0 \pm 0.8$  and  $0.41 \pm 0.09$  respectively, a factor of  $5 \pm 1$  difference. The XMn/XV ratio would thus seem to be a clear discriminator between these aerosols. The reasons for this difference are not quite understood, but probably have to do with the fact that oil is used more commonly as fuel in the USA than in Eurasia.

During transport and aging, the XMn/XV ratio will decrease, for the same reasons that the enrichment factors change, but the decrease will be much smaller than for the enrichment factors, because Mn and V have nearly the same particle size. Data show that the XMn/XV ratio of Eurasian air seems to decrease by factors of 3-4 during winter transport to the Norwegian Arctic (Rahn et al., 1980) and by factors of 2-4 during summer transport to Iceland (Borys and Rahn, 1981).

## 2.5 Seasonal and Episodic Variations of XV and XMn

As soon as the first year of chemical data became available it was recognized that the concentration of the pollution aerosol at Barrow undergoes a tremendous seasonal variation (Rahn and McCaffrey, 1980). Fig. 2 presents mean monthly concentrations of XV and XMn for the period September 1976 - September 1980. From a minimum during summer, concentrations rise gradually during fall, reach a plateau during January/February, and rise to a pronounced maximum in March. Concentrations rapidly decrease towards the summer. The similarity of the two curves is supported by a correlation coefficient between XMn and XV (monthly data) of  $r = 0.88$ . We notice that concentrations of XMn are higher than the ones of XV during fall and early winter. During February - April concentrations of XV are similar to those of XMn or even higher in March. This observation will be discussed further.

During the course of the year, concentrations of XMn and XV vary by

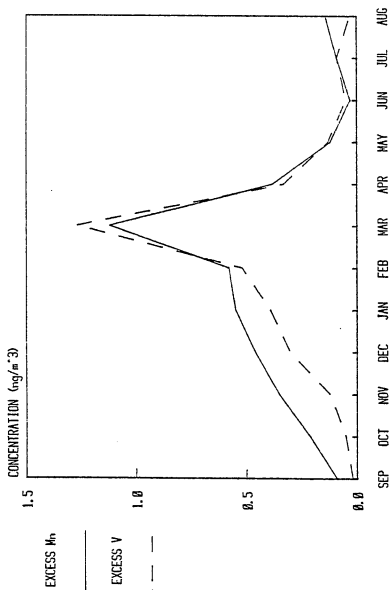


Fig. 2: Mean monthly concentration of excess vanadium and excess manganese (1976-1980).

factors of 33 and 82, respectively. In contrast, the seasonal variation of mid-latitude pollution aerosols is an order of magnitude smaller. Typical winter-summer ratios of XV range between 3-5 (Rahn and McCaffrey, 1980). The seasonality of vanadium and manganese at Barrow, therefore, cannot be explained by the seasonality at the source region.

Although an interannual variability of the seasonal variation is expected, it is remarkable how well the general features of the seasonal variation are preserved from year to year. Fig. 3a presents the monthly concentrations of XV for the four winter seasons. The seasonal variation of 1977/78 and 1978/79 are very similar and reflect the mean conditions described in Fig. 2. During the winters of 1976/77 and 1979/80 it appears that a secondary maximum is present during December. The monthly concentrations of XMn for the winter seasons are presented in Fig. 3b. The overall seasonal variation looks different than in the case of XV. The maximum in March is still preserved, but it appears that a secondary maximum in December is a permanent feature of the seasonal variation. During 1978/79 this maximum is shifted towards January. This fact is reflected in Fig. 2 by the higher concentration of XMn during fall and early winter.

Besides the dominant seasonal variation, the pollution aerosol possesses another important characteristic: it is episodic, which means that short periods of high concentrations are followed by short periods of low concentrations. This can be seen in Fig. 4 and 5, especially in the plots of 1978/79 and 1979/80 when the sampling times were short. The numbers in Fig. 4 and 5 indicate the sample numbers associated with

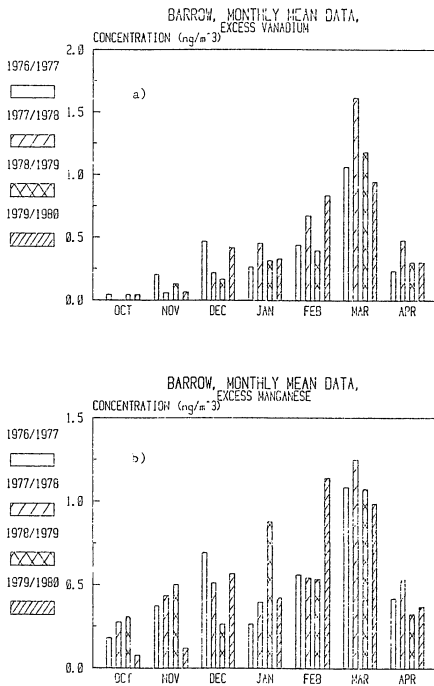


Fig. 3: Monthly mean concentration of a) excess vanadium  
b) excess manganese

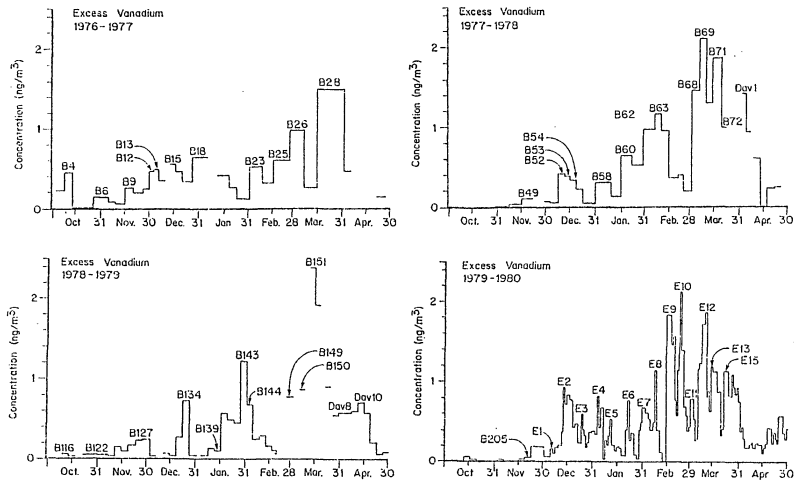


Fig. 4: Time series of concentrations of excess vanadium for the four winter seasons.

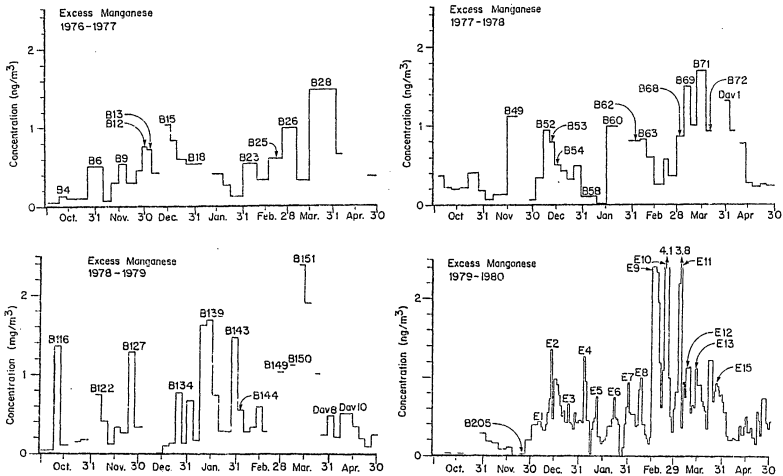


Fig. 5: Time series of concentrations of excess manganese for the four winter seasons.

a pollution episode to be defined in Section 4.2. We note that some spikes in concentration of XMn are not present in the corresponding XV plot, for example, B6, B49, B60, B116, B127. Nevertheless, the correlation between the daily concentration of XMn and XV during December 1979 - April 1980 is still  $r = 0.59$ .

## 2.6 Seasonal Variation of the XMn/XV Ratio

Fig. 6a presents a frequency distribution of the XMn/XV ratio for the period September 1976 - November 1979. The most frequent ratios lie in the 0.8-1.2 interval, followed by ratios in the 1.2-1.6 interval. There are also occasionally large ratios present (from 2.4 to 3.2) which are collected in the column to the right in Fig. 6. Following the discussion of Section 2.4 we surmise that Barrow is mainly influenced by air masses originating in Eurasia. Rahn (1981e) presented similar data for Barrow and compared the XMn/XV ratios at Barrow with the XMn/XV ratios characteristic of Bear Island. Bear Island, closer to European sources has a mean ratio of 0.6 whereas Barrow has a mean ratio of 1.3. It is hypothesized that one can differentiate between Eurasian sources: West European sources should have similar low XMn/XV ratios as North American sources due to a comparable use of oil, on the other hand, Rahn (1981c) concluded that the high ratios at Barrow are consistent with an unrecognized precursor with a very high XMn/XV ratio, probably from pollution sources within East Europe and the Soviet Union.

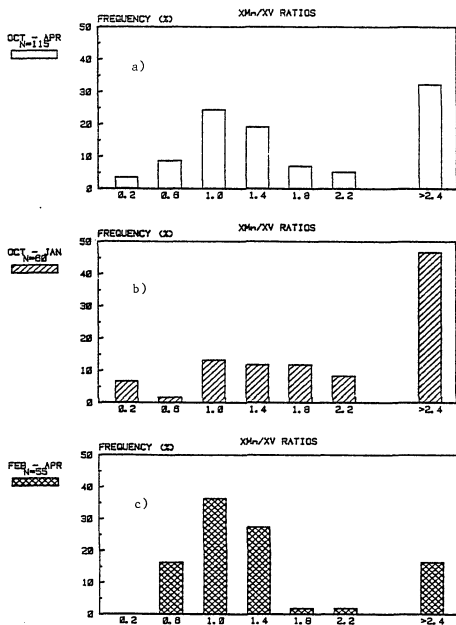


Fig. 6: Frequency distribution of XMn/XV ratios: a) October-April  
b) October-January, c) February-April.

The winter season has been divided into two parts, and two frequency distributions for the months October-January and February-April, respectively, were obtained (Fig. 6b, c). Interestingly, it appears that during October-January large ratios are more frequent than during February-April. A similar result is found in Fig. 7 based on the daily data during December 1979-April 1980. During December-February, ratios are usually larger than unity; during March/April ratios are smaller than unity. We recall that in Fig. 2 concentrations of XMn are higher than those of XV during fall and early winter and less or equal later on during spring. This fact is reflected in the seasonal variation of the XMn/XV ratio.

Rosen et al., (1981) presented data on the chemical composition of the arctic aerosol at Barrow during winter 1979/80. They showed that different elements undergo different seasonal variations. Total carbon (graphite) concentrations have their maximum in December and sulfur concentrations have their maximum in March at the same time when XMn and XV have their maximum. Thus, other ratios like V/C,  $SO_4/C$  (Rahn et al., 1980b) show a seasonal change in the chemical composition of the arctic aerosol as well. We conclude that the pollution aerosol at Barrow originates from a source during early winter which is different from the source during spring. This also implies that there should be a seasonal change in the atmospheric circulation which provides the transport mechanism.

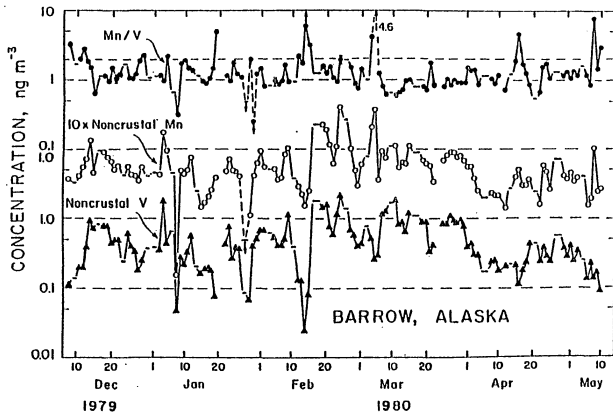


Fig. 7: Excess (noncrustal) manganese, excess (noncrustal) vanadium and the  $X_{Mn}/X_V$  ratio in daily samples during winter 1979/80 (after N. Lewis, personal communication).

For this work, it is assumed that very low  $X_{Mn}/X_V$  ratios at Barrow are indicative of North American sources, ratios  $<1$  for European sources and ratios  $>1$  of Soviet sources. This assumption will be tested in this dissertation.

III METEOROLOGICAL CHARACTERISTICS OF POLLUTED AIR MASSES AT  
BARROW, ALASKA

3.1 The Climate of Barrow

3.1.1 Introduction

Point Barrow ( $71.17^{\circ}\text{N}$ ,  $156.47^{\circ}\text{W}$ ) is located at the Beaufort Sea coast of Alaska. Due to its latitude the sun sets on November 19 and remains beneath the horizon until January 23.

From Barrow it is about 150 km south to the nearest elevation in excess of 60 m and 300 m to the foothills of the Brooks Range (at around  $68^{\circ}\text{N}$ ). Thus, the climate of Barrow is influenced very little by local topographic features. In contrast, winds at Barter Island turn about  $140^{\circ}$  with height due to the mountain barrier effects caused by the Brooks Range. During the same synoptic conditions, surface winds at Barter Island and Barrow, which is not affected by the Range, can differ by  $140^{\circ}$  (Kozo, 1980). The Brooks Range separates the arctic climate of the North Slope, including Barrow, from the continental climate in the interior of Alaska. Either land or sea-breezes are possible during the summer (Moritz, 1977). During the winter, however, the low-lying surfaces surrounding Barrow in all directions are snow covered and sea ice and tundra take on the same appearance beneath the snow.

The climate at Barrow is determined by the presence of the Arctic Ocean, which is covered year-round by sea ice. During favorable years summer melting and off-shore winds can create an open water-way along the Beaufort Sea coast for up to two months. The average "breakup" date is July 15 (Barry, 1977).

### 3.1.2 Winter Circulation Patterns

Using an objective method, Moritz (1979) identified 21 circulation patterns over Alaska and the Beaufort Sea. The circulation regime seems to be remarkably simple in the first approximation, with northern high pressure features (Beaufort Sea anticyclone or Arctic anticyclone) and lows (Aleutian cyclone) to the south in winter, and a seasonal reversal with a ridge to the southeast and lows to the west, southwest, north and northeast during summer. According to Moritz the circulation patterns (CP's) can be grouped into circulation seasons: winter (September-May), spring (May-July), summer (July-August), and autumn (August-September). The transitional seasons do not have characteristic CP's of their own. Rather they represent a decrease of winter CP's and an increase of summer CP's and vice versa.

The winter patterns (CP1, 3, 4), presented in Fig. 8, are caused by arrival and stagnation of cyclonic storms in the Bering Sea-Gulf of Alaska region and high anticyclone frequency areas from the Yukon across the Beaufort Sea towards Siberia (Reed, 1959; Keegan, 1958). Fig. 8

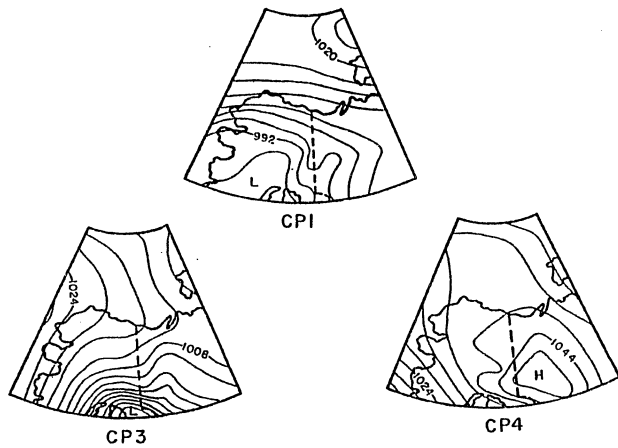


Fig. 8: Characteristic winter circulation patterns (after Moritz, 1979).

shows the pressure pattern of the three main winter circulation patterns. Fig. 9 presents the seasonal variation of the frequency of occurrence of these winter CP's.

CP1 is the most frequent circulation pattern over Alaska. It is characterized by low pressures in the south, higher pressures in the north, and cyclonic curvature over Alaska south of the Brooks Range. The strongest pressure gradient is found over NW Alaska where the isobars are nearly zonal in orientation. Thus, typically Barrow is characterized by easterly geostrophic flow (Section 3.1.3). The isobars over the southeastern part of Alaska turn almost due south. The weather conditions at Barrow associated with CP1 are: ENE winds with speeds of  $5.6 \text{ m sec}^{-1}$ , small temperature departures from the winter mean temperature, 5.2 tenths of cloud cover and little precipitation. The maximum of occurrence of CP1 is in May. Overall, CP1 represents the average climatic winter conditions at Barrow.

CP3 has the lowest pressure and the most intense pressure gradient in the northern part of Alaska. A strong Gulf of Alaska low is located east of the Alaska Peninsula. Highest pressures take the form of a relatively weak ridge along the Beaufort Sea coast from the west, although this feature is invariably much weaker than the low. This ridge often represents an eastward extension of the anticyclone over east Siberia which is, in turn, an extension of the Asiatic anticyclone (Sections 4.3.5 and 4.4.4). The weather conditions at Barrow associated with CP3 are: variable wind directions with light speeds below the winter average, large temperature departure of  $-3.6^{\circ}\text{C}$  from the winter

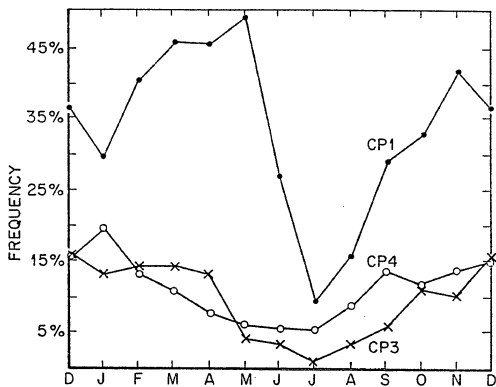


Fig. 9: Seasonal variation of frequency of occurrence of winter circulation patterns (after Moritz, 1979).

mean temperature, 5.2 tenths of cloud cover and little precipitation. CP3 is the coldest of all major winter patterns. Evidently the Beaufort Sea coast is completely cut off from the surface circulation of the Pacific region. The maximum of occurrence of CP3 is in December.

CP4 is characterized by a high pressure center over the southern Yukon which weakens as it extends northward into the Arctic Ocean. A relatively strong northeast-southwest pressure fall occupies the SW corner of Alaska. The weather conditions at Barrow associated with CP4 are: ESE winds with normal speeds, daily temperature departures range from  $-16^{\circ}\text{C}$  to  $+20^{\circ}\text{C}$  because of the variable extent of the Pacific low pressure systems, and 5.9 tenths of cloud cover. CP4 has its maximum of occurrence in January.

Moritz (1979) also found that CP1 has a median persistence of 3.1 days, CP3 of 1.8 and CP4 of 1.7 days.

### 3.1.3 Seasonal Variation of Monthly Mean Meteorological Elements

On the average, July is the warmest month, and the coldest month is February. The annual curve of mean monthly temperature is relatively "flat" in mid-winter (December-March) and in summer (June-September). By contrast, the temperature rise in spring and the autumn cooling are quite rapid. Wendler and Eaton (1981) found that clear days in April, May and the first part of June were still colder than cloudy ones, despite the increased direct solar radiation. The variability in daily

temperature departures from normal is greatest in mid-winter, declines to minima in spring and again in fall, and takes on intermediate, rather low values in the summer. The physical explanations must be related to the great interdiurnal variability of surface air temperature during formation and breakdown of the inversion in winter (e.g. Wilson, 1969). During the transitional seasons, the temperature variation is damped by effects of snow and ice phase changes acting as heat sinks (sources) in the spring (fall).

During the period 1976-1980 (Fig. 10) the coldest months were March 1977, February 1978, February 1979 and January 1980. It seems that the coldest temperature is not correlated with the maximum of pollution aerosol concentration, which always occurred in March. During 1979/80, however, when a broad maximum of pollution concentrations during February/March was present, the temperatures of February and March were similar. We note, that January is warmer than December and February in 1977, 1978, and 1979.

Surface inversions are characteristic of Barrow's climate and are well reflected in the monthly data. They are present almost all year long, but weak and sometimes missing during summer and fall. For our analysis, temperature data were available at 50 mb intervals, and we have also classified those cases as surface inversion when the inversion started at the 1000 mb level instead at the surface. This situation is possible when strong surface winds mix the lowest layer of the atmosphere (Wilson, 1969). During the period 1976-1980 (Fig. 11), surface inversions had their largest vertical extent in February 1977,

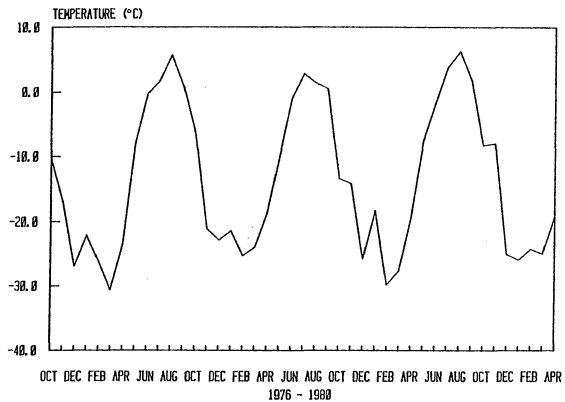


Fig. 10: Seasonal variation of monthly mean surface air temperature.

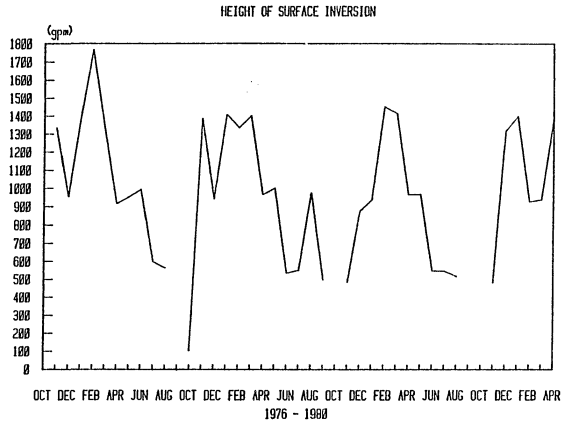


Fig. 11: Seasonal variation of monthly mean height of surface temperature inversion.

January/March 1978, February 1979 and January 1980. The intensity of the surface inversions, expressed as the temperature difference at the top and the surface, during the period 1976-1980 (Fig. 12) was largest (between 10-14 °C) in February 1977, January 1978, February 1979 and March 1980.

During the period 1976-1980, the highest mean surface pressures were present during December 1977, March 1978, February 1979 and January 1980 (Fig. 13). Except for 1978/79, highest pressure did not occur during the coldest months.

On the average, the prevailing wind directions are mainly easterly which is in general agreement with the frequent pressure patterns as discussed in Section 3.1.2. Mean wind speeds are moderately high ( $\sim 5$  m  $\text{sec}^{-1}$ ), with the strongest mean winds occurring from August to November. Fig. 14 presents wind roses for the winter seasons 1976/77, 1977/78, and 1978/79 compiled by Harris et al. (1980). There are differences among the years for the months October-December and April. January-March, on the other hand, seem to show a persistent characteristic.

On the average, a pronounced increase in mean monthly sky cover takes place between April and May and lasts until October. Clouds are primarily low level fog/stratus types, particularly during the summer. The minimum in sky cover is 4.8 tenths in March, the maximum is 9.2 tenths in September. During the period 1976-1980 (Fig. 15), minima of cloud cover occurred in March 1977, March/April 1978, March 1979 and March 1980. Thus, the minimum of cloudiness is a very persistent

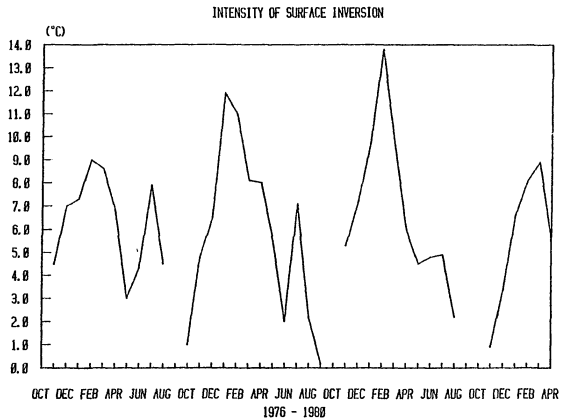


Fig. 12: Seasonal variation of monthly mean intensity of surface temperature inversion.

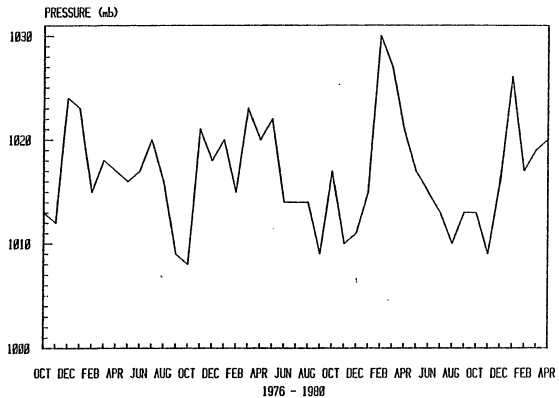
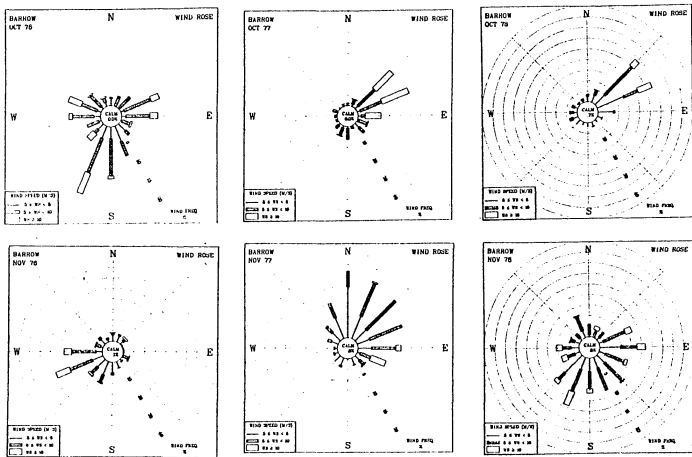


Fig. 13: Seasonal variation of monthly mean surface pressure.



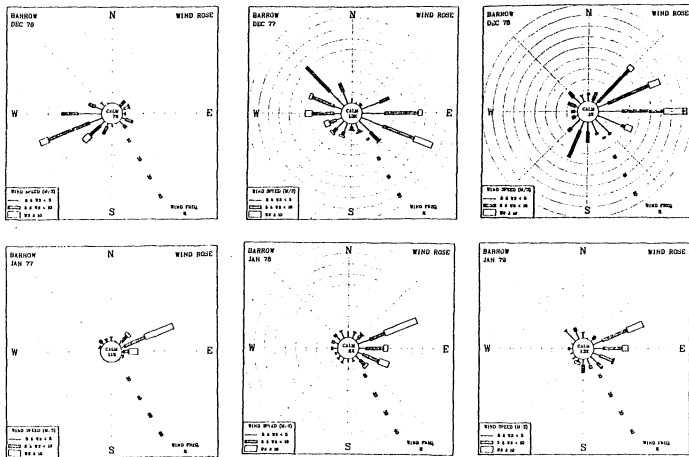


Fig. 14 continued

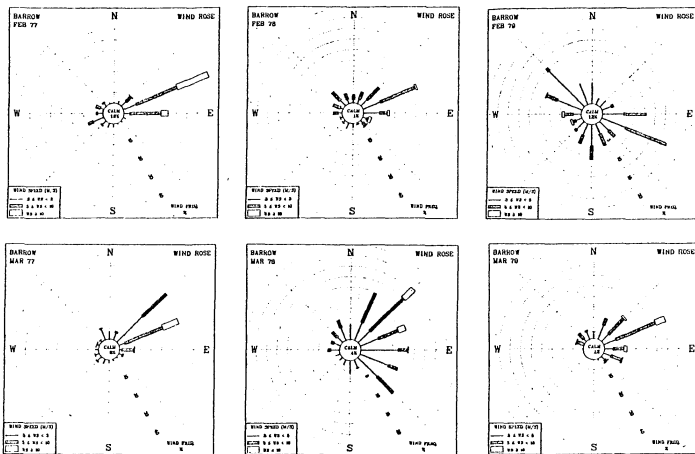


Fig. 14 continued

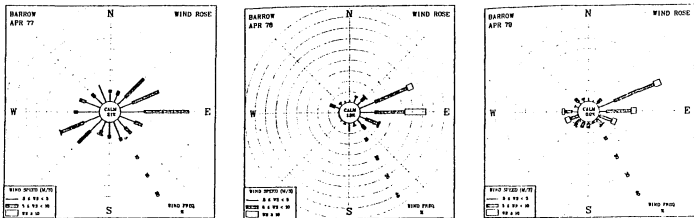


Fig. 14 continued

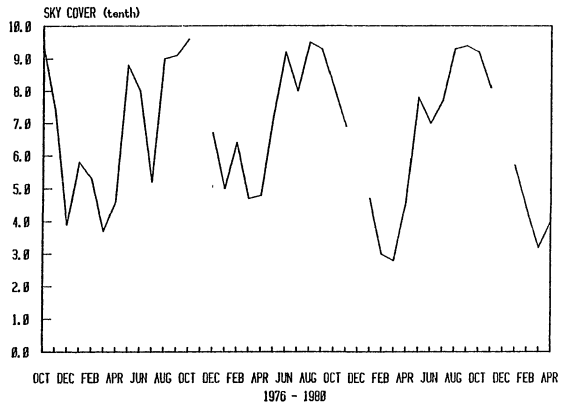


Fig. 15: Seasonal variation of monthly mean total cloud amount.

feature and correlates well with the maximum of pollution concentration. Such a correlation has been suggested by Shaw (1981).

The mean annual precipitation total is 124 mm, of which about 40% falls as summer rain. During winter, precipitation is difficult to measure, and it is estimated that actual falls are about 3 times the amount recorded (Benson, 1982). The summer precipitation maximum coincides with the seasonal increase of coastal cyclone frequency and with the greater availability of local moisture after the tundra thaws and the Arctic Ocean begins to break up (Moritz, 1979). Fig. 16 shows that during the period 1976-1980 precipitation was generally lower during the winter months.

Wendler (1978) investigated the occurrence of blowing snow at Barrow. Blowing snow usually occurs when the ground is snow covered and winds exceed  $7 \text{ m sec}^{-1}$ . The monthly frequency distribution of winds larger than  $7 \text{ m sec}^{-1}$  during 1965-1974 shows a maximum in November and a secondary maximum in January.

We have summarized the occurrence of the extreme values of the concentration of pollution aerosol and those of some meteorological elements (Table 2). The first month listed in each column indicated the main maximum (minimum), the second one indicates the secondary maximum (minimum). During 1976/77, it appears that the maximum of the concentration of the pollution aerosol occurred at the same time as the minima of temperature and cloudiness. During 1977/78, there seems to be a weak correlation only between the pollution concentration and the temperature. During 1978/79, a strong correlation between the pollution

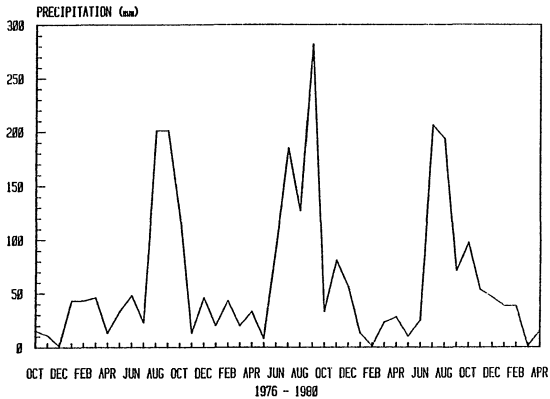


Fig. 16: Seasonal variation of monthly mean precipitation amount.

Table 2: Occurrence of extreme values of concentration of pollution aerosol and other meteorological parameters

	1976/77	1977/78	1978/79	1979/80
maximum concentration of XV	Mar/Dec	Mar/Feb	Mar/Feb	Mar/Feb
maximum concentration of XMn	Mar/Dec	Mar/Feb	Mar/Jan	Feb/Mar
minimum temperature	Mar/Dec	Feb/Mar	Feb/Mar	Jan/Dec
maximum height of surface inversion	Feb/Jan	Jan/Mar	Feb/Mar	Jan/Dec
maximum intensity of surface inversion	Feb/Mar	Jan/Feb	Feb/Mar	Mar/Feb
maximum pressure	Dec/Jan	Mar/May	Feb/Mar	Jan/Feb
minimum cloudiness	Mar/Dec	Mar/Apr	Mar/Feb	Mar/Apr
minimum precipitation	Dec/Apr	Mar/May	Feb/Jan	Mar/Apr

concentration and several meteorological elements is suggested. During 1979/80, only the intensity of the surface inversion seems to be correlated with the concentration maximum.

Overall, the occurrence of the maximum of pollution concentration falls into a period when temperatures are low, surface inversions are a permanent feature, pressures are anticyclonic, winds come from the east, and cloudiness and precipitation are low. A correlation is sometimes suggested but the seasonal and interannual variations cannot explain satisfactorily the seasonal and interannual variation of the concentrations of the pollution aerosol.

### 3.2 Meteorological Characteristics of Polluted Air Masses

#### 3.2.1 On the Origin of the Polluted Air Mass

In meteorological usage, an air mass is assumed to represent a vast body of air whose physical properties possess horizontal uniformity, while distinct changes are found along its boundaries, usually indicated on weather maps as frontal zones. Air masses form in semi-permanent circulation systems which have a tendency to be situated either over land (e.g., the polar continental highs) or over oceans (e.g., the subtropical anticyclones). The air that takes part in the circulation around any such system will become subject to the prolonged influences of the underlying surface, with the result that there will be a tendency

for distinct properties to be acquired, for example, continental cold and dry or marine warm and moist (Petterssen, 1956). As the air mass travels it may be modified continuously by differential advection, vertical stretching and shrinking, and by interactions between the atmosphere and the earth's surface; the last of which turns out to be the most important mechanism.

The simplest approach to distinguishing air masses at Barrow is to investigate the daily meteorological surface data (Table 3). Temperature and dew point temperature seem to be suitable for differentiating between air masses. A change of air masses occurred between the 4th and 5th of January. Surface pressure is less suitable and wind direction, wind speed, and cloud cover completely fail to indicate the arrival of a different air mass. Table 3 presents the data for one sampling period (B18) and it becomes evident that the sampling time was too long, because the question arises: which one of the two air masses carried the pollutants?

Unfortunately, most sampling times were fairly long with varying meteorological conditions present during the sampling (Section 2.1). These long sampling times are a serious problem in our attempt to describe the meteorological conditions. First, we selected only those samples during which the atmospheric conditions remained homogeneous, i.e. temperatures did not deviate more than about 3°C and the wind direction remained within the same quarter. Only 16 samples out of 114 satisfied these conditions. The mean values of several meteorological elements for the homogeneous samples are presented in Table 4. The

Table 3: Daily meteorological surface data at Barrow,  
December 28, 1976 - January 6, 1977

	December 1976				January 1977					
	28	29	30	31	1	2	3	4	5	6
Temperature ( $^{\circ}\text{C}$ )	-23.9	-25.6	-26.1	-21.7	-22.2	-21.1	-23.9	-20.6	-16.4	-15.0
Dew point temperature ( $^{\circ}\text{C}$ )	-27.2	-28.3	-28.3	-23.2	-25.6	-23.3	-26.1	-21.7	-15.6	-17.8
Pressure (mb)	1019.4	1024.5	1024.1	1022.2	1020.8	1016.7	1018.8	1008.3	1009.6	1026.9
Resultant wind direction (degrees)	80	90	60	70	60	60	60	70	80	90
Resultant wind speed (m/sec)	2.8	2.3	5.5	5.5	7.9	8.0	6.1	11.3	7.6	5.0
Sky cover (tenths)	10	6	7	10	9	10	7	7	10	4

Table 4: Characteristics of samples with homogeneous meteorological conditions

Sample	Sampling period	Concentration (ng/m <sup>3</sup> )		Temperature (°C)	Pressure (mb)	Wind direction (degrees)	Wind speed (m/sec)	Sky cover (tenths)
		XV	XMn					
B3	Oct 2-7, '76	0.023	0.050	-4.2	1016	67	14.2	10
B12	Nov 30-Dec 2	0.475	0.764	-22.5	1020	303	9.0	2
B13	Dec 3-5	0.498	0.737	-29.3	1040	86	7.9	3
B16	Dec 17-20	0.470	0.839	-30.1	1025	65	4.2	2.3
B42	Oct 7-11, '77	-	0.222	-1.9	1011	104	19.4	10
B44	Oct 17-21	-	0.219	-7.9	1010	56	21.5	10
B70	Mar 10-13, '78	1.318	1.047	-19.3	1016	73	5.5	7.3
Dav1	Apr 1-3	1.422	1.310	-26.9	1028	77	7.6	1
Dav2	Apr 4-6	0.941	0.931	-24.4	1020	63	13.7	2
B75	Apr 22-25	0.253	0.352	-14.4	1021	80	19.8	3.5
B115	Oct 5-8, '78	-	0.036	-8.1	1020	65	21.8	9.5
B120	Oct 26-29	0.055	0.175	-20.5	1015	93	7.0	6.3
B138	Jan 1-8, '79	0.132	1.630	-15.7	1025	73	13.3	1.3
B150	Mar 6-8	0.875	1.134	-28.3	-	60	12.1	2
B152	Mar 15-18	0.921	1.441	-26.8	1019	323	11.1	3.8
Dav10	Apr 11-14	0.515	0.524	-27.9	1040	75	11.1	0

correlation between XV and the temperature ( $r = -0.735$ ) revealed that the highest concentrations of XV are associated with the coldest temperatures. Correlations between XV (or XMn) and the wind direction failed, because almost all samples are associated with easterly winds.

Next we investigated the daily samples taken in 1979/80 which represent another data set allowing for a direct correlation between the chemical and meteorological data. The correlation between XV and the temperature turned out to be very poor ( $r = -0.1$ ). Fig. 17 presents the frequency distribution of wind directions for different XV and XMn concentrations. As expected east winds are the most common ones (see Section 3.1.3), but it appears that winds from the north are associated with higher concentrations. Table 5 presents the frequency distribution of wind directions for the ten highest and the ten smallest XV and XMn concentrations, respectively. Again, easterly winds are most frequent, but north winds are frequent with high concentrations and not present with low concentrations.

Peterson et al. (1980) investigated the dependence of  $\text{CO}_2$  concentrations, aerosol (measured by condensation nuclei concentration and by integrated light scattering at four wavelenghts), and ozone concentrations on air mass origin at Barrow during January-March periods of 1977 and 1978. The air mass origin was determined by calculating back-trajectories. It was found that ozone concentrations had no dependence on wind direction, whereas  $\text{CO}_2$  and aerosol values did show directional dependence; higher values occurred more often with trajectories leading into the Arctic Basin than with trajectories

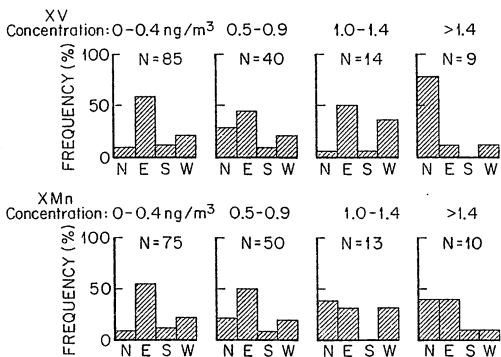


Fig. 17: Frequency distribution of wind directions for different XV and XMn concentrations.

Table 5: Frequency distribution of wind directions for the ten highest and smallest XV and XMu concentrations

	Maximum concentrations	Minimum concentrations
N	7	0
E	9	9
S	0	4
W	4	7

leading to the south. The aerosol analysis supports our results that high pollution concentrations are associated with polar air from the north. The  $\text{CO}_2$  results are less convincing because  $\text{CO}_2$  is released from anthropogenic sources as well as from the ocean through the sea ice as suggested by Gosink and Kelley (personal communication).

From the above analysis we conclude that pollutants reaching Barrow are associated with air masses coming out of the central arctic Basin as indicated by temperature and wind direction.

### 3.2.2 Meteorological Characteristics of the Polluted Air Masses

Another approach to identifying air masses is to use radiosonde data and to construct a height/time cross-section of potential temperature and mixing ratio. This approach is more elaborate because these quantities have to be calculated and plotted. For our analysis the height/time cross sections proved to be most useful in identifying different air masses. We have tried to use the heights of the 1000, 850, 700 and 500 mb levels or the relative topographies of 1000/850 mb and 850/700 mb surfaces, but they have not been useful. Wind directions at different pressure levels also failed to indicate changes of air masses.

The potential temperature at a point is uniquely determined by values of pressure and temperature at that point and represents the temperature a parcel of nonsaturated air would have if it were brought

adiabatically (i.e., without gaining or losing heat) to a standard pressure of 1000 mb. During adiabatic processes, an air parcel can be identified by its potential temperature since this parameter does not change during such a process. In the cross-section (Fig. 18), lines of constant potential temperature sloping upward with increasing time indicate the appearance of colder air at that layer, while lines sloping downward represent the arrival of warmer air. Temperature inversions or isothermal layers are represented by hatched columns. In Fig. 18, which represents the same time interval as Table 3, we find at near-surface levels the arrival of three air masses. There is a change from a cold to a warmer air mass between the 28th and 29th and another change to an even warmer one between the 4th and 5th. The first change is not present at higher levels, suggesting the arrival of a new air mass at low levels only. The second change, on the other hand, takes place at all levels throughout the troposphere. We note, that there are other temperature changes at upper levels not accompanied by changes in the surface layer, which will be discussed later.

The moisture content of an air mass is normally expressed by the relative humidity, however, in the Arctic this quantity is not very useful because although the Arctic is dry in absolute amounts of moisture, it is not so in terms of relative humidity. Relative humidity in the Arctic is normally about 10% higher than in middle latitudes, and only about 5% lower than in the equatorial belt (Petterssen et al., 1956). Therefore relative humidity is of little help in distinguishing between an arctic and a Pacific air mass, for example. A semi-

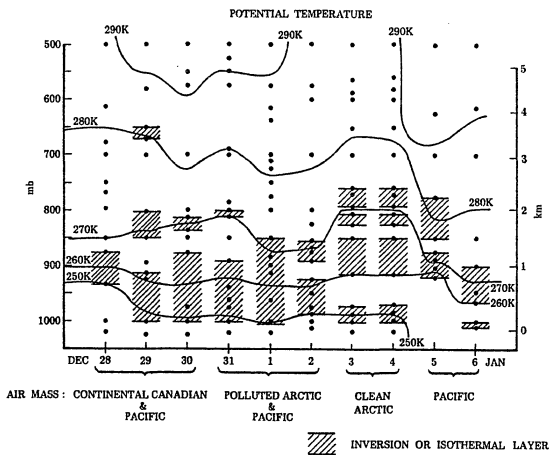


Fig. 18: Height/time cross section of potential temperature.

conservative quantity used to describe an air mass system is the mixing ratio, which describes the moisture content of an air mass, and is defined as the mass of water vapor per unit mass of dry air. The mixing ratio is conservative with respect to adiabatic as well as nonadiabatic temperature changes, but nonconservative with respect to evaporation and condensation. A height/time cross-section of mixing ratio is constructed in a similar way as the one for potential temperature (Fig. 19). It is evident that the mixing ratio provides a way to distinguish air mass systems relatively unambiguously. Regions of high mixing ratios were located at about the 800 mb level on December 18, 30, 31, indicating marine air aloft. There was a region of very dry air at about 775 mb on January 3 and 4. On January 5, a very moist air mass arrived, initially at higher levels, but then also at surface levels on January 6.

The combination of height/time cross-sections of potential temperatures and mixing ratios is very powerful in identifying air masses like cold and dry (continental) or warm and moist (marine). Air mass changes due to subsidence in anticyclones can also be recognized by the appearance of a warm and dry air mass characteristic and by inversions. It is also possible to determine if air mass changes took place only at low or upper levels or throughout the troposphere. One is also able to see when a warm air mass glides on top of a colder air mass and gradually modifies the underlying surface air.

With the help of weather maps, the air masses in Fig. 18, 19 were labelled according to likely origin. During December 29-30, continental

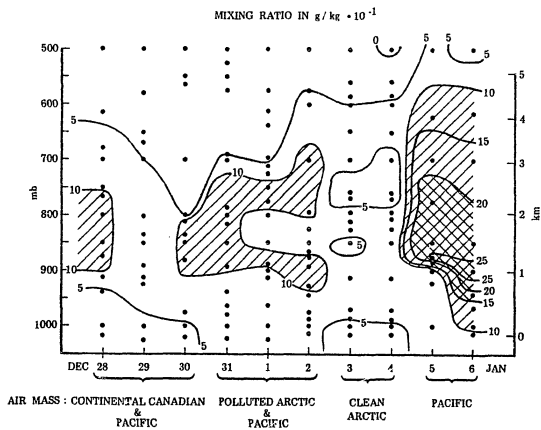


Fig. 19: Height/time cross section of mixing ratio.

Canadian air was present at low levels; at higher levels Pacific air was present, which was replaced by dry Arctic air on December 29. During December 31-January 2, Arctic air was evident in the surface layer, which is assumed to carry the pollution aerosol. These dates are in agreement with a pollution episode to be discussed (Section 4.2). Pacific air was still present aloft. On January 3 and 4, one can identify "clean" arctic air, characterized by slightly colder and less moist surface air and very dry and cold air aloft. This air mass is termed "clean" arctic air because it represents background arctic air which cannot be associated with a pollution episode (see Section 4.2). On January 5 and 6, Pacific air intruded at all levels of the troposphere accompanied by a dramatic change in meteorological conditions. This air mass was the only one detectable in the daily meteorological surface data (Table 3).

Fig. 20 shows the wind direction and wind speed (in  $5 \text{ m sec}^{-1}$  intervals) at different pressure levels during the period of our example. Wind directions at 1000 mb and at 850 mb are from the east throughout the whole period. Thus, no air mass changes are indicated. At 700 mb and 500 mb changes in wind directions are seen, but not always in accordance with the general flow as derived from weather maps. The reason wind directions seem to fail in detecting changes in air masses is Barrow's location with respect to the major synoptic systems. As indicated in Section 3.1.2, CPl is the most frequent circulation pattern influencing Barrow. Barrow lies within a confluence zone in this configuration, with winds always blowing from the east. If the Aleutian

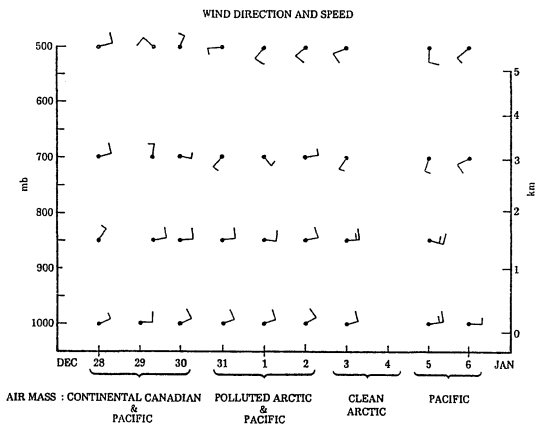


Fig. 20: Height/time cross section of wind direction and speed.

cyclone intensifies slightly, Pacific air will reach Barrow; if the arctic anticyclone intensifies slightly, arctic air will reach Barrow. However, neither the basic pattern nor the wind direction will change. Trajectories calculated for Barrow (e.g., ARL-NOAA trajectories) often fail to reveal the true origin of the polluted air masses for this reason (see also Table 10, Section 4.3.5).

For the samples labelled in Fig. 5 we constructed height/time cross-sections of potential temperature and mixing ratio. We then determined the time interval during which polluted arctic air was present. In most cases this was relatively simple when there was only a choice between Pacific (clean) and arctic air. In the more complicated cases, like Fig. 18 and 19, an approach like the one discussed was used. Timing and direction of the transport pathway of the polluted air were applied as criteria to identify the polluted air mass (Section 4.2). It should be noted that in each case there was an arctic air mass present. We never encountered a case of high concentrations of XV and XMn without the presence of an arctic air mass. This supports the hypothesis that the pollution aerosols originated with air masses out of the Polar Basin.

First results of properties of polluted air masses are given in Table A1 (Appendix). For each sample it was determined how many air masses arrived at Barrow during the period of sampling (column 3). We also specified the period during which the air mass which most likely carried the pollutants was present (column 4). It should be pointed out, that if a polluted air mass was present for three days it does not

necessarily imply that pollutants were also present for three days. Pollutants might be confined to patches which are carried along by the air mass. This possibility will be discussed later (Chapter VI).

Column 6 broadly classifies the types of the polluted air mass in terms of P=Pacific air, A=arctic air,  $A_p$ =arctic air modified by Pacific air, C=continental American air. The following combination  $A_pP$  means arctic air modified by Pacific air near the surface with Pacific air aloft. In column 8 we specify the range of wind direction counted clockwise at 1000 mb and 700 mb obtained from the radiosonde data. Excluding the daily samples E, it was found that 36% of all samples had only one air mass, 25% of all samples had two and three air masses, respectively, 10% of all samples had 3, 4% of all samples had 6 air masses. From column 4 one estimates that the mean duration of the presence of polluted air is about 3 days. A relationship does not seem to exist between the polluted air mass type and the transport pathways taken. It is evident, however, that the combination AP or  $A_p$  occurs quite often, thus, we do not necessarily encounter an arctic air mass by itself. On the other hand, the combination AP suggests that pollutants were contained in the low level layer indicating that in the vicinity of Barrow transport of pollutants takes place at low levels. It should be noted that sample E9 seems associated with moist and warm air coming from the NW Pacific, but an air mass change took place with arctic air modifying the Pacific air.

For the polluted air masses identified and listed in Table A1 (Appendix), column 4 the meteorological characteristics were determined

based on the average daily surface data. The data are displayed in Table A2 (Appendix) and reveal that a wide range of conditions is possible during the times polluted air masses arrive at Barrow. The meteorological characteristics are determined by the season of the year, the origin of the air mass, the transport path and associated travel time and modifications experienced along the path as well as at the receptor site when mixing of two air masses takes place. We have eliminated the annual march by subtracting the monthly mean value. The deviation from the mean (columns 5, 6, 8, 11, 13) are calculated as the deviation from the monthly mean of that particular month and year.

The results indicate that 75% of all polluted air masses have colder temperatures than the monthly mean (Fig. 21a), 56% of all polluted air masses are characterized by higher surface pressure than the monthly mean (Fig. 21b). Remarkably 90% of all polluted air masses arrive with wind speeds higher than the monthly mean (Fig. 22a), and 69% of all polluted air masses are characterized by less sky cover than the monthly mean (Fig. 22b).

Polluted air masses thus carry the characteristics of an arctic anticyclonic air mass. The high frequency of above normal wind speeds and the about normal pressure indicate that polluted air masses arrive along the southern periphery of the arctic anticyclone within a zone of pressure gradients and, therefore, of rapid transport. Polluted air masses do not arrive when the center of the anticyclone is close to or over Barrow.

Next, investigations were carried out to determine if the results

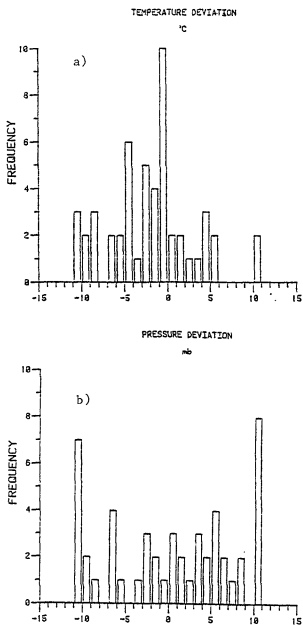


Fig. 21: Frequency of deviations from the monthly mean value (surface data), a) temperature, b) pressure.

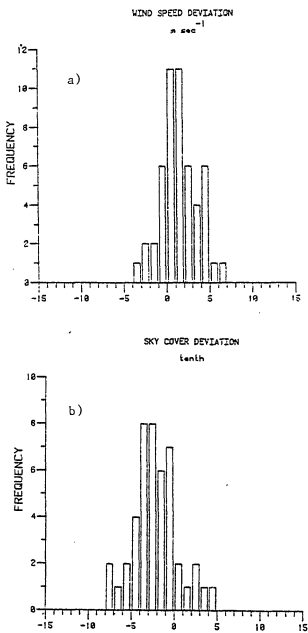


Fig. 22: Frequency of deviations from the monthly mean value (surface data), a) wind speed, b) cloud cover.

would depend on the month during which the polluted air masses arrive. Therefore, the frequency of occurrence of positive and negative departures from the monthly mean for temperature, pressure and sky cover (Fig. 23) was counted. November, March and April appear to be the months during which the polluted air masses deviate the most from the monthly mean. It is conceivable that the meteorological characteristics of the polluted air mass depend on the transport pathway type taken as defined in Section 4.3. The analysis will be presented in Section 4.4.3.

A similar analysis to that presented above was performed for the 850 mb level (Table A3, Appendix), because it is assumed that this level represents the conditions of the lower free atmosphere without the local surface influences which affect the surface data. For this analysis the upper air soundings at 00:00 GMT were usually used. Similar results are found: 68% of all polluted air masses are colder than the monthly average (Fig. 24a), and even 80% of all polluted air masses are associated with wind speeds higher than the monthly mean (Fig. 24b). Temperature inversions were analyzed by calculating the temperature difference between the surface and the 850 mb level. It was found that inversions with temperature differences between  $-6$  and  $-9^{\circ}\text{C}$  occur frequently (Fig. 25); 88% of all polluted air masses were characterized by surface inversions reaching up to 850 mb.

In summary, air masses, carrying pollutants to Barrow had travelled within the Polar Basin. Due to Barrow's position between the influence of the arctic anticyclone and the Aleutian cyclone the classification of

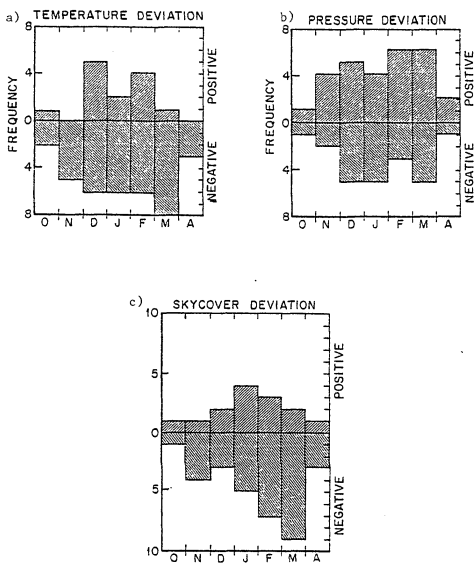


Fig. 23: Seasonal variation of frequency of positive and negative deviations, a) temperature, b) pressure, c) sky cover.

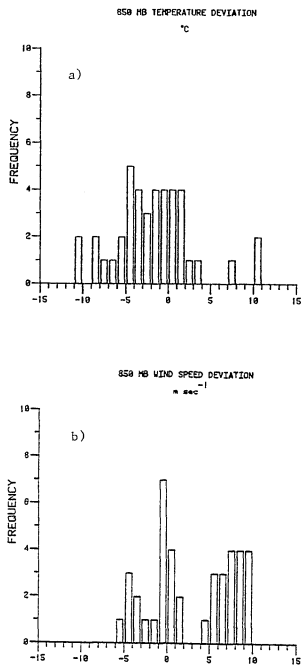


Fig. 24: Frequency of deviations from the monthly mean value (850 mb), a) temperature, b) wind speed.

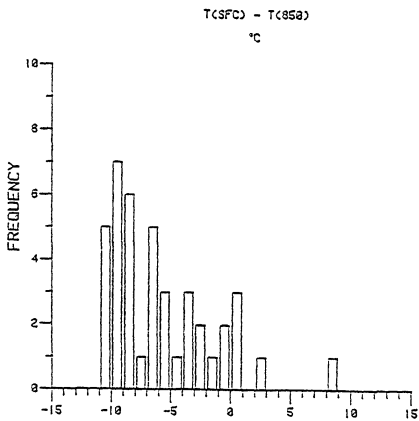


Fig. 25: Frequency of surface temperature inversions.

air masses was best accomplished by using a combination of height/time cross sections of potential temperature and mixing ratio. High levels of pollutants are always associated with the presence of an arctic air mass. The occurrence of the combination of two air masses present at the same time (AP), arctic air at low levels and Pacific air aloft, supports the hypothesis that the transport of pollutants should take place in the lower troposphere, at least in the vicinity of Barrow. The polluted air mass carried characteristics of anticyclonic arctic air, being colder and less cloudy than the monthly mean conditions and containing surface inversions. Interestingly, polluted air masses are characterized by above-normal wind speeds.

### 3.2.3 Spectrum and Cross Spectrum Analysis

Time series of data can be analyzed by spectrum analysis in order to estimate which oscillations of a specific frequency (periods) contribute significant portions to the total variance of the time series. In this way, a spectrum of a time series is analogous to an optical spectrum, indicating the contribution of different wave lengths or frequencies to the total energy of radiation.

An estimate of the power spectrum is computed by applying harmonic analysis to the autocorrelation coefficients of the series. The resulting coefficients are smoothed by a weighted moving average to produce a stable spectrum (Panofsky and Brier, 1968).

When two time series appear to be correlated the question may be asked whether this correlation is due to a correlation between high frequency components (small periods) or low frequency components (large periods) of the data. Or, two time series may appear to be uncorrelated, because the low frequency components actually are negatively correlated, and the high frequency components are positively correlated. This question can be answered by performing a cross spectrum analysis (Panofsky and Brier, 1968) which includes the determination of the coherence.

The coherence varies from 0 to 1 and is analogous to the square of a correlation coefficient, except that the coherence is a function of frequency. The coherence represents a frequency dependent correlation coefficient.

We subjected the daily data of XV, XMn, surface temperature and pressure during December 5-April 30, 1979/80 to a spectrum and cross spectrum analysis program (SAS 79 by SAS Institute, Cary, N.C.) available on the IBM computer of the University of Rhode Island.

Gaps in the chemical data series were closed by filling in the data of the previous day. Sometimes samples were collected over two days instead of over one. However, two day samples did not coincide with weekends, for example, thus producing an artificial period in the spectrum. We removed the seasonal trend by calculating mean values for each element and each month and subtracting them from the actual data. Thus, our data set of temperature, pressure, XMn and XV concentrations represents daily deviations from the monthly mean. Inspection of the

time series of the deviations showed that removing the monthly trend did not cause a distortion of the original time series. In Fig. 26 the power spectra for XV and XMn are presented. In each case we have indicated the 80%-confidence limit, so that the true value lies within this range. Both spectra reveal a similar appearance with plenty of detail. XV reveals significant periods at 24.6-18.5 days, 7.7-7.0 days and 4.1-3.8 days. XMn reveals significant periods at 8.7-7.7 days, 49.3-29.6 days, 4.7-4.4 days and 2.5 days. It appears that the periods of XMn compared to those of XV are slightly shifted towards larger periods. It was noted in Section 2.5 that XV and XMn show a similar trend and a good monthly correlation. In Table 6 the daily data are correlated showing a correlation between XV and XMn of  $r = 0.56$ . The cross spectrum analysis revealed that high coherency of 0.93 and 0.78 was present in the periods of 7.0-6.4 days and 21.1-16.4 days, respectively. It should be noted that highest coherency was found at the shoulders of the peaks in the spectra and not at the peak itself. This high coherency, however, seems to support the overall high correlation coefficient between XV and XMn.

The power spectra for temperature and pressure are presented in Fig. 27. It is obvious that these spectra are similar to each other but differ from the power spectra of XV and XMn. The spectra of temperature and pressure fall off rapidly with smaller periods and do not show as much detail as the spectra of XV and XMn. Pressure reveals significant periods at 29.6-21.1 days and 6.4-5.9 days. Temperature reveals significant periods at 21.1-16.4 days and 4.9-3.8 days. In this case,

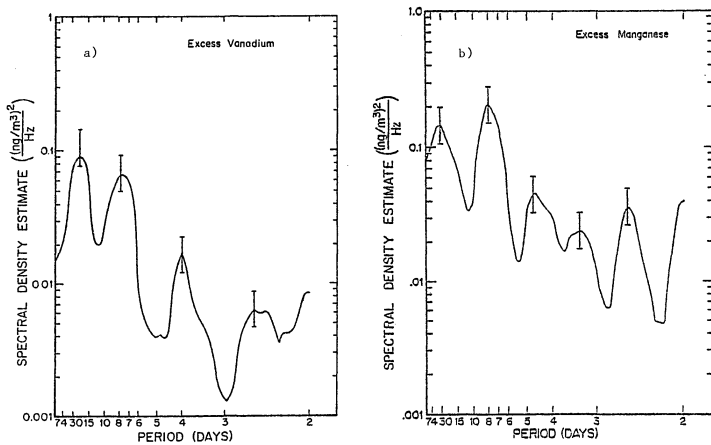


Fig. 26: Power spectrum for a) excess vanadium, b) excess manganese.

Table 6: Correlation coefficients between daily chemical and meteorological data

	ln XV	ln XMn	P	T
ln XV	1			
ln XMn	.56	1		
P	-.02	-.11	1	
T	-.15	-.15	-.15	1

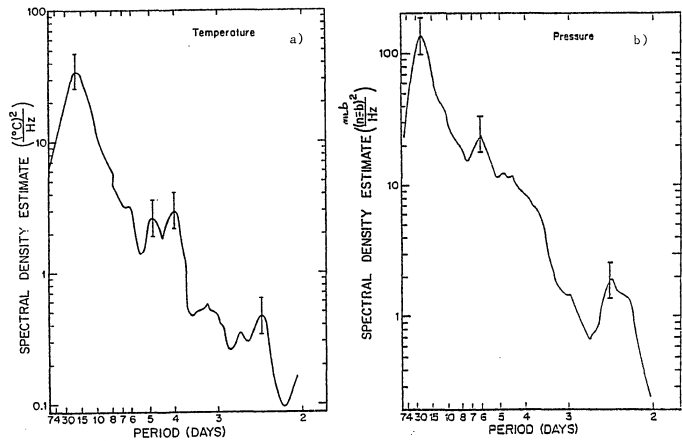


Fig. 27: Power spectrum for a) temperature, b) pressure.

the spectrum of pressure seems to be slightly shifted to larger periods than the spectrum of temperature, analogous to XMn and XV. In Table 6 the daily data of pressure and temperature are correlated with a weak correlation of  $r = -0.1$ . Applying a cross spectrum analysis on temperature and pressure resulted in a coherency of 0.86 in the period of 4.3-4.0 d ys. Again strong coherency was not present between the centers of the peaks but displaced to the shoulders of the peaks. Cross spectrum analysis between the meteorological elements and the chemical elements resulted in overall weak coherences. Some stronger coherences were suggested but never occurred within the significant periods. Therefore, the significance of these coherences appears doubtful. Linear correlations between temperature, pressure, XV and XMn are presented in Table 6 and are insignificant.

The following hypothesis is presented in order to explain the significant periods found in the spectra: from Table A5 (Appendix), E samples only, it can be estimated that about every 6-7 days a surge took place over source regions in mid-latitudes. On the average, a surge lasted for about 4-5 days. These two periods seem to be reflected in the spectra of XV and XMn. Investigating height/time cross sections of potential temperature and mixing ratio at Barrow for December-March it was found that the presence of arctic and Pacific air masses seem to alternate with a period of about 18 days. The presence of Pacific air at Barrow lasted for about 4-5 days, arctic air was usually present over a longer time. Therefore, it appears that the large period peaks in all four spectra can be associated with the varying influence of Pacific and

polar air, or in other words, the large scale synoptic situation. Pacific air is clean, arctic air is polluted. The peak at smaller periods in the pressure and temperature spectra might reflect the duration of Pacific air present.

In summary, spectrum and cross spectrum analyses suggest that the large scale variations of the atmosphere are represented in the long periods of the spectra of all four elements investigated. The peaks in the smaller periods, however, are due to different physical processes and therefore, are not correlated with each other. In the case of XV and XMn, the peaks can be explained based on the frequency and duration of pollution surges in mid-latitudes. Peaks in the spectra of temperature and pressure can be explained by the local synoptic conditions.

The results of the above analysis agree with findings documented for other locations. Differences are expected due to the different climatic/synoptic setting of each location. Shapiro and Stolov (1970) investigated surface pressure variations in the Polar Regions by spectrum analysis and found 31 day and 15 day periods at Resolute Bay and Thule. McGuirk and Reiter (1976) observed a strong persistent and significant oscillation of about 24-day periodicity in hemispheric-scale energy parameters during the winter season. Panofsky and Wolff (1957) found that most of the variation of the westerly index at 60°N were produced by oscillations with periods on the order of 25 days. Hartmann (1974) investigated data from Atlantic weather ships during winter and found that zonal wind as well as temperature revealed a significant

period of 15-30 days. Winter temperature and precipitation at Woodstock College, Maryland possessed significant periods of 5-7 days and of 3 days due to the synoptic regimes (Landsberg and Mitchell, 1959). Hartman (1974) found periods of 4-5 days in the temperature and the meridional wind component and a period of 3-5 days in the meridional transport of temperature. Tilley and McBean (1973) associated peaks at about 3 days in the SO<sub>2</sub>, wind and temperature data with synoptic weather variations.

#### IV TRANSPORT PATHWAYS OF MID-LATITUDINAL AEROSOLS

##### 4.1 Industrial Mid-Latitude Source Areas of Pollutants

The mid-latitudes of the Northern Hemisphere represent a densely populated and highly economically developed area of the world. Economic development is associated with industrial activities which contribute a major portion of total anthropogenic air pollution. It does not matter on which side of the political world the industries are located, "industrialization is the primary cause of environmental disruption" (Goldman, 1970).

The industrial areas are usually clustered in regions due to the presence of exploitable raw materials, available energy resources, and transportation facilities. The term "point sources" is used in this connection describing a cluster of industries of recognizable size, for example, the Ohio Valley, the Ruhr area, or the Volga-Urals Region. "Area sources", on the other hand, are associated with population centers and include large numbers of low-level residential pollution sources. They are of little interest to the problem of long-range transport. Point (industrial) sources, however, have become more and more important in the problem of long range transport, because in order to avoid local pollution, large stacks have been built. For example, prior to 1970 only two stacks exceeding 150 m were in existence in the US; in 1981, there were more than 175 such stacks (Anonymous, 1981).

Pollutants from such stacks are emitted into higher layers of the atmosphere and can readily be transported, in contrast to pollutants from low-level sources. Shaw (1981) considered the industrial areas of mid-latitudes as a quasi-homogeneous band of emission sources surrounding the Arctic. In this investigation the industrial areas are considered to be differentiable sources with individual chemical characteristics and with varying importance as contributors to the arctic pollution aerosols because of the varying synoptic conditions leading to or not allowing transport of their emitted gases and aerosols.

It is known that the United States is the foremost nation in the western hemisphere in population and economic development. The centers of population and major heavy industries are located in the northeastern part of the United States, i.e. in the states of Illinois, Indiana, Ohio, Pennsylvania, and New Jersey. Four states in the Ohio River Valley - Ohio, Indiana, Illinois, and Kentucky - are responsible for nearly one fourth of all the  $SO_2$  produced in the US each year (Anonymous, 1981). Canadian centers of population and major heavy industries are located in the southeastern part of the country, namely Ontario and Quebec (Voldner et al., 1980). During the past decade the annual emissions of sulfur from the Sudbury smelter in Ontario have about equaled the amount thought to have been emitted by all the volcanoes of the world (Likens et al., 1979). Smog and acid rain are well known features of air pollution in North America.

In western Europe, major industrial areas are: the Glasgow and the Manchester area (United Kingdom), the Lorraine province and the northeastern corner of France, the valleys of the Sambre and Maas rivers in Belgium, and the Ruhr area of West Germany. The main industrial areas of eastern Europe lie within the triangle Lodz (Poland), Erfurt (East Germany) and Budapest (Hungary). In general, northeastern Europe is more industrialized than southeastern Europe (Turnock, 1978). Air pollution in eastern Europe has been reported by Dienes (1974), Bruneau (1981), Turnock (1978).

In the Soviet Union heavy industry is still favored in development over the consumer industry. To become independent of imports of raw materials deposits were exploited even in areas of little population regardless of profitability. This led to the result that the Soviet Union's North is more developed than the American North. Major industrial areas are: the Kola Peninsula and the Moscow/Leningrad areas (western USSR), the great band of the Dneper River and the Donets Basin (Ukraine), the Volga-Urals region (southern Urals), and the Kuznetsk Basin (western Siberia) (Dewdney, 1976; Kish, 1971). Goldman (1970) has reported on air pollution in the USSR.

Major industrial areas of East Asia are Korea and Japan. According to Rahn (1981a) these sources are unlikely to be major contributors to the arctic pollution aerosol, because pollutants from these sources would have to travel a marine pathway along which precipitation is likely to remove the aerosols.

Shaw (1981) summarized estimates of northern hemispheric anthropogenic sulfur production at latitudes north of  $35^{\circ}\text{N}$ . It is of interest to note that the main industrial areas of the Soviet Union are located at about  $50\text{--}55^{\circ}\text{N}$ , followed by western Europe at  $50^{\circ}\text{N}$ , eastern Europe and Canada at  $45^{\circ}\text{N}$ , and the USA at  $40^{\circ}\text{N}$ . Industrial areas of East Asia are farthest away from the Arctic at  $30\text{--}35^{\circ}\text{N}$ . Thus, from their geographical position one would expect that the Soviet Union is probably more important than the USA in releasing pollutants into the Arctic.

#### 4.2 Method for Identifying Transport Pathways of Pollutants

Shaw (1981) argued that any cloud of pollutants emitted from an industrial point source would disperse after one week over an area comparable to large scale synoptic features and after several weeks would approach the size of the Arctic itself. In addition, polluted air masses from different source regions would mix with each other. Thus, one would expect to find a well-mixed and homogeneous aerosol at the end of the transport pathway. Barrie et al. (1981) suggested a "bathtub" model in which the arctic atmosphere is a horizontally mixed reservoir into which air from mid-latitudes is periodically injected. Due to the annual variation in scavenging processes in and around the Arctic, the flux of pollutants into the reservoir and their residence times while in it are lower in summer than in winter. Throughout the winter the

reservoir becomes progressively dirtier as demonstrated by a steadily increasing "background".

Referring back to Fig. 5, 6, 7 (Sections 2.5 and 2.6) we recall the following observations:

- 1) The arctic pollution aerosol does not seem to acquire a uniform chemical characteristic as indicated by the change of the XMn/XV ratio from winter to spring (Fig. 6).

- 2) XMn concentrations during December/January are sometimes almost comparable to those during March with periods of lower concentrations in between (Fig. 5).

- 3) Samples show large fluctuations in concentration and ratio characteristics within arctic air masses which cannot be explained by the local synoptic conditions at Barrow (Fig. 7).

Thus, it appears that individual injections of pollutants have retained their individual characteristics and the reservoir does not build up progressively. Therefore, we will investigate episodes of high pollution concentrations at Barrow in order to find the main transport pathways and the synoptic systems creating these. However, it is anticipated that we are investigating selected favorable conditions leading to high concentrations at Barrow which could include abnormally large accumulation of pollutants over the source area, extremely little scavenging along the pathways, short travel times, stationary and persistent pathways, etc..

The analysis employed the following procedure:

- 1) Identify a peak in the pollution concentration. Samples

selected are indicated in Fig. 5. Occasionally peaks were present in the XMn data but not in the XV data as already mentioned (Section 2.5).

2) Construct height/time cross sections of potential temperature and mixing ratio, respectively, at Barrow in order to find out during which days of the sampling period arctic air reached the station (Section 3.2.2).

3) Search for a possible source area which has been under anticyclonic influence (stagnation) for several days, possibly accumulating pollutants (Section 4.4.1).

4) Determine if the period of stagnation over the source area was followed by a surge of air northward due to an approaching cyclone (Section 4.4.1).

5) Identify a possible transport pathway from this source area to Barrow on surface, 850mb and 500 mb daily weather maps (Section 4.3).

6) Check if the approximate travel time along this transport pathway is consistent with the occurrence of the surge and the arrival of arctic air at Barrow (Section 4.4.2).

7) Check if the proposed transport pathway is supported by back-trajectories at Barrow and by 5 day mean 700 mb maps (Section 4.3.5).

8) See if there are any other possible source areas satisfying the above mentioned criteria 3) and 4). Repeat the procedure for these source regions.

Depending on the complexity of the actual situation, this procedure was sometimes repeated, sometimes with changed order, but the overall objective was to obtain a consistent set of information on the

conditions at the source region, the location of the pathway, the travel time and the conditions at Barrow. This method of investigation is comparable to an iteration process; bits of information are gathered, compared, re-evaluated and re-used to continue the iteration process. As in all iterations, at some point the process has to be terminated. The quality of the available data, the subjectivity of the analysis, and the available resources were the factors deciding the termination of this iteration for the present study.

Samples satisfying the above conditions will be referred to as "pollution episodes" in contrast to the common usage of pollution episodes which describes only high concentrations of pollution at the source region.

#### 4.3 Transport Pathway Types of Pollution Aerosol

##### 4.3.1 Introduction

As indicated in Fig. 5, a total of 61 peaks of XV and XMn concentration at Barrow were investigated. Fifty samples could be associated with a pollution episode as defined in Section 4.2. Seven peaks did not have their own episode but rather represented a continuation of the previous sample and its pollution episode. These samples were B16, B59, B64, B70, Dav2, B152, E14. One sample (E11) with high XV and XMn concentration can be explained by the transport of

volcanic material following the eruption of Klyuchevskaya on the Kamchatka Peninsula (Noelle Lewis, personal communication). Three samples (B57, B136, B138) could not be associated with a pollution episode. The number of documented pollution episodes is fairly evenly distributed over the 4 winter seasons analyzed. During 1976/77 11 episodes were documented, 13 episodes in 1977/78, 12 episodes in 1978/79, and 14 episodes in 1979/80.

Although one could imagine a large number of possible transport pathways from source regions to Barrow, we were able to distinguish 9 major types in which to classify the transport pathways. The classification scheme is based on the three major source areas identified. Type I includes North American sources, type II includes West and East European sources, type III includes Soviet and East European sources. Subcategories a, b, etc. were based on the major synoptic pressure systems creating the path and the path's geographical location within the Arctic Basin. Obviously some of the individual transport pathways fit better into this classification than others, because of the varying synoptic conditions and varying degree of development of the transport pathway. In Table A4, column 4 (Appendix), the fit of the individual transport pathways into the general classification is estimated. 43% of all individual transport pathways obtained a rating of "good" with respect to their type, 37% obtained a rating of "moderate" and only 20% of all individual cases have to be considered as "poor" matches of the transport pathway types. Table A4 (Appendix) will be discussed further in Section 4.3.5.

#### 4.3.2 Transport Pathway Types from North American Source Regions

Identifying transport pathways from North American sources to Barrow was difficult because only small peaks seem to be associated with a pollution episode relating to North American sources (B58, B63, B64). Thus, the initial approach of investigating major peaks discriminated against North American sources. An alternative approach was to use very low  $X_{Mn}/X_V$  ratios to identify aerosols from North American sources (Section 2.4). All samples with  $X_{Mn}/X_V$  ratio less than 0.7 are listed in Table 7, except for Dav10 which could be associated with an American source although the ratio was 1.0. Note that, in general, concentrations of  $X_{Mn}$  and  $X_V$  are low, thus it is possible that analytical uncertainties in the determination of  $X_{Mn}$  and  $X_V$  become important and create unrealistic ratios. Unfortunately, low  $X_{Mn}/X_V$  ratios are also characteristic of West European sources and a clear distinction based on the ratio between North American and West European sources is not yet possible. We investigated the synoptic conditions and possible transport pathways for each of the samples listed in Table 7 in order to find the source area. To make things even worse it turned out that often two pathways were present at the same time, one relating to an European source, the other one relating to a North American source. Consequently, only those samples were selected where the synoptic situation suggested that the influence of an European source was unlikely or impossible, whereas a transport path from North American sources seemed possible. Only five samples remained, and the proposed

Table 7: Samples with XMn/XV ratio less than 0.7

Sample	Sampling period	XMn/XV	concentration (ng/m <sup>3</sup> ) XMn XV	European source	American source
B58	Dec 31-Jan 8, '78	0.32	0.103 0.315	unlikely	possible
B59	Jan 10-15	0.03	0.005 0.145	unlikely	possible
B64	Feb 10-14	0.62	0.595 0.965	unlikely	possible
B68	Mar 1-5	0.59	0.866 1.476	likely	possible
B131	Dec 11-14	0.18	0.012 0.066	no distinct pattern	no distinct pattern
B133	Dec 19-22	0.51	0.138 0.273	no distinct pattern	no distinct pattern
Dav8	Apr 3-6, '79	0.56	0.218 0.389	unlikely	possible
Dav10	Apr 11-14	1.02	0.525 0.515	unlikely	possible
B205	Nov 23-25	0.16	0.030 0.195	unlikely	possible
B230	Mar 10-13, '80	0.63	1.273 2.024	likely	possible
B232	Mar 18-21	0.49	0.561 1.152	likely	possible

North American transport pathways are to be accepted with extreme reservation. The possibility exists that we are trying to attach a transport pathway to a "background" pollution aerosol.

Transport pathway type Ia (Fig. 28):

A continental anticyclone dominates the surface circulation of North America. It can extend from the Beaufort Sea area to Texas as one huge system with individual cells possible over the Beaufort Sea, Hudson Bay, and the subtropical cell. Polar air flows southward along eastern Canada and eastern USA, is gradually modified and picks up pollutants from the Great Lakes area and the east coast states. The air moves northward east of the Rocky Mountains which act as a barrier to intrusions of Pacific air. The extension of the Rocky Mountains into Alaska is represented by the Brooks Range which acts as a similar barrier. At 500 mb the Hudson Bay anticyclone is also developed, splitting the westerlies into two branches. This pattern is known as a blocking situation and can be very persistent and stationary.

Transport pathway type Ib (Fig. 29):

The North American continent is under weak anticyclonic influence. The path, in contrast to Ia, is not stationary but develops due to a northward moving cyclone and anticyclone. The beginning of the episode is characterized by a cyclone over the east coast south of New

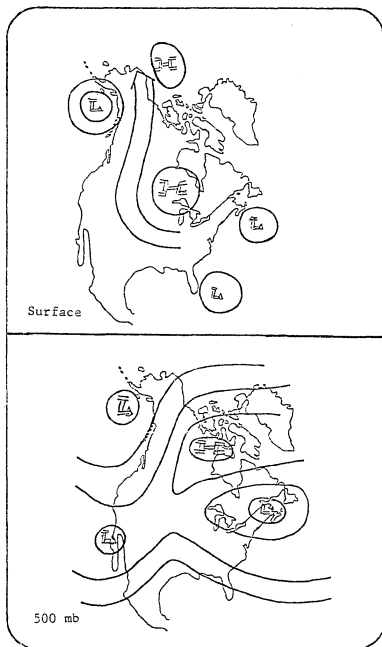


Fig. 28: Transport pathway type Ia

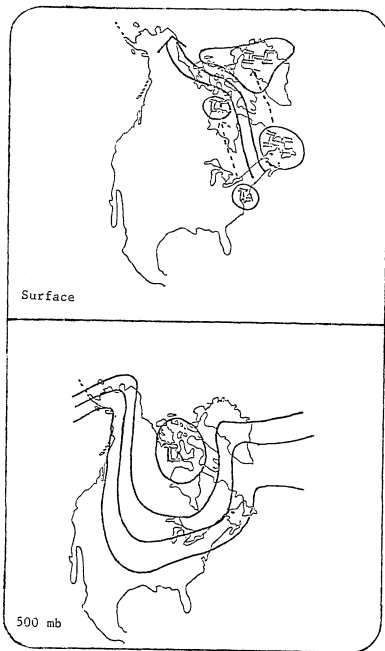


Fig. 29: Transport pathway type Ib

York City and an anticyclone over Newfoundland. Both systems move northward, the anticyclone spreads out over Greenland and the north Canadian coast and the cyclone moves into Keewatin. At 500 mb the Baffin Island cyclone north of Hudson Bay is developed as well as a ridge over the Davis Strait. This creates a northward (meridional) flow along the North American east coast which apparently steered the surface pressure systems, and the Baffin Island cyclone steers the flow along the Canadian Archipelago towards the Beaufort Sea.

Although our data are not convincing, they seem to suggest that a marine path along the North Atlantic via Davis Strait or Denmark Strait as suggested by Rahn and McCaffrey (1980) and Reiter (1981) is not a transport path into the Arctic and Barrow. The data rather suggest that one should look for a continental pathway, during situations when the prevailing westerlies are interrupted by a blocking situation and a retrograde motion at the surface. We will discuss this result again in Chapter VI.

#### 4.3.3 Transport Pathway Types from European Source Regions

In contrast to Section 4.3.2, it was generally easier to associate samples with pollution episodes (as defined in Section 4.2) leading to European pollution sources. The transport pathways were better developed and a good set of maps describing the European source regions was available.

Transport pathway type IIa (Fig. 30):

Preceding the establishment of the path is a blocking anticyclone over western Europe. The surge of polluted air northward (as defined in Section 4.4.1) starts when the blocking anticyclone moves eastward due to a strong Icelandic cyclone approaching the European continent. This configuration creates a straight northward flow from central Europe, and the air enters the Arctic between Greenland and Svalbard. A broad arctic anticyclone then establishes the path to Barrow along the west of the Canadian Archipelago. At 500 mb the surface circulation is supported by an Icelandic cyclone, by a split of the westerlies with strong meridionality from Great Britain to Svalbard due to the dynamic anticyclone cell over Scandinavia (characteristic of blocking), by a Baffin Island cyclone, which is usually weak or absent at the surface, and an anticyclonic ridge supporting the arctic anticyclone. Variations of this path can include: a) a displacement of the surge slightly further to the east, but the flow should not bend further east than the Kola Peninsula, otherwise it would be classified as IIb; b) a displacement of the surge further to the west.

Possible source regions included in this transport path are central Europe and possibly eastern Europe. No significant amount of pollutants should be picked up along this path after it has left Europe.

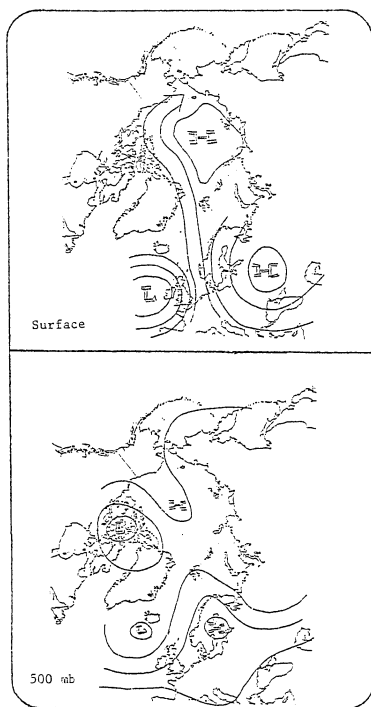


Fig. 30: Transport pathway type IIa

Transport path type Iib (Fig. 31):

The surge of polluted air northward is characterized by a so-called "return flow pattern" (Rahn et al., 1980b). The return flow is composed of a system of cyclones located over Ireland and off the northern Scandinavian coast. Sometimes a cyclone can also be located west of Novaya Zemlya. This system of cyclones is stationary, because the extension of the Asiatic anticyclone over southeastern Europe blocks further penetration of cyclones eastward. Due to this configuration a strong flow across Europe results. The direction is northeastward and the flow bends into the Arctic between the Kola Peninsula and Novaya Zemlya. Rahn (1979) has termed this path also a short path. The air mass is then taken along the backside of the cyclonic system and can travel northwestward reaching Svalbard (Rahn et al., 1980b) or even Iceland (Borys and Rahn, 1981). A path to Barrow is established again by the arctic anticyclone which continues the flow along the coast of the Canadian Archipelago. The surface flow is supported at 500 mb by a cyclone west of Great Britain and a cyclone close to Svalbard; the blocking action due to the westward extension of the Asiatic anticyclone is evident by the splitting of the westerlies and by a ridge over Novaya Zemlya supporting the injection into the Arctic. The flow across the Arctic is supported at 500 mb by the Baffin Island cyclone and the arctic anticyclone. Thus, transport pathway type Iib is well established throughout the troposphere.

Variations of this path are determined by the position of the

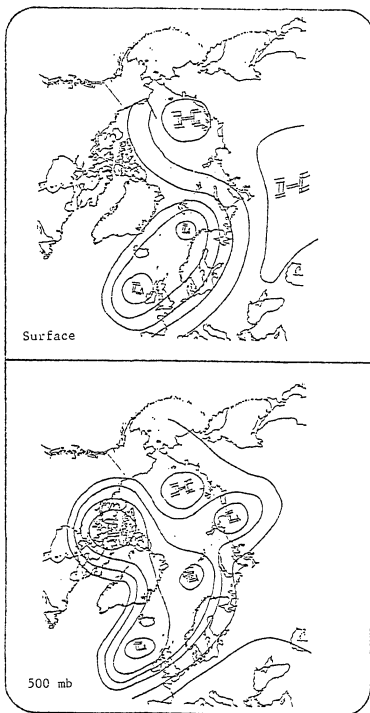


Fig. 31: Transport pathway type 11b

return flow pattern, i.e. the position of the cyclonic system. If it is located to the west, injections enter the Arctic via the Kola Peninsula and major contributions of West European aerosols are likely; if it is located to the east, injections enter the Arctic via Novaya Zemlya and contributions of West and East European sources are then likely. If the return flow pattern is located farther to the east, i.e., air entering the Arctic over the Taymyr Peninsula, then this path will be classified as IIIb. Due to the configuration, it is imaginable that this transport pathway probably will pass over a variety of source regions in West and East Europe and in the European USSR.

Transport pathway type IIc (Fig. 32):

The return flow pattern has extended its influence and is created by three cyclonic cells over Great Britain, Svalbard and the Taymyr Peninsula, respectively. A blocking anticyclone is located over eastern Europe creating a northward (meridional) flow over Europe towards Scandinavia and then eastward along the arctic coast of the USSR, thus keeping it away from East European/western Soviet sources. The arctic anticyclone has combined with the Asiatic anticyclone and is located over east Siberia. Thus the final flow from Europe is along the Soviet Arctic, practically zonal in direction. At 500 mb the blocking over eastern Europe is reflected in the splitting of the westerlies and a small ridge over Scandinavia. The return flow pattern is supported by cyclones over Great Britain, Novaya Zemlya and the Taymyr Peninsula,

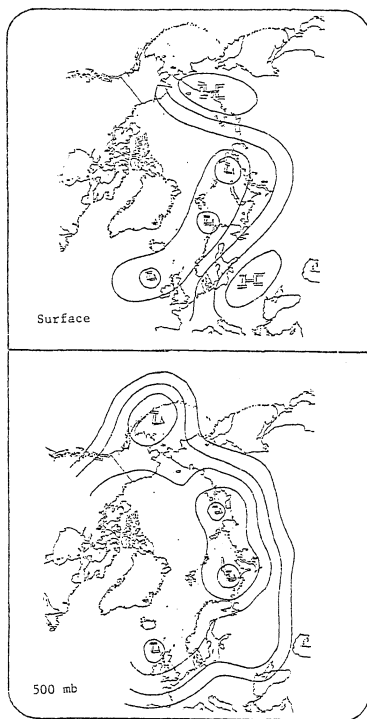


Fig. 32: Transport pathway type IIc

respectively. The arctic anticyclone, in general, is weak and at best reflected as a ridge over the Chukchi Sea. Thus, the transport pathway IIC is well established throughout the troposphere.

Type IIC differs from type IIB in that a) the return flow is not strong enough to bring the aerosol westward on its backside, b) the arctic anticyclone is displaced farther to the south towards the East Siberian continent and therefore the path is along the Soviet Arctic instead of along the American Arctic, c) IIC is basically a zonal flow except for the surge northward whereas IIB is a meridional flow.

Major source regions for this transport pathway type are West and East Europe. Along its path this type should pick up little pollution from other sources, except for sources on the Kola Peninsula.

#### 4.3.4 Transport Pathway Types from Soviet Source Regions

Transport pathway type IIIa (Fig. 33):

A broad anticyclone covers most of the Asiatic continent; its influence is restricted to the continent and its extension towards the Chukchi Peninsula is weak or not present. The arctic anticyclone is not developed. A system of cyclones with varying influence is present along the northern parts of Europe and the USSR. The surge of polluted air can be accomplished in two ways: a) an extended return flow pattern is present over Scandinavia and creates a northward flow over East Europe,

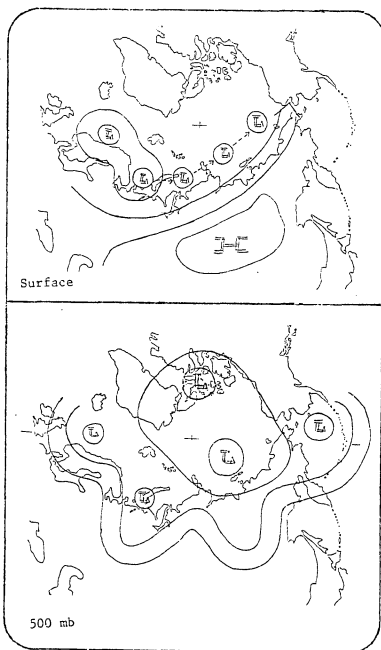


Fig. 33: Transport pathway type IIIa

b) a cyclone over Novaya Zemlya is strongly established creating a flow from west Soviet and Volga-Urals sources northeastward. The flow to Barrow along the Soviet arctic coast is accomplished by old cyclones moving eastward as far as the New Siberian Islands.

At 500 mb the pathway is supported by a polar vortex resulting in a cyclonic pattern. Characteristic are the ridge over Fennoscandia and over the Taymyr Peninsula, respectively, and a trough over the Urals. This trough is especially well developed when the surge of polluted air is caused by the cyclone over Novaya Zemlya. Sometimes the trough can create an organized northeastward flow from Turkey up to the Taymyr Peninsula. The central arctic region is determined by a circumpolar vortex. Thus, the final path from the Taymyr Peninsula to Barrow is zonal and in an eastward direction.

Important source areas for this transport pathway type are probably the western USSR, the Volga-Urals region and West Siberia.

Transport pathway type IIIb (Fig. 34):

This type is identical to pathway type I Ib except that its surge of polluted air occurs farther to the east including Soviet instead of European sources. Its position farther to the east also implies a more aged return flow pattern due to the occluding cyclonic pressure systems. Blocking occurs east of the Urals and is well supported at 500 mb by an anticyclone and by splitting of the westerlies. The injection is northward over eastern Europe/western USSR and the path bends along

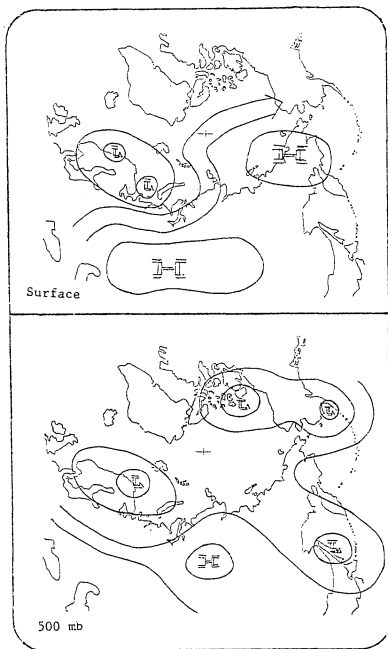


Fig. 34: Transport pathway type IIIb

the Soviet arctic coast up the Taymyr Peninsula where it enters the Arctic. The arctic surface anticyclone over the Soviet Pacific Arctic is supported by a ridge at 500 mb. It seems that the arctic anticyclone is usually weaker than in the cases of a transport pathway type IIb, resulting in the fact that the flow across the Arctic remains more within the central arctic region instead of penetrating farther into the American Arctic.

Transport pathway type IIIc (Fig. 35):

The surge of polluted air is caused by a blocking anticyclone east of the Urals and a system of cyclones over East Europe and Scandinavia. The blocking is indicated at 500 mb as an anticyclone or as a ridge over the Urals. The cyclonic system can be represented by an old extended return flow pattern. Thus, the injection northward west of the Urals is well supported. In addition, an anticyclone over the Taymyr Peninsula is well developed at the surface as well as at 500 mb. Its influence can reach over the Arctic. Another anticyclone representing an extension of the Asiatic anticyclone is located over the Magadan Region at the surface as well as at 500 mb. The anticyclones over the Taymyr Peninsula and over the Magadan Region, respectively, may combine into one system exerting an anticyclonic influence over the entire Soviet Arctic. The flow enters the Arctic over Novaya Zemlya and crosses the central Polar Basin along the western sides of the anticyclones.

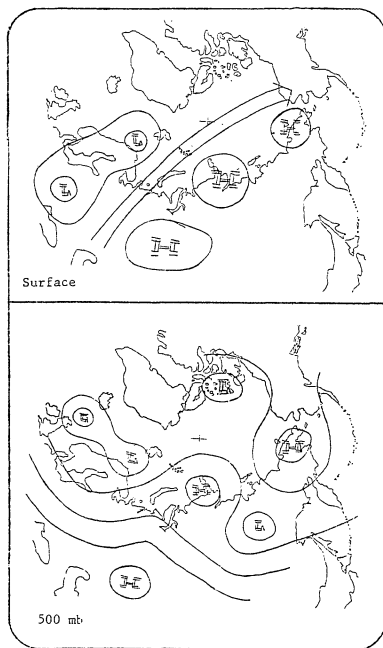


Fig. 35: Transport pathway type IIIc

Transport pathway type IIIId (Fig. 36):

The Asian continent east of the Urals is dominated by the Asiatic anticyclone and an extension over the Magadan Region. The Asiatic anticyclone east of the Urals is reflected at 500 mb as a large ridge extending up to the Arctic in the region between the Taymyr Peninsula and the New Siberian Islands. It is usually stronger than the one over the Magadan Region which is reflected at 500 mb only as a small ridge. The path is completely determined by this anticyclonic system and sometimes can be seen at 500 mb as well. Its position is usually close to the Soviet arctic coast. The surge of polluted air is accomplished by a cyclone over the southern tip of Novaya Zemlya. It is supported at 500 mb by a trough located over the Urals. This transport pathway type is located over the Soviet Union farthest to the east compared to IIIa, b, c including source areas east of the Urals only.

#### 4.3.5 Quasi-persistent Modes of the Atmospheric Circulation in the Arctic and Mid-Latitudes

As mentioned earlier (Section 4.3.1) 50 episodes of pollution transport were investigated. Ten percent of these episodes were related to North American sources (type I), 42% to European sources (type II) and 48% to Soviet sources (type III). A total of 9 different transport pathway types was found. Their synoptic characteristics (4.3.2-4.3.4)

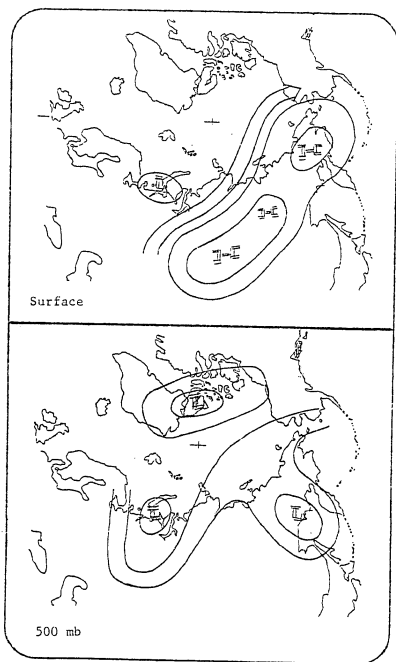


Fig. 36: Transport pathway type IIIId

suggest that these transport pathway types represent quasi-stationary circulation configurations in the Arctic and in the mid-latitudes. As indicated in Table A4 (Appendix) most of these transport pathways were supported at the 500 mb level indicating well developed circulation features throughout the troposphere. Fifty-six percent of all transport pathways are even indicated on the 5 day mean 700 mb maps (published in the "Monthly Weather Review" journal). In some cases (18%) the transport pathways were not reflected due to the averaging process (Table A4, column 6, Appendix). Back-trajectories calculated for the lower troposphere, centered at 850 mb (Miller, 1981), supported our identified transport pathways in 58% of all episodes (Table A4, column 7, Appendix). Trajectories, however, are less supportive because during certain synoptic conditions, as discussed in Section 3.2.2, they fail to identify the polluted air mass. All types of transport pathways are characterized by a strong meridional flow (northward) over the source region and, depending on the location of the source region and season, by a meridional or zonal flow across the Arctic. Meridionality is necessary to accomplish an exchange of air masses between mid-latitudes and the polar region.

Namias (1958) noted that in arctic circulation patterns there is a tendency of a particular type to persist in broad scale from day to day, and to persistently recur in the same season after only brief interruptions. It was his impression that there is not one general circulation over the Arctic but rather several modes, each of which possesses remarkable stability. Wilson (1967) pointed out that the

variability of the arctic circulation can be explained by (1) the persistence of large-scale patterns, (2) the importance of dynamic barriers (blocking anticyclones) in the modification of the tracks and frequency of surface cyclones and anticyclones, and (3) the effect of the degree of expansion or contraction of the polar vortex and the subsequent abnormal displacement of the upper westerlies. A study of the day-to-day persistency of the large-scale sea-level pressure patterns over the Arctic for the year 1955 (Wilson, 1958) gave the following results:

1) Well-defined periods of quasi-persistent large-scale patterns existed, averaging 6 days and twice extending over 11 days.

2) A total of 28 of these persistent periods were determined, 12 of them indicate pathways from Europe and the Soviet Union to Barrow; 8 out of these 12 occurred during the period October-April.

3) The periods of persistence were most marked from December to May and were separated by brief interludes of abrupt change, when the circulation seemed to "flip" from one pattern of stability to another.

4) From June to November the general level of persistence was lower and the changes less clear-cut than with the intense patterns of winter.

5) Frequently, smaller-scale traveling disturbances were very active during these large-scale stable situations.

6) An approximate 14-15 day period in persistence can be seen in the January to May season, but no regularities seem evident during the summer season.

7) The main causes of change of a persistent large-scale pattern are identified as a) a general breakdown of the circulation both at 500 mb and the surface, b) a regional change with slackening or strengthening of the zonal flow at 500 mb, especially over north Asia, and c) a rapid reorientation of the large-scale systems through eastward progression or westward retrogression.

In mid-latitudes, persistent quasi-stationary circulation types over Europe were recognized by Baur around 1944 who introduced the concept of Grosswetterlagen. Hess and Brezowsky (1969) extended Baur's catalogue of Grosswetterlagen. The Grosswetterlage (large scale weather pattern) is a circulation type over a region, i.e. Europe, determined by the position of steering centers (upper anticyclones and cyclones, upper troughs), by the position of frontal zones, and distinct surface pressure patterns. The Grosswetterlage is also determined by similar weather conditions during the course of a few days (~3 days). Thus, the concept of Grosswetterlage constitutes a description of the average state of the circulation over space and time, or a circulation mode.

The following Grosswetterlagen as listed in Hess and Brezowsky's (1969) catalogue can provide the first part of the transport pathways type II from Europe to Barrow:

IIa: SEA, HFA, HNA, HNFA

IIb: SWE, SA, HM

IIc: SEZ, SA, HFA

Transport of European aerosol to Iceland has been documented by Borys and Rahn (1981) which occurred due to the Grosswetterlage SEA, and

by Rahn (1981d) due to NEA according to our analysis. Unfortunately, there are no corresponding catalogues of Grosswetterlagen for North America and the Soviet Union available.

Dmitriev (1968) noticed that the presence of the extension of the Asiatic anticyclone over the Magadan Region (including the Chukchi Peninsula) exerts a large influence on the weather and climatic regime in that region. This is because the extension has considerable stability, only slightly less than the Asiatic anticyclone itself. This synoptic situation is mainly responsible for the formation of the transport pathway IIId.

The strong horizontal temperature gradient between the subtropics and the subpolar region creates the prevalence of westerly winds in the troposphere over the mid-latitudes. This "normal" (zonal) situation is also known as a "high index" circulation pattern. At 500 mb the jet stream runs between a low pressure system in the north and a high pressure system in the south, practically parallel with the latitude circle. On the other hand, an "abnormal" (meridional) situation is known as a "low index" circulation pattern. The normal westerly jet stream is stopped or blocked by a dynamic anticyclonic pressure system, called a blocking high. Treidl et al. (1981) used the following criteria to define a blocking high: 1) Closed isopleths must be present simultaneously in the surface and 500 mb charts, splitting the westerly current aloft into two branches. 2) The latitude belt where the high occurs extends northward from  $30^{\circ}\text{N}$ . 3) The minimum duration of the high is of the order of a few days.

For this study these criteria were relaxed and an anticyclone was called a blocking high if the surface high was supported by a ridge at 500 mb giving the westerlies a strong meridional component. This characteristic of blocking is the most important for exchanging mid-latitude and polar air masses. The other criteria are of minor importance. Treidl et al. (1981) found a median block duration of 8 days with preferred areas of blocking around  $10^{\circ}\text{W}$ ,  $30\text{--}40^{\circ}\text{E}$  and  $120\text{--}160^{\circ}\text{W}$ . The area of blocking at  $10^{\circ}\text{W}$  and  $120\text{--}160^{\circ}\text{W}$ , respectively, are unimportant for injecting pollutants into the Arctic because they are not close to a source region. The area of frequent blocking at  $30\text{--}40^{\circ}\text{E}$ , however, is important in creating a meridional flow of European and western Soviet pollutants into the Arctic. Thus, blocking highs can put the mid-latitude circulation into a mode of strong meridional exchange with the polar region, allowing for the surge of pollutants into the Arctic.

An investigation of tracks of cyclones and anticyclones is of little interest to us, because most of the transport pathways are due to quasi-stationary synoptic systems. However, IIIa can be recognized in the cyclone track along the Soviet arctic coast as described by Klein (1957).

If high concentrations of XMn and XV at Barrow can be related to quasi-stationary synoptic systems creating a pathway, then it should be possible to explain the seasonal variation of concentrations due to the seasonal variation in the position and intensity of the quasi-stationary synoptic systems. This will be done in Section 4.4.4 and Chapter VI.

#### 4.4 Characteristics of Transport Pathway Types

##### 4.4.1 Synoptic Conditions Over the Mid-Latitude Source Areas

As mentioned in Section 1.4 we do not have any chemical data to describe the accumulation of pollutants over the source region and to define the beginning of a pollution episode. Therefore, one has to speculate on the beginning of such an episode based on meteorological/synoptic evidence.

According to Boettger (1961) air pollution potential may be defined from the meteorological standpoint as a set of weather conditions conducive to the accumulation of air pollutants in the atmosphere. One of the meteorological elements involved is stagnation defined by light surface and upper winds, subsidence below 600 mb and persistency for at least 30 hours. The combination of these criteria is most likely to persist in an area near the center of a stagnating warm anticyclone. Elsom and Chandler (1978) investigated the control of meteorological factors upon ground level concentrations of smoke and sulphur dioxide. Of numerous parameters investigated, wind speed, degree-day temperature and mixing height were shown to be most important. One of our criteria for defining a pollution episode was therefore to find a source region which had experienced stagnation conditions in order to accumulate pollutants (Section 4.2). As seen from Table A5 (Appendix) this condition was satisfied by almost all pollution episodes identified.

Reports of haze and smoke were usually present on the daily surface weather maps.

Stagnating anticyclones, however, do not allow for a rapid transport of pollutants due to the weak pressure gradients necessarily present. A surge of pollutants northward is generally accomplished when a moving cyclone approaches the stationary anticyclone, or, in some cases, when the anticyclone builds up and approaches an occluded, quasi-stationary cyclone. Pressure gradients steepen and a narrow zone of strong winds northward is created, "flushing" the source region and transporting pollutants rapidly. It is important, however, that the transport takes place along the western side of the anticyclone where precipitation is absent. Once pollutants become part of the cyclone they inevitably become scavenged out (Twomey, 1977, p. 162), leading to the phenomenon known as acid rain.

An example of the development and the associated weather phenomena of a surge is given in Fig. 37 for the European region. The anticyclone is located over the western USSR with predominantly clear skies and sub-freezing surface temperatures. Along the western periphery of the anticyclone there is a zone of ground fog occurrence and farther to the west there is a small zone with stations reporting haze. Rain bands are associated with the various fronts of the Icelandic cyclone. This example also shows a zone of stronger pressure gradients along the southern periphery of the anticyclone. Thus, such a situation would also allow for the possibility that pollutants from the southern quadrant of the anticyclone could be transported efficiently to the west

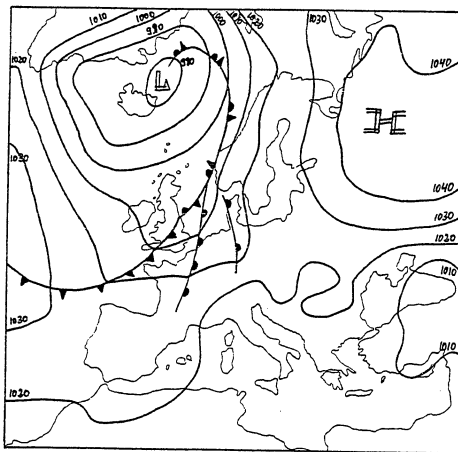


Fig. 37: Synoptic conditions over Europe during a surge.

and then to the north.

Due to the presence of blocking anticyclones, however, it seems to happen quite frequently that the approaching cyclone slows down, occludes and finally becomes stationary or even dies. In this case, the wet regions of the cyclone do not catch up with the traveling pollutants, allowing them to "escape" into the Arctic. For almost all pollution episodes identified surges were present over the source regions (Table A5, Appendix). Based on these data we estimate a surge's mean duration of 3.9 days with a standard deviation of 2.6 days. A similar estimate has been derived previously based on the occurrence of surges during the 1979/80 season only (Section 3.2.3.). Brezowsky et al. (1951) noted that Grosswetterlagen with blocking action have an average duration of 4.1 days.

In Table A5 (Appendix) the  $X_{Mn}/X_V$  ratio for each transport pathway is listed as well as the proposed source region. It appears that each transport pathway type is characterized by a distinct  $X_{Mn}/X_V$  ratio which in turn is due to the source region (Table 8). The transport pathway types IIb, IIc, and IIIc have the smallest standard deviations. The mean  $X_{Mn}/X_V$  of IIa is not based on enough data to be representative. As anticipated, European sources are characterized by relatively low  $X_{Mn}/X_V$  ratios whereas Soviet sources are characterized by relatively large ratios with IIIId having the highest value. Interestingly, IIb is the transport pathway type having one of the smallest standard deviations even though it has the largest number of occurrences and its position over the European continent passes over a variety of source areas.

Table 8: Mean XMn/KV ratio for each transport pathway type

Transport pathway type	Mean	Standard deviation	Number of cases
IIa	1.9	1.5	2
IIb	0.8	0.1	10
IIc	1.1	0.4	9
IIIa	3.8	4.7	8
IIIb	3.3	5.1	8
IIIc	1.2	0.1	4
IIId	9.2	8.6	4

Among the Soviet transport pathway types, IIIc has the lowest ratio indicating that it includes western Soviet sources or sources close to European sources. In contrast, transport pathway type IIIId is characterized by the highest  $X_{Mn}/X_V$  ratios which are mainly caused by source regions east of the Urals. Obviously some transport pathways and their ratios deviate significantly from their mean.

Assuming that there are characteristic  $X_{Mn}/X_V$  ratios for each individual source region (an assumption which has yet to be proven by chemical data) the discrepancy is mainly due to the subjective analysis of the possible source regions. Refinements would undoubtedly be possible with a more detailed analysis based on better and more detailed weather maps of the mid-latitudes. Since chemical data about the source regions are not yet available, this analysis supports the notion that different source regions can indeed be distinguished by their different  $X_{Mn}/X_V$  ratios as proposed by Rahn (1981c).

Over the European continent where different source areas are located close to each other our meteorological analysis has not been able to distinguish between source areas on a regional scale. But it seems that it can be done, for the different ratios obtained indicate that during a pollution episode aerosols from one source area can be picked up whereas aerosol from another source area at about the same latitude but further to the east or west cannot be picked up. There are several reasons for this observation. We have argued that blocking anticyclones are favorable for the accumulation of pollutants, but it is also noted that blocking anticyclones hinder the eastward progression of

cyclones, thus the anticyclone prevents aerosols from source areas farther to the east from being incorporated into the northward surge. In addition, Wallen (1970) pointed out that during "low index" circulation and the consequent blocking of the westerlies the upper air jet stream meanders around the high pressure ridges and the low pressure troughs, indicating that at the surface the polar front runs in a similar fashion. Consequently, the cyclonic activity takes place along south-north tracks or north-south tracks rather than along the more common west-east tracks. At the surface this meridional circulation is reflected in weather conditions which change rapidly from west to east. The weather of a particular band stretching north-south will, then, depend completely upon where the band is situated in relation to the upper air ridge and trough. Thus, source areas along the same latitude but separated by some distance can experience quite different weather conditions allowing for the accumulation of pollutants or their suppression.

Ludlam (1980, p. 333) showed that isobaric charts for a blocking situation give the misleading impression that over most of its length the air flows across the axis of the trough from west to east. In contrast, the isentropic analysis shows that on the eastern flank of the trough there is a confluence of two distinct airstreams. One of these enters the southeastern quadrant of the trough and ascends as it flows northward and accelerates, and the other enters the northwestern quadrant and generally descends as it flows southward. The confluence line lies in the frontal zone, marked by a crowding of isobars which

indicates the steepening of the isentropic surface and by marked horizontal temperature contrast. This supports the suggestion made previously that pollution aerosol stays along the western side of the anticyclone separated from the cyclone by the position of the polar front.

We also observe that European pathways (i.e. IIb) passing over Soviet sources do not seem to acquire a Soviet signature, maybe because accumulation time over the Soviet sources was too brief, so that a negligible amount of Soviet pollution aerosols was added to the traveling European aerosol.

It has been observed that hazy air masses due to the accumulation of anthropogenic ozone were usually present at the western side of stagnating or slow-moving anticyclones (Samson and Ragland, 1977; Lyons and Husar, 1976; Lyons et al., 1978; Hall et al., 1973). Vukovich et al. (1977) made similar observations and developed a model concerning residence times of air parcels within an anticyclonic system. The validity of the model was tested as well (King and Vukovich, 1982). Based on their observations, Vukovich et al. (1977) argued that over the eastern United States emission sources were injecting precursors of ozone equally into all quadrants of the anticyclone, thus, the observed ozone maximum in the west should be due to the different residence times of air parcels in the anticyclonic system. Vukovich's et al. (1977) model incorporates two equations, one describing the pressure distribution of the anticyclone, the other representing the equation of motion of an air parcel. This system of equations was used to calculate

trajectories and to determine residence times. Two important results were obtained:

1) Air parcels entering the anticyclone in the northeast will spend the longest time in the system. The slower the speed of the anticyclone the greater the number of days. Thus, stagnating anticyclones are associated with longest life expectancies for air parcels.

2) The number of days air parcels have already spent in the anticyclonic system is maximal in the western portion of the anticyclone. For small system speeds the maximum is found in the SW quadrant, for larger speeds it is found in the NW quadrant.

Although the model is based purely on mathematical prediction, there are also several meteorological observations supporting the calculations. Bohr et al. (1974) described the weather conditions associated with warm anticyclones. Due to the near surface outflowing air this loss is compensated by air from upper levels, thus a descending motion develops leading to the dissipation of clouds. Within the anticyclone air motions are usually weak and, therefore, air masses within the anticyclonic region remain there for a long time, age, become modified and in general also become drier. In summer, the air mass warms up due to the predominant insolation, in winter, the air mass cools due to radiative losses. Cloud cover (Cu, Sc) is significant in the NE and E sector of the anticyclone, less in the SE and very limited in the S and SW sectors. Tropical maritime air is able to penetrate into the western flank of the anticyclone which leads to fog formation

in the early morning due to the advected humidity. Fog formation is supported by subsidence inversions which are present at low levels, prohibiting significant turbulence within the surface layer. During the summer the amount of solar radiation is sufficient to destroy the ground fog fairly rapidly; during winter, however, this fog can persist for several days. These conditions lead to the well-known smog episodes (Schulz, 1963; McCormick, 1970). Samson and Ragland (1977) concluded that large-scale pollution episodes are produced on the western half of a slow-moving anticyclone because a) the preceding stagnant conditions in the area of small pressure gradients have made possible the accumulation of pollutants in a relatively small volume of air, b) a well-mixed but capped boundary layer is present which serves to trap pollutants in a definite layer during the day and c) transport is aided by near geostrophic winds close to the surface inversion at night. In our analysis we almost always found reports of haze and fog occurring at the same time over Europe. Thus, without chemical data, one could use the presence of fog under anticyclonic conditions as an indicator for the presence of pollution. Dallavalle et al. (1975) found that in the lower troposphere subsidence generally has its maximum on the eastern side of the surface anticyclone in a region of pronounced cold advection. Subsidence over the high center is weak. Holzworth (1972) found that during the peak of the pollution episode the subsidence inversion had combined with the radiation surface inversion creating a high degree of stability throughout a layer more than 600 m thick.

#### 4.4.2 Synoptic Conditions Along the Transport Pathway and Associated Travel Times

In the discussion about possible source areas Carlson (1981) hypothesized that arctic aerosols originate north of the polar front where the meridional potential temperature gradient between source region and the Arctic is relatively weak. When warm air travels northward it will rise, condensate, and pollutants will be scavenged out. We speculate that only pollutants within warm but very dry air would have a chance to survive but would end up at high altitudes and not near the surface as in the case of the arctic pollution aerosol, e.g. Asian desert dust transport (see Chapter V). For the formulation of his hypothesis Carlson (1981) used monthly mean vertical isentropic cross sections which certainly do not reflect the daily individual synoptic conditions. He also chose an arbitrary cross section which did not follow a transport pathway. We have constructed a few isentropic cross sections along an identified transport path and tried to follow the conditions as the air mass moved. The results were inconclusive because a) the position of the polluted air mass could not be accurately determined without any chemical "checkpoint" along the path and b) most portions of a path were located over the Arctic Ocean where there are no synoptic data available and even the data from the Asian continent were scarce.

The analysis, however, pointed out the fact that the air over the Asian continent during winter is usually colder than the air over the

Arctic because heat conduction through the ice is a significant source of heat (Wexler, 1936). Thus, aerosol from Soviet sources will be emitted into an airmass which is as cold as the arctic air itself. No dramatic ascent with condensation has to take place. Over Europe those conditions are not given in such extremity, but blocking situations occurring in association with the accumulation of pollutants are known to bring the coldest temperatures in this region (Wallen, 1970; Schueepp and Schirmer, 1970). Cold continental air masses are usually also dry, thus, ascending motion will be accompanied by little cloud formation. Conditions in the Arctic are reported to be relatively clear during winter (Huschke, 1969; Vowinckel, 1962). Overall, one could imagine that pollutants, especially from European sources, will have a tendency to rise but without too much scavenging involved and will descend again to lower levels when under the influence of the arctic anticyclone.

We have estimated the travel times of pollution aerosols based on two independent analyses discussed earlier. In Section 3.2.2, Table A1 (Appendix), it was determined when polluted arctic air was present at Barrow for each pollution episode. In Section 4.4.1, Table A5 (Appendix), the occurrence and duration of the initial surge of pollutants was determined. Both columns of data are presented again in Table A6 (Appendix). One can then infer the minimum and maximum travel times, respectively. In some cases travel times of 5 days or less were suggested which were rejected because 5 day back-trajectories (Miller, 1981) indicated that these trajectories never leave the Arctic but just barely reach the northern peripheries of the European and Asian

continents. In Table 9 mean travel times for each transport pathway type are presented. IIa has the shortest travel time of 6.4 days, which is expected because this transport pathway creates a direct connection between Europe and Barrow. IIIId is also associated with a relatively short travel time due to the proximity of east Soviet sources to Barrow. IIb and IIIb have similar travel times, which agrees very well with the definition of the transport pathway types, because they represent the same atmospheric circulation mode except for a slight shift of the position of the surge to the east over the source region. IIIa represents the transport pathway type with the longest travel time and connects west Soviet sources (farthest away from Barrow) with Barrow by a zonal flow, accomplished by transient cyclones along the Soviet arctic coast.

In general, travel times of aerosols from Soviet sources are longer by about one day than travel times from European sources. It should be noted that travel time (speed) is also a function of the season, most rapid speeds are expected during spring when the atmospheric circulation is most intense (e.g. Namias, 1958; Wilson, 1967). As will be discussed in Section 4.4.4, transport pathway types III occur predominantly during winter, pathway types II occur during spring in agreement with an increased travel speed.

Thus, the proposed travel times average less than 10 days which should be associated with high wind speeds along the path. This is in accordance with the observation made that polluted air masses arriving at Barrow are characterized by wind speeds larger than the monthly

Table 9: Mean travel times for different transport pathway types

Type	Travel times (days)		
	Mean	Standard deviation	Number of cases
Ia	13.1	0.97	2
Ib		no data	
IIa	6.4	0.89	2
IIb	7.09	0.56	8
IIc	7.33	0.39	9
II	7.16	0.30	19
IIIa	9.65	0.48	6
IIIb	7.09	0.59	7
IIIc	7.85	0.84	4
IIId	7.04	0.65	4
III	8.18	0.30	21

average (Section 3.2.2, Fig. 22, 23). Travel times less than 10 days agree with Carlson's (1981) suggestion, but disagree with Patterson and Husar's (1981) findings of travel times between 12 and 20 days based on 850 mb trajectories. Also, Rahn and McCaffrey (1980) suggested that there is evidence that arctic pollution aerosols seem to have a residence time of about 20 days. We speculate that rapid transport is performed by stationary anticyclonic systems more efficiently than by moving cyclones or moving anticyclones.

#### 4.4.3 Meteorological Characteristics of Transport Pathway Types Reaching Barrow

It is known that regions under stagnant anticyclones are source regions for the formation of air masses with distinct characteristics due to the under-lying surface (Petterssen, 1956). It was shown that the pollutant transporting air masses originate in stagnating anticyclones over certain source regions and acquire a characteristic chemical signature as indicated by the  $X_{Mn}/X_V$  ratio. It is therefore also conceivable that these air masses will acquire meteorological characteristics based on the humidity and temperature conditions over the source region. The meteorological characteristics of polluted air masses as observed at Barrow were inspected based on the different transport pathway types taken. Based on Tables A2, A3 (Appendix), discussed in Section 3.2.2, the mean values of the temperature

deviations ( $\Delta T$ ), the pressure deviations ( $\Delta P$ ), the wind speed deviations ( $\Delta WS$ ), and the sky cover deviations ( $\Delta SC$ ) for the surface level were calculated. Mean values of the temperature and wind speed deviations ( $\Delta T$ ,  $\Delta WS$ ) at the 850 mb level as well as the mean value of the temperature difference between the surface and 850 mb were also determined. The results are listed in Table 10.  $\sigma$  denotes the standard deviation,  $N$  the number of samples.

Overall, the results are very disappointing because each transport pathway type is characterized by a number of varying meteorological characteristics resulting in large standard deviations. Even general trends do not seem to be preserved. For example, one would expect IIIId to be associated with the coldest temperatures because this transport pathway type is mainly due to the Asiatic anticyclone. In Section 3.2.2, Table A1 (Appendix) showed that pollution episodes were quite often associated with two air masses present at the same time. It appears, therefore, that the air mass leaving a source region acquires meteorological characteristics from the synoptic systems creating the transport pathway as well as experiencing modification due to the frequently present Pacific air within the confluence zone at Barrow. This result is in agreement with the findings in Section 3.2.3 which showed that the significant periods in the power spectra of temperature and pressure were related to local synoptic conditions.

Table 10: Mean values of meteorological parameters for different transport pathway types

Type	Surface											
	$\Delta T$	$\sigma$	N	$\Delta P$	$\sigma$	N	$\Delta WS$	$\sigma$	N	$\Delta SC$	$\sigma$	N
Ia	-2.8	7.3	2	0.7	3.1	2	0.9	0.6	2	0.7	1.8	2
Ib	-5.8	1.9	3	-2.0	15.1	3	4.3	1.0	3	-2.4	2.0	2
IIa	4.1	6.0	3	-11.3	4.9	3	4.0	1.2	3	1.4	1.9	3
IIb	-2.3	3.4	11	3.7	5.3	11	2.2	1.9	11	-1.4	2.1	11
IIc	-0.3	4.8	8	-2.5	9.0	8	2.5	1.8	8	-1.0	1.6	7
II		4.8	22	-0.6	8.5	22	2.5	1.9	22	-0.9	2.1	21
IIIa	-3.1	5.4	8	4.5	10.1	8	3.2	2.1	8	-3.4	3.9	5
IIIb	-0.1	2.5	8	-4.4	6.7	7	3.1	1.7	8	-0.2	2.1	8
IIIc	-8.1	3.9	4	9.8	8.2	4	-0.8	1.4	4	-2.8	1.4	4
IIId	-0.3	5.8	4	5.1	4.3	4	2.6	2.1	4	-0.7	2.1	2
III	-2.5	5.3	24	2.8	9.5	23	2.4	2.3	24	-1.5	3.0	19

Type	850 mb									
	$\Delta T$	$\sigma$	N	$\Delta WS$	$\sigma$	N	$T_{Sfc} - T_{850}$	$\sigma$	N	
Ia	-9.3	11.4	2	1.4	0.1	2	-5.1	1.1	2	
Ib	-	-	-	-	-	-	-	-	-	
IIa	-4.5	0.6	2	3.3	4.0	2	3.0	7.6	2	
IIb	-2.4	4.1	8	2.0	4.7	8	-6.4	3.4	8	
IIc	3.0	6.9	9	7.1	5.6	9	-8.9	3.8	9	
II	-0.1	6.1	19	4.5	5.5	19	-7.0	4.7	19	
IIIa	-1.5	3.5	8	5.6	5.6	8	-4.4	5.9	8	
IIIb	-1.2	2.4	5	5.2	4.0	5	-6.9	3.1	5	
IIIc	-3.1	4.7	3	-1.0	2.6	3	-8.4	2.0	3	
IIId	-3.2	2.7	4	7.0	4.0	4	-3.7	4.2	4	
III	-2.7	3.9	20	3.7	5.1	20	-5.5	4.5	20	

#### 4.4.4 On the Seasonal Variation of Transport Pathway Types

Based on the seasonal variation of the  $X_{Mn}/X_V$  ratio, it was speculated that there should be a seasonal change in the atmospheric circulation types or transport pathway types (Section 2.6) in order to transport pollution aerosol from different source regions to Barrow. After having identified the transport pathway types (Section 4.3) the number of occurrences per month was counted for each type (Table 11). A distinct seasonal variation is seen. Transport pathways relating to mainly Soviet sources dominate during October through January and transport pathways relating to mainly European sources are predominant during February and March.

As noted previously (Section 4.4.1) some transport pathway types may include several different source regions as expressed by a variety of  $X_{Mn}/X_V$  ratios. In order to resolve the occurrence of different source regions the monthly mean  $X_{Mn}/X_V$  ratio for each transport pathway type was calculated (Table 12). Note that sometimes only one or two data points are available. Transport pathway type III<sub>d</sub> seems to have a larger  $X_{Mn}/X_V$  ratio in October than in November, III<sub>a</sub> seems to have a larger  $X_{Mn}/X_V$  ratio in November than in December, and III<sub>b</sub> seems to have larger ratios during November/December than February with January probably being anomalous. III<sub>c</sub> has similar ratios during January and February. II<sub>b</sub> has similar ratios during all months of its occurrence. II<sub>a</sub> nicely separates the two ratios by possessing the larger ratio during October and a smaller ratio during March. Thus, we seem to

Table 11: Seasonal variation of frequency of occurrence of transport pathway types

Type	October	November	December	January	February	March
III d	2	2				
III a		5	3			
III b		1	2	3	2	
III c				2	2	
II c			2	2	4	1
II b			2	1	2	5
II a	1					1
Total	3	8	9	8	10	7

Table 12: Seasonal variation of mean  $X_{Mn}/X_V$  ratios for each transport pathway type

Type	October	November	December	January	February	March
III d	12.2 $\pm$ 12.4	6.2 $\pm$ 5.6				
III a		5.3 $\pm$ 5.6	1.2 $\pm$ 0.3			
III b		1.6	1.7 $\pm$ 0.4	6.2 $\pm$ 8.4	1.3 $\pm$ 0	
III c				1.3 $\pm$ 0.1	1.2 $\pm$ 0.1	
II c			1.5 $\pm$ 0.6	0.9 $\pm$ 0.1	1.1 $\pm$ 0.5	0.9
II b			0.8 $\pm$ 0.1	0.8	0.7 $\pm$ 0.1	0.9 $\pm$ 0.04
II a	2.9					0.8

obtain a consistent result that during winter source regions with relatively large ratios ( $\sim >1$ ) contribute pollution aerosols, whereas during spring source regions with relatively lower ratios ( $\sim <1$ ) become of importance.

In order to understand the seasonal variation of the transport pathway types one should investigate the seasonal variation of the major synoptic systems creating these pathways, e.g. the Asiatic anticyclone, the arctic anticyclone and blocking situations over Europe. Transport pathway type III<sub>d</sub> is the one which appears first during October/November and it is mainly determined by the presence of the Asiatic anticyclone and its extension over the Magadan Region. Intrusions of cold arctic air over eastern Siberia lead to widespread cooling in that region which causes the formation of the Asiatic anticyclone. With such occurrences the beginning of the Asiatic anticyclone becomes discernible as early as the first of October. The winter circulation over Asia definitely takes over about the middle of November when the Asiatic anticyclone becomes well established near Lake Baykal (Lydolph, 1977). The Asiatic anticyclone develops an eastward extension over the Magadan region (including the Chukchi Peninsula) which is at times as persistent and well developed as the main Asiatic anticyclone itself. The maximum of occurrence of the extension is during November through January (Dmitriev, 1968). This extension is also part of the circulation pattern CP3 as identified by Moritz (1979) (Section 3.1.2) which has its maximum of occurrence during December.

During the course of winter the Asiatic anticyclone expands and

increases its influence further to the west. During this time the arctic circulation is zonal and cyclonic in character (Namias, 1958) creating pathway type IIIa associated with a cyclone track along the Soviet arctic coast (Klein 1957). During winter this track enters the Arctic over the Atlantic Ocean and follows the Soviet and Canadian arctic coasts. During spring, however, this track terminates over the Kara Sea due to the persistent presence of the arctic anticyclone over the Beaufort Sea. IIIb is created when the westward extension of the Asiatic anticyclone reaches the Urals and the arctic circulation changes into an anticyclonic circulation type (Namias, 1958) which is characteristic of April.

The extension of the Asiatic anticyclone over Europe is most frequent during spring (Lydolph, 1977; Reinel, 1960) and its eastern portion is partially or completely collapsed during February/March (Lydolph, 1977; Dmitriev, 1968). The extension of ridges of the subtropical anticyclone on top of the cold extension of the Asiatic anticyclone creates blocking anticyclones (Reinel, 1960). All transport pathway types II are characterized by initial blocking over Europe and either a cyclonic (less frequent) or anticyclonic arctic circulation. According to Treidl et al. (1981), on an annual basis the blocking frequency near  $10^{\circ}\text{W}$  is most important, clearly dominating all other peaks which appear to lose their significance. Whereas winter exhibits a commanding peak at  $0-20^{\circ}\text{W}$  and a weak secondary peak at  $40-50^{\circ}\text{E}$ , the main peak is weakened in spring while a strong peak appears at  $20-50^{\circ}\text{E}$ . This peak can be associated with the initial formation of

transport pathway types II because it is located over and to the east of European source regions. The main peak at  $0-20^{\circ}\text{W}$  is of no interest because it is located over the Atlantic.

Hess and Brezowsky (1969) presented a seasonal variation of the occurrence of Grosswetterlagen. Grosswetterlagen characterized by meridional circulation over Europe have a maximum of occurrence during March-May and dominate the zonal and mixed circulation types.

All anticyclonic systems with closed isobars within the Pacific Hemisphere ( $90^{\circ}\text{W}-90^{\circ}\text{E}$ ) of the Arctic north of  $70^{\circ}\text{N}$  were counted for the period October 1976 - September 1979. The October and September means, respectively, are based on two year data only. The frequency of occurrence of the arctic anticyclone over the Pacific sector of the Arctic undergoes a surprisingly weak seasonal variation and it seems more important to consider its mean monthly intensity which exhibits a strong seasonal variation with maximum values during January through March (Fig. 38). According to Barry and Perry (1973, p. 75) only during spring can one speak of a true "polar" anticyclone which is then present over the Canadian Arctic.

Lir, referenced by Borisov (1965) divided the circulation over Eurasia into four phases which support the seasonal variation of the transport pathway types and of the individual pressure systems outlined above:

- 1) Winter: The southerly displacement of the (sub-)tropical zone of high pressure; reduced pressure in the Arctic; the strengthening of the zonal circulation with an inflow towards the polar regions.

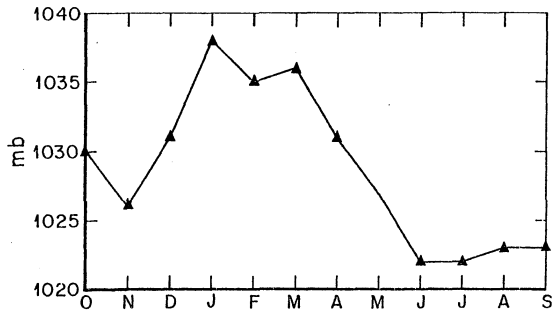


Fig. 38: Mean monthly intensity of the arctic anticyclone when located over the Pacific Arctic.

2) Spring: The same disposition of the (sub-)tropical zone; high pressure in the Arctic; disturbances of the zonal circulation.

3) Summer: The northerly displacement of the (sub-)tropical zone of high pressure; high pressure in the Arctic; the weakening of the zonal circulation with an outflow from the polar regions.

4) Autumn: The same disposition of the (sub-)tropical zone; low pressure in the Arctic; the restoration of zonal circulation.

In summary, the seasonal variation of the frequency of occurrence of transport pathway types is related to the seasonal variations of the arctic and mid-latitude circulations. It appears that the presence of certain transport pathways depends mainly on the presence and absence of the Asiatic anticyclone over certain areas of the Eurasian continent. During summer, when the Asiatic anticyclone has disappeared, no significant amounts of pollution aerosols are collected at Barrow. This will be discussed further in Chapter VI.

V OBSERVATIONS OF "ARCTIC HAZE" DURING THE "PTARMIGAN" WEATHER  
RECONNAISSANCE FLIGHTS, 1948-1961

5.1 Introduction

The term "Arctic Haze" was used for the first time by Murray Mitchell, Jr. in 1956 describing the haze encountered during the "Ptarmigan" weather reconnaissance flights. Mitchell's description of Arctic Haze was based on observations and subsequent discussions with several weather officers. They were surprised to find the optical transparency of the arctic atmosphere at times significantly reduced by thick haze layers. This was surprising because the polar regions had been considered as the cleanest regions on earth.

Bodhaine et al. (1981) and Shaw (1981) showed that at Barrow the aerosol light scattering undergoes a seasonal variation similar to the seasonal variation of the arctic pollution aerosol. Shaw (1982b) observed that during the presence of pollution-derived aerosols at the ground near Fairbanks haze bands aloft were also present. Therefore, although still very speculative, Rahn and Shaw have suggested that Arctic Haze observed during the fifties was a manifestation of anthropogenic pollution in the Arctic. On the other hand, during their first experiment near Barrow they found that the crustal particles collected in the haze bands had had their origin in the deserts of Far East Asia (Rahn et al., 1977; Rahn et al., 1981).

As Mitchell's description of Arctic Haze was based on a small data set we decided to obtain the complete "Ptarmigan" records in order to systematically investigate the meteorological/synoptic conditions present during the observations of Arctic Haze and to decide whether Arctic Haze was a natural or anthropogenic phenomenon. In contrast to the pollution aerosol described in Chapters II-IV, we do not have chemical information on the composition of Arctic Haze. Instead we hope to obtain information on the horizontal and vertical extent and the occurrence of Arctic Haze within the Arctic Basin.

## 5.2 The "Ptarmigan" Data Set

The "Ptarmigan" flight reports were obtained on microfilm from the National Climatic Data Center, Asheville, and cover the period January 1949 through December 1967. Table 13 shows that in the beginning, flights were made only 2 or 3 times a week, but later on flights were made almost daily. The flight altitude was close to the 500 mb surface in most cases, and in some cases close to the 700 mb surface. Although the flight paths were occasionally changed, the flights were always restricted to the Alaskan sector of the Arctic; i.e., approximately within the region defined by the three points:  $70^{\circ}\text{N}$ ,  $160^{\circ}\text{W}$ ;  $70^{\circ}\text{N}$ ,  $110^{\circ}\text{E}$  and the North Pole. Haynes (1949) described his experience during one of the "Ptarmigan" flights.

A "Ptarmigan" flight record entry made at 1/2 hour intervals

Table 13: Monthly frequency of "Ptarmigan" weather reconnaissance flights

Year	Jan	Feb	Mar	Apr	May	Jun	Jul	Aug	Sep	Oct	Nov	Dec	Total
1949	11	13	15	14	14	15	14	16	13	10	9	0	144
1950	2	9	3	4	8	11	9	13	15	12	10	10	106
51	2	4	15	24	27	17	17	15	13	16	15	12	177
52	5	5	9	2	3	13	16	18	22	14	27	28	162
53	23	23	27	28	31	27	32	30	24	13	21	22	301
54	14	18	31	32	32	30	32	31	29	29	26	27	331
55	32	27	33	31	31	30	31	32	31	31	31	31	371
56	31	29	33	30	32	31	31	31	31	31	32	33	375
57	25	8	0	0	19	15	20	22	14	27	27	30	207
58	30	27	11	25	31	31	31	2	30	39	29	31	317
59	31	27	31	30	31	29	33	31	30	31	31	31	366
1960	31	20	19	16	0	2	5	16	12	11	13	31	176
61	3	12	31	20	25	30	26	10	37	19	13	15	241
Total	240	222	258	256	284	281	297	267	301	283	284	301	3274

contained the following information: date, time, position, altitude, visibility, wind, cloud amount and types, air temperature, (sometimes) dewpoint, and height of 500 mb or 700 mb surface above ground. Sometimes other information was given also, like turbulence, icing of the aircraft, state of sea underneath, etc., and vertical temperature profiles made using dropsondes.

Some of the instrumentation used was described by Vederman and Smith (1950) but we do not have any information on the reliability of the observation procedures and instrumentation. There is also a great deal of uncertainty attached to those visual observations made during the polar night or twilight. For this analysis we are considering only those "Ptarmigan" flight reports in which the occurrence of haze was actually spelled out as a comment, because the coded report on "present weather" conditions does not distinguish between "fog" or "thick dust haze", and on the other hand, in writing out the word "haze" it must have appeared to the observers as something worth mentioning. This restriction reduces our data set to 114 "Ptarmigan" flights. But we are still faced with the problem that a very thin cloud might have been mistaken as a haze layer or the observer simply missed seeing the haze when it was present, that is, the data set is subjective. Mitchell (1956), however, noticed that there is a distinct difference between haze and thin cirrostratus. Haze has a different color (grey-blue in anti-solar directions and a reddish-brown hue in the direction of the sun), diffuse boundaries, and is without optical effects.

### 5.3 On the Occurrence of Arctic Haze

Presenting the available data of 114 flights, with about 400 haze reports to be analyzed, in the form of Table 14 we can already deduce some information on the seasonal and interannual variation of the occurrence of Arctic Haze. There seems to be a seasonal variation with a repeatable spring maximum. Mitchell (1956) did not mention this, perhaps because of the more limited data set he had available. The spring maximum apparently is real, that is, it is not caused by an increased number of flights and therefore an increased number of observations during spring (Table 13). It is possible that the number of occurrences of haze can be higher during the winter, when visual observations are questionable due to the lack of proper illumination. We note that the three months of March, April and May include 62% of all flights with haze reports. Thus, the spring maximum seems to be significant.

The spring maximum of Arctic Haze is, to first order, in agreement with findings of the seasonal variation of the pollution-derived elements manganese and vanadium (Section 2.5) found at Barrow, Alaska. Breaking it up into months, May has the maximum of "Ptarmigan" Arctic Haze reports, which seems to be displaced by about 1-2 months with respect to the pollution-derived aerosol which tends to peak in March. There are also a number of haze reports during the summer, which seem to contradict the concept of a pollution-derived haze. During summer the concentrations of pollution-derived elements are very low. For example,

Table 14: Monthly frequency of "Ptarmigan" weather reconnaissance flights with haze reports

Year	Jan	Feb	Mar	Apr	May	Jun	Jul	Aug	Sep	Oct	Nov	Dec	Total
1949	3	4	2	4	0	1	0	2	1	0	2	-	19
1950	1	0	0	2	5	1	0	2	3	4	2	2	22
51	1	2	4	8	7	2	1	0	1	0	1	0	27
52	0	0	1	0	0	0	0	0	0	0	0	0	1
53	0	0	1	2	7	1	3	3	1	0	0	3	21
54	0	0	5	2	0	1	0	0	0	0	0	1	9
55	1	0	3	1	3	0	0	0	0	0	0	0	8
56	0	0	0	1	1	0	2	0	0	0	0	0	4
57	0	0	-	-	0	0	0	0	0	0	0	0	0
58	0	0	0	0	0	0	0	0	0	0	0	0	0
59	0	0	2	0	0	0	0	0	0	0	0	0	2
1960	0	0	0	0	-	0	0	0	0	0	0	0	0
61	0	0	0	0	1	0	0	0	0	0	0	0	1
Total	6	6	18	20	24	6	6	7	6	4	5	6	114

the concentration of vanadium at Barrow is lower by about a factor of 80 (Section 2.5).

A spring maximum, on the other hand, would also be consistent with the idea of a desert dust-derived haze, because spring is the season of desert dust storms in the eastern deserts of Asia (Watts, 1969). Dust concentrations in the atmosphere over Northern Kazakhstan and southern Central Asia are high during May through September (Makhon'ko and Rabotnova, 1981). According to Duce et al. (1980) there is a significant transport of continental aerosols out of Asia north of 20°N during the spring and extending into the summer. Arao et al. (1979) reported a maximum of yellow sand occurrence over Nagasaki, Japan, during April.

Surprisingly, there is an almost equal number of haze observations during the early fifties (except 1952), but after that, the accounts of Arctic Haze drop off and become scarce. The years 1949-1954 represent 87% of all flights with haze report. We have checked for the possibility of a change in flight path patterns, flight altitude, use of observers, and change in observation procedures, but these factors have not revealed any significant changes.

As shown (section 4.3.5) Eurasia is the most important region contributing to the pollution-derived aerosols collected at Barrow. For a pollution-derived haze we would expect a monotonic increase of haze occurrence with time associated with increasing anthropogenic activity. It appears unlikely that this drop in haze occurrence could have been caused by a change from coal to oil as the major fossil fuel

in Europe (Semb, 1978), because this change occurred during the late fifties and early sixties. We assume that increased consumption of oil in the Soviet Union occurred even later than in Europe, around the mid-sixties, when large discoveries were made (Shabad, 1977).

If Arctic Haze is desert dust-derived a possible explanation would be an increased number of dust storms during the early fifties due to exceptional dryness in Asia. Arao et al. (1979) showed a time series of the number of days with yellow sand over Nagasaki, Japan, (Fig. 39). Between 1952 and 1955 there is a pronounced increase in the occurrence of yellow sand, flanked by very low values during the late forties and during the late fifties.

For both possibilities (a pollution-derived haze or a desert dust-derived haze) a change in the effectiveness of removal mechanisms (i.e. clouds and precipitation) along the transport path as well as changes in the transport path itself due to circulation changes could also explain a change in the frequency of Arctic Haze occurrence. Raatz (1981) reported a pronounced increase in cloudiness over Barrow which occurred during the mid-forties, however.

Because of the dramatic drop in haze reports the "Ptarmigan" data from 1962-1967 were not analyzed and are, therefore, not included in this investigation. Reports of Arctic Haze remained very scarce until the end of the record in 1967.

From the frequency of haze reports during one flight we find that Arctic Haze was more widespread over the Arctic during spring than during the rest of the year (Table 15). Note, however, that some of the

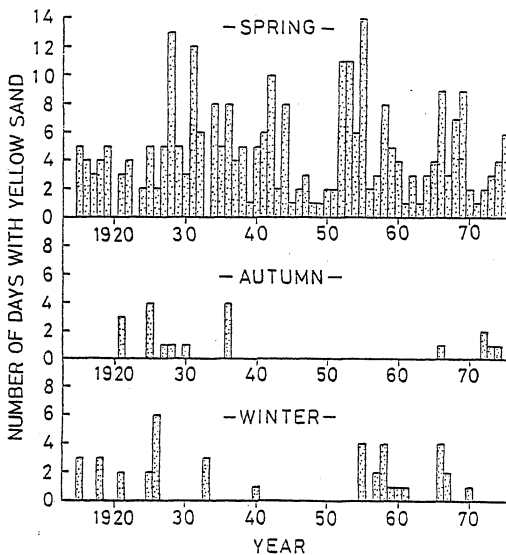


Fig. 39: Number of days with yellow sand over Nagasaki, Japan (after Arao et al., 1979).

Table 15: Monthly frequency distribution of frequency of haze observations during one flight

Month	Numbers of haze observations during one flight														Total	Average
	1	2	3	4	5	6	7	8	9	10	11	12	13	14		
Jan	1	1	2		1			1							6	3.7
Feb	2	2		1		1									6	2.7
Mar	2	4	3	3		1		1	2	1			1		18	4.8
Apr	4	6	1	3	3			1			1	1			20	3.9
May	9	3	3	2	4			1			1	1			24	3.4
Jun	2	1	1			1	1								6	3.3
Jul	4	1						1							6	2.3
Aug	4		1	1	1										7	2.3
Sep	4	1	1												6	1.5
Oct	2		1		1										4	2.5
Nov	3	1		1											5	1.8
Dec	3						1			1				1	6	5.7
Year	40	20	13	11	10	3	3	4	2	2	2	2	1	1	114	3.5

calculated average numbers of haze observations during one flight can be misleading; e.g. December, when there were only few data available. For the whole data set, on the average 3.5 haze observations were made during one flight. We also find that Arctic Haze usually seems to be confined to patches limited to certain areas. This is in agreement with Mitchell's (1956) findings which estimate an average horizontal extent of 800-1300 km. But there were also two cases when Arctic Haze was reported in every flight record, thus covering a distance of about 3200 km.

Fig. 40 shows the frequency of observations of Arctic Haze per quadrant with sides of  $4^{\circ}$  latitude and  $5^{\circ}$  longitude. We have made no adjustments for the decreasing size of the quadrants with latitude. At  $32^{\circ}\text{N}$  and  $86^{\circ}\text{N}$  we increased the length of the longitude side to  $10^{\circ}$  and  $20^{\circ}$ , respectively, for better visual presentation. There is practically no area where Arctic Haze has not been observed. There seem to be certain areas where Arctic Haze was encountered more frequently, but by studying the most common flight path patterns, those areas of maximal Arctic Haze are the ones most often overflown. The spatial frequency distribution is therefore inconclusive. We noticed, however, that Arctic Haze was almost always reported during anticyclonic surface pressure conditions, most often at the northern periphery of the Beaufort Sea anticyclone. Haze reports were also frequent within the northwestern quadrant of the anticyclone. In mid-latitudes hazes are often observed during anticyclonic conditions and Arctic Haze does not seem to be different.



Forty percent of all haze observations were specified with an altitude estimate. Arctic Haze was observed everywhere between the surface and 6 km altitude, i.e. below the tropopause (Fig. 41). In most cases the altitude of the haze was given as "haze at and below flight level", in other cases the top of the haze layer was estimated. Therefore, it is not too surprising to find the most frequent haze altitude to coincide with the main flight level at 500 mb (5.6 km). A secondary maximum is observed at the other main flight level at 700 mb (~ 4.4 km). Mitchell (1956) remarked that Arctic Haze was characterized by considerable vertical thickness.

However, it is interesting to note the large number of observations of Arctic Haze occurrence at the 500 mb level, because more recent investigations seem to suggest a haze at lower levels. For example, Holmgren et al. (1974) found an Arctic Haze layer near 2 km altitude, Shaw (1982c) reported haze layers at 1.2 km and between 2 and 3 km, respectively, and Rahn et al. (1981) observed bands of haze between 2 and 2.6 km with evidence of another layer above 3 km. These recent investigations, however, were carried out with small airplanes which could not ascend up to 500 mb. Assuming that haze reports without specified altitude represent low level haze because the observer could not estimate the altitude, we found that during the period November-April there are as many haze reports without specified altitude as during the period May-October. The data set does not suggest, for example, that low level haze prevails during the winter months and upper level haze during the summer months.

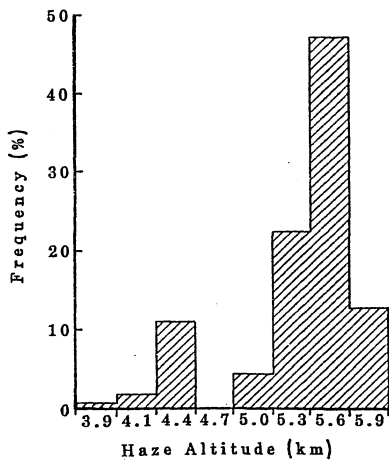


Fig. 41: Frequency distribution of altitude of occurrence of Arctic Haze.

#### 5.4 Synoptic Conditions During Observations of Arctic Haze

Present weather, cloud types and amount were reported for a cylindrical portion of the atmosphere, approximately 50 km in radius about the plane at the time of the observation. It has been noted by Mitchell (1956) that Arctic Haze was usually found during otherwise "clear" weather conditions. Mitchell's statement is verified for the period November-April (Fig. 42a). But for the period May-October Arctic Haze is observed most often during conditions of "continuous layers of clouds" (Fig. 42b). This may only be related to the fact that during the winter arctic skies are usually clear, but they are overcast during the summer (Henderson, 1967). On the other hand, it might suggest that clear skies are not a necessary prerequisite for the appearance of Arctic Haze. From the analysis of haze observations at flight level during weather conditions with clouds, we find that in most cases the haze was at a different altitude than the cloud layers, making it easier to distinguish haze from thin clouds.

If there were clouds present, Arctic Haze was most frequently associated with cirrostratus clouds. The high percentage of cirrostratus clouds is surprising, because it does not reflect the normal conditions as indicated by "Ptarmigan" data over the Beaufort Sea (Henderson, 1967) and the data at Resolute (Vowinckel, 1962), where middle layer clouds are most frequent. Voskresenskij and Karimova (1964) noted that the number of days with clouds in the upper atmospheric layer has a maximum over the Arctic between the end of the

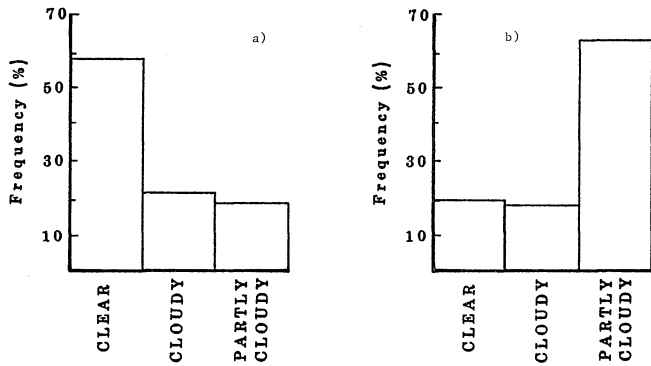


Fig. 42: Frequency of weather conditions during haze reports  
a) November-April, b) May-October.

winter and the beginning of spring (March/April). They also mention that the formation of cirrostratus clouds is usually due to the regular rise of air in the zone of high level fronts. This is consistent with the findings that haze was observed in zones of strong surface pressure gradients which can be associated with fronts aloft.

According to Section 3.2.1, pollution episodes at Barrow are associated with northerly winds. Clean air usually has its origin at southern latitudes. On the "Ptarmigan" flights wind was determined by aerial navigation methods and Fig. 43 shows the frequency of wind directions associated with observations of Arctic Haze. It should be kept in mind that the wind was determined at flight level, which is not always necessarily the same at the altitude of the haze layer. Because winds are reported at flight level, which was usually at 500 mb, it is not surprising to find a predominant west wind. During November-April, haze observations frequently coincide with northerly winds, whereas during May-October there are many observations of Arctic Haze with southerly winds.

One of the most obvious features of Arctic Haze is that it restricts horizontal visibility. Horizontal visibility was determined as the maximum distance to which one could see, common to sectors comprising 1/2 or more of the horizon circle at flight level. Unfortunately, two different ranges of estimates were used, so that we represent horizontal visibility in categories composed of these two (Table 16). Surprisingly, even under "clear" sky conditions the horizontal visibility can be reduced appreciably. The effects of haze

## Wind Direction During Haze Report

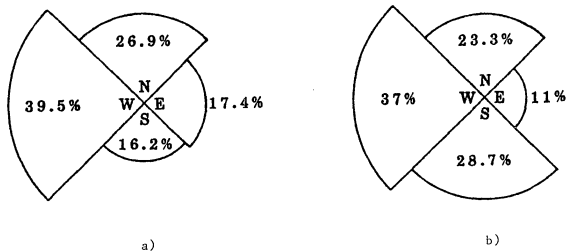


Fig. 43: Frequency of wind direction during haze reports  
a) November-April, b) May-October.

Table 16: Frequency of visibility range during haze reports and different weather conditions

	Visibility Range (km)				
	< 1.8	1.8-5.6	5.6-18.5	18.5-55.6	> 55.6
Clear	15*	4	25	44	90
Partly cloudy	0	0	31	20	22
Continuous layers of clouds	6	6	35	31	49

\* 13 observations during one flight

cannot be eliminated from those due to clouds during conditions of "partly cloudy" or "overcast" skies.

It is difficult to estimate a typical temperature of Arctic Haze because this depends on the type of air mass the haze is in, as well as the altitude of the haze. If, in the case of haze at flight level, we plot altitude of haze versus temperature at that altitude a correlation is found. The relationship is valid for different "present weather" conditions. The lower the altitude the colder the haze temperature. This principle seems valid regardless of whether the wind has a northerly or southerly component. Winds with a southerly component are only slightly warmer. But it seems that the correlation does not represent a new piece of information. It merely reflects the well-known principle that a pressure surface lies higher if the air column underneath is warmer and vice versa. The range of observed haze temperatures is broad, from  $-20^{\circ}\text{C}$  to  $-50^{\circ}\text{C}$ .

During some of the flights, dropsondes were released to obtain vertical temperature profiles. In most cases dew point temperatures were not available. We were able to summarize 16 cases of haze report for which both the synoptic conditions and vertical temperature profiles are available. Some cases are also included when the time of dropsonde release did not correspond with the time of haze report, but in these cases the time difference was no more than one hour, so the aircraft was probably still within the same air mass. In other cases the dropsonde release was in the vicinity of ground stations (Barrow, Mould Bay), and when both were within the same air mass as revealed by similar

temperature profiles, we then obtained the information on the moisture regime from the ground station. A variety of synoptic conditions as well as a variety of vertical temperature profile types are associated with haze reports. No typical Arctic Haze temperature profile is obvious from the data set.

#### 5.5 On the Possible Origin of Arctic Haze

In Chapter IV we were able to identify transport pathways of pollution aerosol from mid-latitudinal source regions to Barrow due to quasi-stationary synoptic pressure systems. If Arctic Haze is pollution-derived, then similar transport pathways should be detected in association with the haze observation. Therefore, we selected the years 1949, 50, 51, and 53, which represent 89 flights, in order to identify pathways similar to the ones described in Section 4.3 on the northern Hemisphere Sea Level and 500 mb charts published by the U.S. Weather Bureau. This analysis was not as detailed as the one used in Section 4.2 and included only a check on what stationary pressure systems were present to create a transport pathway. Since we do not have a chemical tracer for Arctic Haze, we classified possible source areas into the following broad categories only: Soviet Union, Europe, North America, Far East, and of unknown origin. The last category "unknown origin" includes all those cases where no pathway could be detected or when two equally strong pathways were present at the same time. Transport

pathways leading to the USSR, Europe, and North America are assumed to represent paths of mid-latitude anthropogenic pollution aerosols; the ones leading to the Far East are assumed to represent paths along which desert dust-derived aerosols travel.

In general, we found that during winter/spring transport pathways were established on the surface weather maps and quite often supported at the 500 mb level. During the summer, however, transport pathways were usually only suggested at 500 mb. It is known, however, that the arctic atmospheric surface circulation is intense and distinct during the winter, whereas it appears sluggish and indifferent during the summer (i.e. Wilson, 1967). It is therefore possible that transport of aerosols during winter can occur at low levels, while during summer, the transport would tend to take place at higher levels. The data in Table 17 suggest that there is a seasonal trend in what source area contributes to the formation of Arctic Haze. During September-April the Soviet Union is suggested as a source (26% of all cases). The importance of European sources seems to be shifted towards the spring (30% of all cases). There is little evidence that North American sources are important in contributing aerosols (3% of all cases). Sources in Far East Asia, which we will assume to be deserts, are, according to Table 17 predominantly, responsible for Arctic Haze during the summer (26% of all cases), with little or no contributions from the other source areas.

The month of May appears to be transitional with respect to the haze origin. From December to May the haze is mostly of pollution

Table 17: Monthly frequency of occurrence of transport pathways leading to different source regions

	USSR	Europe	America	Far East	Unknown
Sep	3	1		1	1
Oct	2	1		1	
Nov	1	3		1	
Dec	4	1			
Jan	2	2			1
Feb	3	4			
Mar	3	3			2
Apr	4	7	2		4
May	1	5	1	7	5
Jun				6	
Jul				3	
Aug	1	1		5	
Total	24	28	3	24	13

origin; from May to August the haze seems to be desert dust-derived. The strong spring maximum as noted in Table 14 seems to be caused by the simultaneous presence of pollution-derived and a desert dust-derived haze. During April and May 1976 Rahn et al. (1981) noticed pollution episodes and desert dust episodes following each other. Overall, pollution-derived haze was suggested in 59% of all cases, desert dust-derived haze in 26% of all cases and 15% were undetermined.

In summary, Arctic Haze as described by the "Ptarmigan" weather reconnaissance flights, possesses the following characteristics: its occurrence undergoes a seasonal variation with a spring maximum; it was found almost everywhere over the Alaskan Arctic, but it is primarily found at the peripheries of anticyclones and is confined to patches with about 800-1,300 km of horizontal extent; haze was most frequently reported as "at and below flight level" which was usually at 500 mb; Arctic Haze was found under a variety of meteorological conditions but always with the presence of anticyclones and frequently with cirrostratus clouds. The atmospheric circulation patterns suggest that Arctic Haze possesses a dual character of origin: during winter/early spring, it seems to be pollution-derived, during late spring/summer, it seems to be desert dust-derived.

The quality of the "Ptarmigan" data set is highly questionable: 1) How well was the observer able to visually detect haze during twilight and polar night conditions and to distinguish haze from clouds? 2) How motivated was the observer to record the presence of haze? In this respect, the sudden drop of numbers of haze observations still remains

partially unexplained. 3) No chemical data to describe the composition of the haze bands were taken, and a connection between haze and its likely origin is highly speculative. However, the analysis of Arctic Haze during the "Ptarmigan" flights provided supportive, although not conclusive, evidence to the description of tropospheric long-range transport of aerosol from mid-latitudes into the Arctic as discussed in Chapter VI.

## VI DISCUSSION AND CONCLUSION

The present investigation was based on the following five assumptions: a) noncrustal vanadium and noncrustal manganese can be used as tracers for polluted air masses originating in mid-latitudes; b) the pollution aerosol at Barrow reveals an episodic character embedded in the overall seasonal variation with distinct characteristics; c) the  $X_{Mn}/X_V$  ratio is a suitable tracer to distinguish individual industrial point sources in mid-latitudes; d) the climatology of major anticyclonic pressure systems in the Arctic and in mid-latitudes explains the seasonal variation of the concentrations of the pollution aerosols; e) tropospheric long-range transport on the order of 10,000 km is possible.

In the preceding chapters a coherent analysis was presented supporting these five assumptions. Dedicated experiments using aircrafts and detailed analysis of individual pollution episodes are certainly needed to upgrade the present analysis.

1.  $X_V$  and  $X_{Mn}$  are suitable tracers for pollution aerosols in the Arctic

The noncrustal component of V can be used as a good indicator for mid-latitude pollution aerosols at Barrow, because it originates mainly

from the combustion of heavy residual oil (Zoller et al., 1973), whereas the lighter fuels used in the Arctic do not contain any significant amounts of vanadium (Hofstader et al., 1976). Rahn (personal communication) has found no possible sources in Barrow, and the Narwhal experiment (Conway and Rahn, personal communication) confirms that there are no local sources of vanadium (Section 2.3). Although manganese has a larger crustal component and its pollution component originates from a larger variety of anthropogenic sources (Section 2.3), its overall good correlation with XV (Sections 2.5 and 3.2.3) supports its usefulness as a tracer for pollution aerosol. Although this investigation of the arctic pollution aerosol was restricted to one arctic site only, it should be pointed out that similar seasonal variations of XV and XMn concentrations are observed at Fairbanks (Rahn and McCaffrey, 1980), at Mould Bay and Igloodik (Barrie et al., 1981), at five stations in Greenland (Heidam, 1981), at Bear Island and Ny Alesund (Larssen and Hanssen, 1979). Differences among the stations can be explained by the local synoptic influences.

In the initial analysis, a mid-latitude source area could not be found for sample Ell (March 4-6, 1980) until Noelle Lewis (personal communication) explained this peak due to the eruption of a volcano on Kamchatka. The ratio of XMn/XV is unusually high with a value of about 14, in contrast to a mean ratio of 1.3 at Barrow. It is still unknown if significant amounts of stratospheric aerosol penetrate into the lower arctic atmosphere during winter and how much XV and XMn would be associated with it. However, Reiter (1963) and Feely (1979) suggested

that stratospheric aerosols will descend in the mid-latitude anticyclones south of the polar front and then will be subjected to the same low level tropospheric transport processes as the anthropogenic pollution aerosols. Therefore, the results of the present analysis on transport pathways would not be affected.

A total of 61 peaks of concentration of XV and XMn at Barrow were investigated, and only 3 peaks could not be explained by the method of attaching a pollution episode to it (Section 4.2). Investigating the synoptic conditions at Barrow during times of high pollution concentration revealed that conditions were usually associated with cold temperatures, clear skies, stable vertical conditions and high pressures, or generally anticyclonic conditions (Sections 3.1.3, 3.2.1, 3.2.2). Anticyclonic conditions are usually characterized by light winds. Polluted air masses, however, arrived at Barrow with wind speeds higher than the monthly mean. This suggests that the transport was anticyclonic in character but took place along the periphery of the anticyclone.

Air masses had to be identified by constructing height/time cross sections of potential temperature and mixing ratio, because standard elements like temperature, pressure and wind often failed to indicate an air mass change. Air masses which originated from different source areas and had travelled along different transport pathways did not differ significantly in their meteorological characteristics (Sections 3.2.2 and 4.4.3). It appears that they quite often acquired properties of the major synoptic systems providing the transport pathway and those

of the local air masses at Barrow, especially in cases when Pacific air was overriding the arctic air (Section 3.2.2). Spectrum and cross spectrum analysis provided an elegant means of showing that polluted air masses retain the chemical characteristics from their source region but acquire meteorological characteristics en route or locally (Section 3.2.3). These findings are supported by the "Ptarmigan" data, where no characteristic synoptic conditions with the occurrence of Arctic Haze could be identified. Haze was always associated with the synoptic conditions characteristic of the particular season. Vertical temperature profiles varied as well according to the synoptic conditions present (Section 5.4).

It should be noted, however, that XV and XMn are not the only possible tracers for anthropogenic pollution at Barrow. Sulfate (Rahn and McCaffrey, 1980), soot (Rosen et al., 1981b), organics (Daisey et al., 1981; Weschler, 1981), trace gases (Peterson et al., 1980; Rasmusson and Khalil, 1982) and pollen (Barrie et al., 1981) undergo seasonal variations similar to that of XV and XMn, and in some cases might be better tracers. The available data base restricted us, however, to the use of XV and XMn (Section 2.2).

## 2. The Pollution Aerosol Exhibits An Episodic Character

It was noticed that on top of the seasonal variation of the concentration of the pollution aerosol there were fluctuations on a

smaller time scale with different  $X_{Mn}/X_V$  ratios (Section 2.5). Assuming that this observation was of importance, it was concluded that these peaks must have been caused by "favorable" conditions either at the source, along the transport pathway, or at Barrow itself. Peaks in concentration were examined to see whether they could be associated with a pollution episode, having the following set of conditions (Section 4.2): a) Stagnation over the source area to allow for accumulation of pollutants; b) a surge of polluted air northward due to an approaching cyclone; c) a distinct transport pathway persistent enough to allow for transport across the Arctic; d) the presence of arctic air during the sampling period characterized by abnormally high concentrations.

This approach was successful because these conditions were satisfied in most cases investigated (Section 4.3.1). The analysis presumably identifies the "signal" part of the arctic pollution aerosol in contrast to Shaw's (1981) diffusion model which might be valid for the "noise" or background aerosol.

Several observations indicated that the arctic pollution aerosol should be episodic in character: a) stagnant conditions over the source area are due to Grosswetterlagen, which have a mean duration of 4 days (Brezowsky et al., 1951); b) a surge following a period of stagnation is present for a limited time only, lasting for about 4 days (Section 4.4.1); c) persistent transport pathways through the Arctic are present for a few days (Wilson, 1967; Namias, 1958), before the circulation changes into another persistent mode; d) observations from the "Ptarmigan" records describe Arctic Haze as being patchy (Section 5.3)

and quite often haze was observed over one area but was not observed the following day over the same area during similar synoptic situations.

### 3. The $X_{Mn}/X_V$ Ratio Proved to Be Able to Distinguish Between Different Source Areas

Rahn (1981c) suggested that the  $X_{Mn}/X_V$  ratio was capable of discriminating between North American and Eurasian sources and that the high  $X_{Mn}/X_V$  ratios at Barrow probably were due to unknown Soviet sources. West-European sources were assumed to have similar  $X_{Mn}/X_V$  ratios as North American sources due to the similar use of oil. The analysis of the transport pathways was in general agreement with the  $X_{Mn}/X_V$  ratio, i.e. transport pathways leading to European source areas were characterized by relatively low  $X_{Mn}/X_V$  ratios ( $<1.0$ ), transport pathways to Soviet source areas were characterized by relatively large  $X_{Mn}/X_V$  ratios ( $>1.0$ ). Minor discrepancies can be explained by the inadequate meteorological data set available which did not allow for a detailed study; however, no major discrepancies were detected. The analysis also showed that the influence of North American sources to the pollution aerosol at Barrow is of little importance.

The seasonal change of the  $X_{Mn}/X_V$  ratio and therefore of different source areas is well reflected in the seasonal change of the transport pathways (Section 4.4.4). This result is also supported by the "Ptarmigan" data (Section 5.5). During winter, Soviet sources

contribute predominantly to the arctic pollution aerosol; during spring, European sources contribute predominantly. In addition, the "Ptarmigan" data suggest that during the summer, desert areas of Far East Asia are the main cause of Arctic Haze. During summer no transport pathways to anthropogenic pollution areas are indicated. It is hypothesized that Arctic Haze is pollution-derived during winter/spring because a) the occurrence of Arctic Haze seems to undergo a similar seasonal variation as the pollution aerosol concentration and b) the occurrence of Arctic Haze is associated with pathways leading to industrial mid-latitude source areas. This hypothesis is suggested by observations by Shaw (1981, 1982b) that high concentrations of pollution aerosols are often associated with haze bands aloft, although the chemical composition of the haze bands has not been determined. On the other hand, it is hypothesized that Arctic Haze is desert dust-derived during spring/summer because a) there is no pollution-derived aerosol present during the occurrence of spring/summer Arctic Haze, and b) the occurrence of spring/summer Arctic Haze is associated with pathways at upper atmospheric levels only, leading to desert areas of Eastern Asia.

The different  $X_{Mn}/X_{V}$  ratios support the notion that industrial areas can be regarded as point sources with a distinct chemical characteristic. Pollution episodes seem to pick up pollutants from selected source areas only because stagnant conditions are necessary to accumulate pollutants, a condition not satisfied by many source areas at the same time. In addition, the atmospheric circulation, which is characterized by blocking, forcing the polar front to run in the north-

south manner, separates sources west of the front, which will come under cyclonic influence (rainout), from sources east of the front, which remain under anticyclonic conditions (Section 4.4.1).

Interestingly, aerosols traveling along transport pathways passing over a series of different source areas seem to retain their original chemical characteristic without mixing with other sources. This might be explained by the "breathing" effect of the boundary layer (Sisterson et al., 1979). During the day, pollutants are incorporated into a growing boundary layer; during the night, this layer becomes uncoupled from the constraints imposed by the underlying surface, and pollutants can be transported. If, on the following day over the area where the pollutants are now present at higher levels, the heating is not strong enough (especially in cases when the air mass has traveled northward), the new forming boundary layer will not reach high enough to mix the pollutants contained in the upper layer with those in the boundary layer. Thus, the original chemical characteristics are preserved.

#### 4. Climatology of the Arctic and Mid-Latitudes Is Decisive in

##### Explaining the Seasonal Variation of the Arctic Pollution Aerosol

It was most important to recognize that the transport pathways were most often created by quasi-stationary pressure systems (Section 4.3.5) creating preferred modes of the arctic and mid-latitude atmospheric circulation (Wilson, 1967; Namias, 1958; Hess and Brezowsky, 1969).

Consequently the seasonal variation of the pollution aerosol can be explained by the seasonal variation of the transport pathways and the quasi-stationary pressure systems (Section 4.4.4). The most important quasi-stationary pressure systems were all anticyclones: the arctic anticyclone, the Asiatic anticyclone, the Asiatic anticyclone's eastward extension over the Magadan Region and westward extension reflected in blocking over East Europe. Following Keegan's (1958) opinion that the arctic anticyclone over the Beaufort Sea is partially an offspring of the Asiatic anticyclone, one might conclude that all anticyclones listed are a part of the Asiatic anticyclone. Therefore, it is suggested that the seasonal variation of Arctic Haze and the arctic pollution aerosol can be explained by the seasonal variation of the Asiatic anticyclone, implying that conditions along the path are anticyclonic. During summer, when there is no Asiatic anticyclone, no significant amounts of pollution aerosol can be detected in the Arctic. Arctic Haze observed during the summer appears to contain desert dust (Section 5.5) raised to upper levels by cyclonic activity and injected into the Arctic by high-level transport processes in contrast to low level transport during winter/spring. Note, that in April the arctic anticyclone is still fairly strong, the Asiatic anticyclone is still present and blocking is at its maximum. On the other hand, concentrations of pollutants are rapidly declining at Barrow. In Table 18, the frequency of occurrence of transport pathway types IIb and IIIb is listed, indicating a seasonal variation with a maximum in March and a rapid decrease towards summer. However, the presence of a certain synoptic pattern and an associated

Table 18: Monthly frequency of occurrence of transport pathway types 11b and 111b

Year	Jan	Feb	Mar	Apr	May	Jun	Jul	Aug	Sep	Oct	Nov	Dec
1977	10	6	2			1	1		1	7	5	1
1978			2	1						3		
1979	1	2	7						1			
1980		3	5	5								3
Total	11	9	16	6	0	1	1	0	2	10	5	4

transport pathway does not necessarily lead to the creation of a pollution episode as defined in Section 4.2. A suite of "favorable" conditions such as a stable atmosphere, inversions, clear skies, persistency of the path, etc., have to be fulfilled in order to create such an episode. During April, for example, increased solar radiation over the source area leads to more turbulent mixing and less anticyclonic conditions over the continents, thus supporting the accumulation of pollutants. Thus, although anticyclones are still present during April, the associated anticyclonic conditions, especially over the continents, begin to deteriorate.

North America and Japan do not have a corresponding Asiatic anticyclone because their land mass is not as large as the Eurasian continent. We notice that the Asiatic anticyclone over Eurasia is located always east of the source area, the weak continental Hudson Bay anticyclone, however, is located west of the industrial areas of the US east coast requiring a retrograde motion and not allowing for a surge due to approaching cyclones.

##### 5. Tropospheric Long-Range Transport Is Possible

Long-range transport of desert soils is characterized by initial cyclonic activity in order to raise the crustal particles to high levels (e.g. Ing, 1972). In contrast, long-range transport of industrial pollution is characterized by initial emission of pollutants from high

stacks into a stable atmosphere, characterized by stagnation. These conditions lead to accumulation of pollutants in a layer high enough to be susceptible to atmospheric transport. But stagnating anticyclones do not provide means of fast transport except for transporting aerosols from the east side of the anticyclone to its west side, as suggested by Vukovich's et al. (1977) model. Efficient long-range transport is initiated by a surge of air northward caused by an approaching cyclone (Section 4.4.1). It is, however, essential that the aerosol remains within the influence of the anticyclone. As soon as the aerosol becomes part of the cyclone system, it is likely to be scavenged. Thus, the aerosol has to "escape" along the periphery of the anticyclone ahead of the cloud and rainbands of the cyclone. Ottar (1981) estimated that on an annual basis, dry deposition accounts for about 50% of the emitted sulphur pollutants. About 30% is deposited by precipitation (and rain), and the remaining 20% would be transported ("escape") out of northwestern Europe.

The transport pathways described are mainly along anticyclones in contrast to cyclonic pathways, which necessarily are associated with precipitation. Smith (1981) suggested, that the atmosphere may be subdivided into synoptic-scale systems, 1) regions where there is little or no precipitation (dry regions), and 2) regions where precipitation is occurring (wet region). Thus, there is always the statistical possibility that the pollutants will travel entirely through dry regions along the route.

The transport pathways identified were created by quasi-stationary

systems. Thus, transport was not accompanied by the movement of these systems, as in the case of documented summer anticyclones providing long-range transport (e.g. Wolff et al., 1981; Guicherit and van Dop, 1977; Hall et al., 1973; Samson and Ragland, 1977; Lyons et al., 1978). Instead, the transport takes place in the zones of strong pressure gradients, which was also suggested by the location of the haze episodes observed from the "Ptarmigan" records, and by the fact that polluted air masses arrived at Barrow with wind speeds larger than the monthly mean (Section 3.2.2). Gavrilova (1964) reported that jet streams in polar regions are related to upper frontal zones. These in turn are due to meridional circulation patterns when, in the middle and upper layers of the troposphere, intensive advection of heat is observed along the western periphery of the high ridges. In Section 5.4, a high frequency of cirrostratus clouds was noted in association with haze observations. Cirrostratus clouds are indicative of upper level fronts (Voskresenskij and Karimova, 1964), thus, high winds along the frontal zone provide a rapid transport along a "corridor" as demanded by Selezneva (1979) for long range transport.

Rahn and McCaffrey (1980) and Carlson (1981) suggested that the source regions of the arctic pollution should be located north of the polar front and within the arctic airstream region (Wendland and Bryson, 1981) or should be characterized by a continental climate (Rahn, 1981a). This is consistent with the findings of this study that the source region and the transport pathway are determined by anticyclonic conditions. In general, the atmosphere will be characterized by clear

skies (little scavenging), by cold temperatures (similar to the temperatures encountered at Barrow or even colder), and by inversions which tend to trap the pollutants. Due to the "similar" temperatures at the source region and Barrow some lifting is expected during the surge but with little condensation because of the original continental dry air. Anticyclonic conditions with surface and subsidence inversions probably will restrict the transport to around 850 mb, which is a typical height of the arctic inversions (Vowinckel and Orvig, 1967; Belmont, 1958). On the other hand, the "Ptarmigan" data revealed a high frequency of occurrence of haze at 500 mb even in winter, although Mitchell (1956) noted that Arctic Haze possessed a large vertical extent. The question at which level the pollution aerosol is being transported therefore remains open until more data become available. It was noted that the arctic circulation at low levels is only well developed during winter, whereas the summer circulation is sluggish (Wilson, 1967; Keegan, 1958; Reed, 1959). Thus, it seems understandable that rapid transport of desert dust-derived particles has to take place at upper levels, as indicated by the "Ptarmigan" data (Section 5.5).

## 6. Climatological Aspects

Although four years of chemical data represent a unique time series in air pollution meteorology, it is still questionable how representative the series is in respect to climatological conditions.

It was shown, however, that the spring maximum was very repeatable (Section 2.5). The winters of 1976/77 and 1977/78 were characterized by record cold temperatures in the eastern United States and drought conditions in the west (Namias, 1978; Edmon, 1980; Harnack, 1980). During those two winters, the Aleutian low was stronger than normal and its position displaced to the southeast, the Icelandic low was positioned farther to the southwest, and temperatures were warmer than usual over Alaska, Greenland and the western United States. The lower troposphere was cooler than normal in middle latitudes and warmer than normal in the polar region, resulting in a reduced zonally averaged meridional temperature gradient. The winter of 1978/79 had similar arctic and North Atlantic mean circulations as in the two winters before, except that the mean circulation was quite different over the North Pacific.

A singularity may be defined as the recurrence tendency of some weather characteristic about a specified date in the year. Schulz (1963) presented a time series for central Europe indicating that during certain times of the winter, maxima of surface pressure and associated anticyclonic Grosswetterlagen are present (Fig. 44). Referring back to Fig. 5 (Section 2.5), it seems that some maxima during the spring months occur as well at specific dates. Some results are summarized in Table 19. It appears that some of the singularities during spring over Europe are reflected in the seasonal change in concentration of the arctic pollution aerosol.

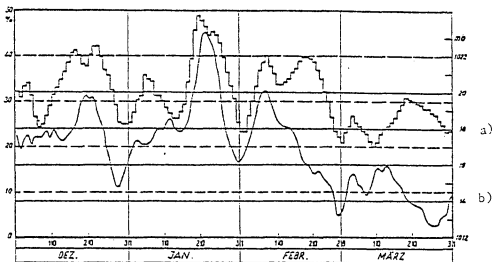


Fig. 44: Singularities over central Europe a) frequency of anticyclonic Grosswetterlagen, b) mean surface pressure. (after Schulz, 1963)

Table 19: Possible correlation between the occurrence of pressure singularities over central Europe and the occurrence of high concentration of pollution aerosol at Barrow, Alaska

Pressure singularity Schulz (1963)	1976/77	1977/78	1978/79	1979/80
December 15	B15/16	B54	B134	E3
January 6	B18	B58	B139	E4
January 20	-	B60	B134	E6
February 14-20	B25	B63/64	-	E9/10
March 15	B28	B71	B152	E13

From the present analysis it seems possible to predict the occurrence of Arctic Haze and the arctic pollution aerosol on a day to day basis due to the synoptic regimes at Barrow and the circulation patterns identified, which determine the presence of mid-latitude anthropogenic pollution. The environmental effects of the arctic pollution aerosol have not yet been fully assessed, but with further increases in industrial pollution perturbations of the arctic radiation budget (Shaw and Starnes, 1978), and the possibility of acid snow (Koerner et al., 1982), for example, will have to be expected.

## REFERENCES

- Anonymous, 1981: Fact sheet on Acid rain. Prepared for the Canadian Embassy by Willford, Wegman, Krulwich, Gold&Hoss. Canadian Embassy, 1771N Street, Washington, DC. 20036, 15 pp.
- Arao, K., Y. Makino and Y. Nagaki, 1979: Some statistical aspects of yellow sand. Science Bulletin of the faculty of Education, Nagasaki University, No. 30, in Japanese.
- Athanassiadis, Y.C., 1969: Preliminary air pollution survey of vanadium and its compounds. US Department of Health, Education, and Welfare.
- Bach, W., 1976: Global air pollution and climatic change. Reviews of Geophysics and Space Physics, Vol. 14, p. 429-474.
- Barrie, L.A., R.M. Hoff and S.M. Daggupaty, 1981: The influence of mid-latitude pollution sources on haze in the Canadian Arctic. Atmospheric Environment, Vol. 15, p. 1407-1419.
- Barry, R.G., 1977: Study of climatic effects on fast ice extent and its seasonal decay along the Beaufort-Chukchi coast. Annual report. In: Environmental Assessment of the Alaskan continental shelf. Vol. XIV, Transport Outer Continental Shelf Environmental Assessment Program, US Department of Commerce, Boulder, Colorado, p. 574-743.
- Barry, R.G., and A.H. Perry, 1973: Synoptic climatology. Methuen, London, 555 pp.
- Belmont, A.D., 1958: Lower tropospheric inversions at Ice-Island T-3. AGARD Symposium. Polar Atmosphere, Oslo, Meteorology Section, Part I, p. 215-284.
- Benson, C.S., 1982: Reassessment of winter precipitation on Alaska's arctic slope and measurements on the flux of wind blown snow. Geophysical Institute Report UAG R-288, University of Alaska, Fairbanks, Alaska, 26 pp.
- Bigg, E.K., 1980: Composition of aerosol at four baseline atmospheric monitoring stations. Journal of applied Meteorology, Vol. 19, p. 521-533.
- Bluethgen, J., 1966: Allgemeine Klimageographie. De Gruyter & Co., Berlin. 720 pp.
- Bodhaine, B.A., J.M. Harris, and G.A. Herbert, 1981: Aerosol light scattering and condensation nuclei measurements at Barrow, Alaska. Atmospheric Environment, Vol. 15, p. 1375-1390.

- Boettger, C.M., 1961: Air pollution potential east of the Rocky Mountains: Fall 1959. Bulletin of the American Meteorological Society, Vol. 42, p. 615-620.
- Bohr, P., P. Hess, T. Meissner and C. Pflugbeil, 1974: Allgemeine Meteorologie. Leitfaeden fuer die Ausbildung im deutschen Wetterdienst, No. 1, Offenbach, 103 pp.
- Borisov, A.A., 1965: Climates of the USSR. Aldine Publishing Company, Chicago, 255 pp.
- Borys, R.D. and K.A. Rahn, 1981: Long-range atmospheric transport of cloud-active aerosol to Iceland. Atmospheric Environment, Vol. 15, p. 1491-1502.
- Brezowsky, H., H. Flohn and P. Hess, 1951: Some remarks on the climatology of blocking action. Tellus, Vol. 3, p. 191-193.
- Brueneau, L., 1980: Pollution from industries in the drainage area of the Baltic. Ambio, Vol. 9, p. 145-152.
- Carlson, T.N., 1981: Speculations on the movement of polluted air to the Arctic. Atmospheric Environment, Vol. 15, p. 1473-1478.
- Carlson, T.N. and J.M. Prospero, 1972: The large-scale movement of Saharan air outbreaks over the Northern Equatorial Atlantic. Journal of applied Meteorology, Vol. 11, p. 283-297.
- Daisey, J.M., R.J. McCaffrey and R.A. Gallagher, 1981: Polycyclic aromatic hydrocarbons and total extractable particulate organic matter in the Arctic aerosol. Atmospheric Environment, Vol. 15, p. 1353-1363.
- Dallavalle, J.A. and L.F. Bosart, 1975: A synoptic investigation of anticyclogenesis accompanying North American polar air outbreaks. Monthly Weather Review, Vol. 103, p. 941-957.
- Dams, R., K.A. Rahn and J.W. Winchester, 1972: Evaluation of filter materials and impaction surfaces for nondestructive neutron activation analysis of aerosols. Environ. Sci. Technol., Vol. 6, 441 pp. Referenced by Ragaini, 1978.
- DeLuisi, J.J. (ed), 1981: Geophysical Monitoring for climatic change, No. 9: Summary Report 1980, NOAA Environmental Research Laboratories, Boulder, Colorado, 163 pp.
- Dewdney, J.C., 1976: The USSR. Studies in industrial Geography. Westview Press, Boulder, 262 pp.

- Dienes, L., 1974: Environmental disruption and its mechanism in east-central Europe. *The Professional Geographer*, Vol. 26, p. 375-381.
- Dmitriev, A.A., 1968: Situations characterizing various states of the Siberian anticyclone and its northeastern extension in the cold period of the year. In: Treshnikov, A.F. (ed.). Problems of the Arctic and the Antarctic, Vol. 29-32, p. 448-455. Jerusalem: Israel Program Science Translation.
- Duce, R.A. and G.L. Hoffman, 1976: Atmospheric vanadium transport to the Ocean. *Atmospheric Environment*, Vol. 10, p. 989-996.
- Duce, R.A., C.K. Unni, B.J. Ray, J.M. Prospero and J.T. Merrill, 1980: Long-range atmospheric transport of soil dust from Asia to the tropical north Pacific: temporal variability. *Science*, Vol. 209, p. 1522-1524.
- Edmon, H.J., 1980: A study of the general circulation over the Northern Hemisphere during the winters of 1976/77 and 1977/78. *Monthly Weather Review*, Vol. 108, p. 1538-1553.
- Eiden, R., 1979: The influence of trace substances on the atmospheric energy budget. In: Bach, W., J. Pankrath and W. Kellogg (eds.). Man's impact on climate. Elsevier, Amsterdam, p. 115-127.
- Elsom, D.M. and T.J. Chandler, 1978: Meteorological controls upon ground level concentrations of smoke and sulphur dioxide in two urban areas of the United Kingdom. *Atmospheric Environment*, Vol. 12, p. 1543-1554.
- Feely, H.W., 1979: Nuclear fallout and high volume aerosol collections. In: Herbert G.A. (ed.): Geophysical Monitoring for climatic change, No. 8. Summary report 1979. NOAA Environmental Laboratories, Boulder, Colorado, p. 94-95.
- Gavrilova, L.A., 1964: Jet stream distribution in the troposphere at high latitudes. In: Meteorological conditions in the Arctic during the IGY and IGC, Moscow. Jerusalem Program, Science Translation.
- Goldman, M.I., 1970: The convergence of environmental disruption. *Science*, Vol. 170, p. 37-42.
- Guicherit, R. and H. van Dop, 1977: Photochemical production of ozone in western Europe (1971-1975) and its relation to Meteorology. *Atmospheric Environment*, Vol. 11, p. 145-155.
- Hall, F.P., C.E. Duchon, L.G. Lee and R.R. Hagan, 1973: Long-range transport of air pollution. A case study, August 1970. *Monthly Weather Review*, Vol. 101, p. 404-411.

- Harnack, R.P., 1980: An appraisal of the circulation and temperature pattern for winter 1978/79 and a comparison with the previous two winters. *Monthly Weather Review*, Vol. 108, p. 37-55.
- Harris, J.M. and G.A. Herbert, 1980: Carbon dioxide, condensation nuclei and wind climatology of the Barrow GMCC observatory (1973-1979). NOAA Data report ERL ARL-2. Silver Spring, Maryland, 112 pp.
- Hartmann, D.L., 1974: Time spectral analysis of mid-latitude disturbances. *Monthly Weather Review*, Vol. 102, p. 348-362.
- Haynes, B.C., 1949: Polar weather flights. *Weather*, Vol. 4, p. 11-15.
- Heidam, N.Z., 1981: On the origin of the Arctic aerosol: a statistical approach. *Atmospheric Environment*, Vol. 15, p. 1421-1427.
- Heintzenberg, J., 1980: Particle size distribution and optical properties of Arctic Haze. *Tellus*, Vol. 32, p. 251-260.
- Heintzenberg, J., 1981: The chemical composition of Arctic Haze at Ny-Alesund, Spitzbergen. *Tellus*, Vol. 33, p. 162-171.
- Henderson, P.M., 1967: Cloud conditions over the Beaufort Sea. Publications in Meteorology, No. 86. McGill University, Montreal. 48 pp.
- Hess, P. and H. Brezowsky, 1969: Katalog der Grosswetterlagen Europas. Berichte des deutschen Wetterdienstes, No. 13, Offenbach, 14 pp.
- Hofstader, R.A., O.I. Milner and J.H. Runnels, 1976: Analysis of petroleum for trace metals. *Advances in Chemistry Series No. 156*, 165 pp.
- Holmgren, B., G. Shaw and G. Weller, 1974: Turbidity in the arctic atmosphere. *AIDJEX Bulletin*, Vol. 27, p. 135-148.
- Holworth, G.C., 1972: Vertical temperature structure during the 1966 Thanksgiving week air pollution episode in New York City. *Monthly Weather Review*, Vol. 100, p. 445-450.
- Huschke, R.E., 1969: Arctic cloud statistics from "air-calibrated" surface weather observations. Rand Corporation, RM-6173-PR, 79 pp.
- Ing, G.K.T., 1972: A duststorm over Central China, April 1969, *Weather*, Vol. 167, p. 136-145.
- Keegan, T.J., 1958: Arctic synoptic activity in winter. *Journal of Meteorology*, Vol. 15, p. 513-521.

- King, W.J. and F.M. Vukovich, 1982: Some dynamic aspects of extended pollution episodes. *Atmospheric Environment*, Vol. 16, p. 1171-1181.
- Kish, G., 1971: Economic atlas of the Soviet Union. University of Michigan Press. Ann Arbor. 2nd ed., 40 pp.
- Klein, W.H., 1957: Principal tracks and mean frequencies of cyclones and anticyclones in the Northern Hemisphere. Research paper No. 40, US Department of Commerce, Weather Bureau, Washington, D.C., 60 pp.
- Koerner, R.M. and D. Fisher, 1982: Acid snow in the Canadian high Arctic. *Nature*, Vol. 295, p. 137-140.
- Kozo, T.L., 1980: Mountain barrier baroclinity effects on surface winds along the Alaskan arctic coast. *Geophysical Research letters*, Vol. 7, p. 377-380.
- Landsberg, H.E. and J.M. Mitchell, 1959: Power spectrum analysis of climatological data for Woodstock Colledge, Maryland. *Monthly Weather Review*, Vol. 87, p. 283-298.
- Larssen, S. and J.E. Hanssen, 1979: Annual variation and origin of aerosol components in the Norwegian Arctic-Subarctic region. WMO conference, Boulder, Colorado (WMO No. 549).
- Likens, G.E., R.F. Wright, J.N. Galloway and T.J. Butler, 1979: Acid Rain. *Scientific American*, Vol. 241, p. 43-51.
- Ludlam, F.H., 1980: Clouds and Storms. Pennsylvania State University Press. University Park. 405 pp.
- Lydolph, P.E., 1977: Climates of the Soviet Union. World Survey of Climatology, Vol. 7, Elsevier, Amsterdam, 443 pp.
- Lyons, W.A. and R.B. Husar, 1976: SMS/GOES Visible images detect a synoptic scale air pollution episode. *Monthly Weather Review*, Vol. 104, p. 1623-1626.
- Lyons, W.A., J.C. Dooley and K.T. Whitby, 1978: Satellite detection of long-range pollution transport and sulfate aerosol hazes. *Atmospheric Environment*, Vol. 12, p. 621-631.
- Makhon'ko, K.P. and F.A. Rabotnova, 1981: The concentration of mineral dust in the atmosphere over the USSR. *Soviet Meteorology and Hydrology*, p. 47-50.
- Mason, B., 1966: Principals of Geochemistry, 3rd ed., Wiley & Sons, Inc., New York, 329 pp.

- McCormick, R.A., 1970: Meteorological aspects of air pollution in urban and industrial districts. In: Meteorological aspects of air pollution. WMO, technical note No. 106, Geneva, p. 1-30.
- McGuirk, J.P. and E.R. Reiter, 1976: A vacillation in atmospheric energy parameters. *Journal of the atmospheric sciences*, Vol. 33, p. 2079-2093.
- Miller, J.M., 1981: A five-year climatology of five-day back trajectories from Barrow, Alaska. *Atmospheric Environment*, Vol. 15, p. 1401-1406.
- Mitchell, J.M., 1956: Visual range in the polar regions with particular reference to the Alaskan Arctic. *Journal of atmospheric and terrestrial physics*, special supplement, p. 195-211.
- Moritz, R.E., 1977: On a possible sea-breeze circulation near Barrow, Alaska. *Arctic and Alpine Research*, Vol. 9, p. 427-431.
- Moritz, R.E., 1979: Synoptic climatology of the Beaufort Sea coast of Alaska. Institute of Arctic and Alpine Research, University of Colorado, Occasional paper No. 30, 176 pp.
- Namias, J., 1958: Synoptic and climatological problems associated with the general circulation of the Arctic. *Transactions American Geophysical Union*, Vol. 39, p. 40-51.
- Namias, J., 1978: Multiple causes of the North American abnormal winter 1976/77. *Monthly Weather Review*, Vol. 106, p. 279-295.
- Ottar, B., 1981: The transfer of airborne pollutants to the Arctic region. *Atmospheric Environment*, Vol. 15, p. 1439-1446.
- Panofsky, H.A. and P. Wolff, 1957: Spectrum and cross spectrum analysis of hemispheric westerly index. *Tellus*, Vol. 9, p. 195-200.
- Panofsky, H.A. and G.B. Brier, 1968: Some applications of statistics to Meteorology. Pennsylvania State University, 224 pp.
- Patterson, D.E. and R.B. Husar, 1981: A direct simulation of hemispheric transport of pollutants. *Atmospheric Environment*, Vol. 15, p. 1479-1482.
- Pearce, F., 1982: The menace of acid rain. *New Scientist*, p. 419-424.
- Peterson, J.T., K.J. Hanson, B.A. Bodhaine and S.J. Oltmans, 1980: Dependence of CO<sub>2</sub>, aerosol, and ozone concentrations on wind direction at Barrow, Alaska during winter. *Geophysical research letters*, Vol. 7, p. 349-352.

- Petterssen, S., Jacobs and Haynes, 1956: Meteorology of the Arctic. Office of the technical assistant to the chief of naval operations for polar projects (Op-03A3) Washington D.C., 207 pp.
- Petterssen, S., 1956: Weather analysis and forecasting, Volume II. McGraw Hill, New York, 266 pp.
- Raatz, W.E., 1981: Trends in cloudiness in the Arctic since 1920. Atmospheric Environment, Vol. 15, p. 1503-1506.
- Ragaini, R.C., 1978: Characterization of atmospheric aerosols by neutron activation analysis. In: Malissa, H. (ed.). Analysis of airborne particles by physical methods, CRC Press, p. 93-123.
- Rahn, K.A., 1976: The chemical composition of the atmospheric aerosol. Technical Report. Graduate School of Oceanography, University of Rhode Island, 265 pp.
- Rahn, K.A., 1978: Sulfate in the Barrow atmosphere. Unpublished.
- Rahn, K.A., 1979: The Eurasian sources of arctic aerosol. Norwegian Institute for air research, Lillestrom, No. 34/79, 36 pp.
- Rahn, K.A., 1980: Current understanding of the origin, characteristics, and significance of Arctic Haze. Presented at the 48th meeting of the Polar Research Board and the US Committee for SCAR. National Academy of Sciences, Washington, D.C..
- Rahn, K.A., 1981a: Relative importance of North America and Eurasia as sources of arctic aerosol. Atmospheric Environment, Vol. 15, p. 1447-1456.
- Rahn, K.A., 1981b: Elemental tracers and sources of atmospheric acidity for the Northeast - A statement of new evidence. Unpublished.
- Rahn, K.A., 1981c: The Mn/V ratio as a tracer of large-scale sources of pollution aerosol for the Arctic. Atmospheric Environment, Vol. 15, p. 1457-1464.
- Rahn, K.A., 1981d: Analysis of two episodes of long-range transport of pollution aerosol to Iceland during winter 1980-81: a progress report on the URJ/JMO study of air quality near Iceland. Unpublished.
- Rahn, K.A., 1981e: Arctic Haze studies at Barrow. In: DeLuisi, J.J. (ed.). Geophysical Monitoring for climatic change, No. 9. Summary report 1980, NOAA Environmental Research Laboratories, Boulder, Colorado, p. 113-116.

- Rahn, K.A., R.D. Borys and G.E. Shaw, 1977: The Asian source of Arctic Haze bands. *Nature*, Vol. 268, p. 713-715.
- Rahn, K.A. and R.J. McCaffrey, 1980: On the origin and transport of the winter arctic aerosol. *Annals of the New York Academy of Sciences*, Vol. 338, p. 486-503.
- Rahn, K.A., C. Brosset, B. Ottar and E.M. Patterson, 1980a: Black and white episodes, chemical evolution of Eurasian air masses, and long-range transport of carbon to the Arctic. Presented at the General Motors Research Symposium. Particulate Carbon: Atmospheric life cycle. Warren, Michigan, 12-14 October 1980.
- Rahn, K.A., E. Joranger, A. Semb and T.J. Conway, 1980b: High winter concentrations of SO<sub>2</sub> in the Norwegian Arctic and transport from Eurasia. *Nature*, Vol. 287, p. 824-826.
- Rahn, K.A., R.D. Borys and G.E. Shaw, 1981: Asian desert dust over Alaska: Anatomy of an Arctic Haze episode. *Geological Society of America*, Special paper No. 186, p. 37-70.
- Rasmussen, R.A. and M.A. Khalil, 1982: Atmospheric trace gases and Arctic Haze at Barrow. In: Bodhaine, B. and J. Harris (eds.) Geophysical Monitoring for climatic change, No. 10. Summary report 1981. NOAA Environmental Research Laboratories, Boulder, Colorado, p. 114-120.
- Reed, R.J., 1959: Arctic weather analysis and forecasting. Department of Meteorology and Climate, University of Washington, Occasional report, No. 11, 78 pp.
- Reinel, H., 1960: Die Zugbahnen der Hochdruckgebiete ueber Europa als klimatologisches Problem. *Mitt. Fraenk. Geogr. Ges.*, Vol. 6, p. 1-73. Referenced by Bluetngen.
- Reiter, E.R., 1963: A case study of radioactive fallout. *Journal of applied Meteorology*, Vol. 2, p. 691-705.
- Reiter, E.R., 1971: Atmospheric transport processes. Part 2: chemical tracers. US Atomic Energy Commission. 382 pp.
- Reiter, E.R., 1981: Planetary-wave behavior and arctic air pollution. *Atmospheric Environment*, Vol. 15, p. 1465-1472.
- Rey, L., B. Ottar, K.A. Rahn and G.E. Shaw, 1983: Arctic environmental issues of energy production at mid-latitudes and the role of long distance air transport of pollutants. Paper to be presented at the 12th congress of the world energy conference, New Delhi, Sep. 18-23, 1983.

- Rosen, H., T. Novakov and B.A. Bodhaine, 1981a: Carbon particles in the arctic aerosol. In: DeLuisi J.J. (ed.). Geophysical monitoring for climatic change, No. 9. Summary report 1980, p. 122-127.
- Rosen, H., T. Novakov and B.A. Bodhaine, 1981b: Soot in the Arctic. Atmospheric Environment, Vol. 15, p. 1371-1374.
- Samson, P.J. and K.W. Ragland, 1977: Ozone and visibility reduction in the Midwest: Evidence for large-scale transport. Journal of applied Meteorology, Vol. 16, p. 1101-1106.
- Schueepp, M. and H. Schirmer, 1970: Climates of central Europe. In: Wallen C. (ed.): Climates of Central and Southern Europe. World Survey of Climatology, Vol. 6, Elsevier, Amsterdam, p. 3-60.
- Schuetz, L., 1980: Long range transport of desert dust with special emphasis on the Sahara. Annals of the New York Academy of Sciences, Vol. 338, p. 515-532.
- Schuetz, L. and K.A. Rahn, 1982: Trace-element concentrations in erodible soils. Atmospheric Environment, Vol. 16, p. 171-176.
- Schulz, L., 1963: Die winterliche Hochdrucklage und ihre Auswirkung auf den Menschen. Berichte des deutschen Wetterdienstes, No. 88, Offenbach, 28 pp.
- Selezneva, YE. S., 1979: Rainout and balance of sulfur in the atmosphere over an industrial region. Izvestiya, Atmospheric and Oceanic Physics, Vol. 15, p. 281-287.
- Semb, A., 1978: Sulphur emissions in Europe. Atmospheric Environment, Vol. 12, p. 455-460.
- Shabad, T., 1977: Gateway to Siberian Resources. Scripta series in Geography.
- Shapiro, R. and H.L. Stolov, 1970: Surface pressure variations in Polar Regions. Journal of the atmospheric sciences, Vol. 27, p. 1021-1026.
- Shaw, G.E., 1979: Considerations on the origin and properties of the antarctic aerosol. Review of Geophysics and Space Physics, Vol. 17, p. 1983-1998.
- Shaw, G.E., 1981: Eddy diffusion transport of Arctic pollution from the mid-latitudes: a preliminary model. Atmospheric Environment, Vol. 15, p. 1483-1490.

- Shaw, G.E., 1982a: Evidence for a central Eurasian source area of Arctic Haze in Alaska. *Nature*, Vol. 299, p. 815-818.
- Shaw, G.E., 1982b: Atmospheric turbidity in the Polar Regions. *Journal of applied Meteorology*, Vol. 21, p. 1080-1088.
- Shaw, G.E., 1983: On the Aitken particle size distribution in Alaskan air mass systems. *Journal of the atmospheric sciences*, to be published in May 1983.
- Shaw, G.E., and G. Wendler, 1972: Atmospheric turbidity measurements at McCall glacier in northern Alaska. Proceedings on the conference on atmospheric radiation, Fort Collins, Colorado, American Meteorological Society, Boston, Mass., p. 181-187.
- Shaw, G.E. and K. Stamnes, 1978: Arctic Haze: Perturbation of the polar radiation budget. *Annals of the New York Academy of Sciences*, Vol. 338, p. 533-539.
- Sisterson, D.L., J.D. Shannon and J.M. Hales, 1979: An examination of regional pollutant structure in the lower troposphere - some results of the diagnostic atmospheric cross-section experiment (DACSE-I). *Journal of applied Meteorology*, Vol. 18, p. 1421-1428.
- Smith, F.B., 1981: The significance of wet and dry synoptic regions on long-range transport of pollution and its deposition. *Atmospheric Environment*, Vol. 15, p. 863-873.
- Sullivan, R.J., 1969: Preliminary air pollution survey of manganese and its compounds. US department of Health, Education and Welfare.
- Tilley, M.A. and G.A. McBean, 1973: An application of spectrum analysis to synoptic-pollution data. *Atmospheric Environment*, Vol. 7, p. 793-801.
- Treidl, R.A., E.C. Birch and P. Sajecki, 1981: Blocking Action in the Northern Hemisphere: A climatological Study. *Atmosphere-Ocean*, Vol. 19, p. 1-23.
- Turnock, D., 1978: Eastern Europe. Studies in industrial geography. Dawson & Sons Ltd., Cannon house Folkestone, England, 273 pp.
- Twomey, S., 1977: Atmospheric Aerosols. Developments in Atmospheric Science, Vol. 7. Elsevier, Amsterdam, 302 pp.
- Vederman, J. and C.D. Smith, 1950: The winter mid-troposphere circulation near the North Pole. *Bulletin of the American Meteorological Society*, Vol. 31, p. 197-205.

- Voldner, E.C., Y. Shah and D.M. Whelpdale, 1980: A preliminary Canadian emissions inventory for sulfur and nitrogen oxides. *Atmospheric Environment*, Vol. 14, p. 419-428.
- Voskresenskij, A.J. and G.U. Karimova, 1964: Frequency and amount of clouds of lower, middle and upper layers in the Arctic during the IGY and IGC. In: Meteorological conditions in the Arctic during the IGY and IGC. Moscow. Jerusalem Program Science translation.
- Vowinckel, E., 1962: Cloud amount and type over the Arctic. Publication in *Meteorology*, Vol. 51, McGill University, Montreal, 27 pp.
- Vowinckel, E. and S. Orvig, 1967: The inversion over the Polar Ocean. WMO Technical Note, No. 87, p. 39-59.
- Vukovich, F.M., W.D. Bach, B.W. Crissman and W.J. King, 1977: On the relationship between high ozone in the rural surface layer and high pressure systems. *Atmospheric Environment*, Vol. 11, p. 967-983.
- Wallen, C., 1970: Introduction. In: Wallen, C. (ed.) Climates of northern and western Europe. World Survey of Climatology, Vol. 5, Elsevier, Amsterdam, p. 1-21.
- Watts, J.E., 1969: Climates of China and Korea. In: Arakawa, H. (ed.) Climates of Northern and Eastern Asia. World Survey of Climatology, Vol. 8, Elsevier, Amsterdam, p. 1-74.
- Wendland, W.M. and R.A. Bryson, 1981: Northern Hemisphere airstream regions. *Monthly Weather Review*, Vol. 109, p. 255-270.
- Wendler, G., 1978: Snow blowing and snow fall on the North Slope, Alaska. Geophysical Institute, University of Alaska, UAGR-259, 23 pp.
- Wendler, G. and F. Eaton, 1981: Radiation balance measurements at Barrow. In: DeLuisi, J.J. (ed.) Geophysical monitoring for climatic change, No. 9. Summary report 1980, NOAA Environmental Research Laboratories, Boulder, Colorado, p. 104-105.
- Weschler, C.J., 1981: Identification of selected organics in the arctic aerosol. *Atmospheric Environment*, Vol. 15, p. 1365-1369.
- Wexler, H., 1936: Cooling in the lower atmosphere and the structure of polar continental air. *Monthly Weather Review*, Vol. 64, p. 122-136.
- Wilson, C., 1958: Synoptic regimes in the lower arctic troposphere during 1955. Publication in *Meteorology* No. 8, McGill University, Montreal, 58 pp.

- Wilson, C., 1967: Climatology of the cold regions. Northern Hemisphere, Part 1. Monograph I-A3a. Cold regions research and engineering laboratory, Hanover, N.H., 142 pp.
- Wilson, C., 1969: Climatology of the cold regions. Northern Hemisphere, Part 2. Monograph I-A3b. Cold regions research and engineering laboratory, Hanover, N.H., 158 pp.
- Wolff, G.T., 1980: Mesoscale and synoptic scale transport of aerosols. *Annals of the New York Academy of sciences*, Vol. 338, p. 379-388.
- Wolff, G.T., N.A. Kelly and M.A. Ferman, 1981: On the sources of summertime haze in the eastern United States. *Science*, Vol. 211, p. 703-704.
- Zoller, W.H., G.E. Gordon, E.S. Gladney and A.G. Jones, 1973: The sources and distribution of vanadium in the atmosphere. in: Kothney, E.L. (ed.). Trace elements in the environment. *Advances in chemistry series*, Vol. 123, p. 31-47.

A P P E N D I X

Table A1: Some properties of polluted air masses

Sample	Sampling period	# of air masses	polluted air mass	type of polluted air mass	air mass type	maximum inversion	WD 1000 mb 700 mb	transport pathway type
B68	Dec 31-Jan 9	4	Dec 31-Jan 4	moist surface layer very moist aloft dry above 700 mb	A <sub>m</sub> <sup>P</sup>	surface - 900 mb	119-295 220-270	1a
B63	Feb 6-9	1	Feb 7-9	dry	A <sub>m</sub>	two inversions between surface and 600 mb merge to one Sfc-850 mb	280-360 80-250	
Dav8	Apr 3-6	}	no data available					1b
Dav10	Apr 11-14							
B205	Nov 23-26							
B4	Oct 8-12	3	Oct 11-12	moist surface layer drier aloft	A	1000-980, 880-865 665-630 mb	290 260	11a
E13	Mar 14-19	1	Mar 14-19	dry surface layer moist and warm aloft especially Mar 16,17	AP	Sfc-900, 930-830 mb	240-350 250-350	

Table A1 continued

Sample	Sampling period	# of air masses	polluted air mass	type of polluted air mass	air mass type	maximum inversion	1000 mb 700 mb	transport pathway type
B18	Dec 27-Jan 5	4	Dec 31-Jan 2	dry surface layer moist Pacific air at intermediate layer dry aloft	APA	1000-875 mb	70 80-120	11b
B28	Mar 15-31	6	Mar 21-23	moderate moist	A	Surface-800 mb	60-75 25-85	
B68	Mar 1-5	2	Mar 5	two mixed air masses	A, P	990-860 mb	260-40 280-30	
B69	Mar 6-9	1	Mar 6-9	cold dry surface layer, Pacific air intruding aloft	AP	Surface-950 mb lifted inversions 980-670 mb	60-70 30-105	
B72	Mar 20-22	1	Mar 20-22	dry and cold	A	Surface-830 mb	795-155 270-325	
Dav1	Apr 1-3	1	Apr 1-3	dry and cold	A	Surface-900 mb	80 15-115	
B144	Feb 1-4	}	no data available					
B151	Mar 12-14							
E6	Jan 5-6	1	Jan 5-6	cold and intermediate moist at Sfc layer, warmer air intruding aloft	AP	Surface-850 mb	90-95 105-210	
E15	Mar 27-30	1	Mar 27-30	cold and dry, remnant moist patches aloft	AA, P	1000-850 mb	50-70 60-80	

Table A1 continued

Sample	Sampling period	# of air masses	polluted air mass	type of polluted air mass	air mass type	maximum inversion	WD 1000 mb 700 mb	transport pathway type
B53	Dec 12-14	1	Dec 12-14	uniform, but intermediate moist	A P	925-825 mb	260 350	11c
B62	Jan 30-Feb 5	1	Jan 30-Feb 5	dry and cold surface layer, moist air aloft	AP	Surface-925 mb, several small inversions between 900-800 mb	25-335 90-280	
B71	Mar 14-19	2	Mar 14-16	cold and dry surface layer, Pacific air intruding aloft	AP	near surface inversion up to 830 mb	115-60 130-290	
E3	Dec 24-25	1	Dec 24-25	dry and cold	A	Surface-880 mb	- 90	
E6	Jan 21-22	1	Jan 21-22	shallow cold and moist surface layer, moist and warm aloft	A P P	950-850 mb	100-160 150-155	
E8	Feb 8	1	Feb 8	shallow cold and moist surface layer, intermediate warm and moist layer, dry aloft	A PA P	950-800 mb	80 170	
E9	Feb 15-16	1	Feb 15-16	very moist throughout warm and rapid cooling	P A	Surface-990 mb 1000-900 mb	230-300 200-260	
E10	Feb 22-25	1	Feb 22-25	cold and dry, Pacific air intruding during last day	A	Surface-930 mb 900-850 mb	10-170 50-160	
E12	Mar 8-10	1	Mar 8-10	dry and cold, some moisture aloft	AA P	1000-800 mb	50-80 10-110	

Table A1 continued

Sample	Sampling period	# of air masses	polluted air mass	type of polluted air mass	air mass type	maximum inversion	1000 mb 700 mb	transport pathway type
B9	Nov 15-19	2	Nov 19-20	mixture of two air masses	A PA P	shallow surface inversion 925-850 mb	70 165	111a
B13	Dec 3-5	1	Dec 3-5	moist surface layer, dry aloft	A	Surface-950 mb	170 60	
B54	Dec 15-18	1	Dec 15-18	uniform and moist	A	surface inversion increasing up to 850 mb, small lifted inversion drops from 700 mb combining with surface inversion	330-130 355-180	
B122	Nov 3-6	3	Nov 7, air mass change Nov 6/7	fairly moist, remnant of Pacific air aloft	A P P	960-910 mb 970-810 mb	330 295	
B127	Nov 24-27	3	Nov 25-26	uniform moist	A P	Surface-850 mb	85-90 65-90	
B134	Dec 23-26	1	Dec 23-26	cold and dry	A	Surface-750 mb	50-155 80-185	
E1	Dec 5-6	1	Dec 5-6	uniform moist	A P	880-830 mb	285 255-280	
E2	Dec 14-18	1	Dec 14-18	uniform moist, cooling	A P	1000-900 mb	310-30 280-10	

Table A1 continued

Sample	Sampling period	# of air masses	polluted air mass	type of polluted air mass	air mass type	maximum inversion	WD 1000 mb 700 mb	Transport pathway type
B12	Nov 30-Dec 2	2	Dec 1-2	cold and dry	A	1000-850 mb	310 300	111b
B15	Dec 13-16	1	Dec 13-16	moist and warm in patches with varying mixing ratio	AA <sup>p</sup>	several small lifted inversions	60 90	
B60	Jan 16-20	2	Jan 21-22	some moisture in surface layer, dry aloft	A	1000-836 mb 770-736 mb	75 50	
B139	Jan 12-15	}	no data available					
B149	Feb 26-Mar 1							
B150	Mar 6-8							
E5	Jan 10-11	1	Jan 10-11	cold and dry	A	1010-890 mb	320-330 340-350	
E7	Jan 30-31	1	Jan 30-31	dry and cold surface layer, remnant Pacific air aloft	AP	1030-920 mb disappearing	320-350 330-10	

Table A1 continued

Sample	Sampling period	# of air masses	polluted air mass	type of polluted air mass	air mass type	maximum inversion	1000 mb 700 mb	transport pathway type	
B23	Feb 1-8	2	Feb 1-4	cold and dry	A	Surface-825 mb	10-105 340-155	111c	
B25	Feb 16-25	3	Feb 24-25	cold and dry	A	Surface-825 mb	70 65		
B26	Feb 26-Mar 3	3	Feb 26-Mar 1	cold and dry surface more moist at intermediate layer, dry aloft	ACA	1000-875 mb small inversion at 800 mb	55-70 350-75		
B143	Jan 28-31			no data available					
B6	Oct 26-Nov 4	4	Nov 1-3	shallow and moist surface layer, cold and dry aloft	A	1020-1010 mb 1000-920 mb	215 20	111d	
B49	Nov 15-21	3	Nov 15-16	moist and warm aloft mixing with surface air	A P	two inversions between surface and 800 mb	60-70 95		
B52	Dec 8-11	3	Dec 8-9	moist surface layer very moist air aloft	A P	Surface-950 mb 2 small inversions between 900 and 800 mb	215-305 290-330		
B116	Oct 9-12	2	Oct 11-12	moist and uniform	A P	875-850 mb	220 140		

Table A2: Meteorological characteristics of polluted air masses (surface data)

Sample	T (°C)	T <sub>d</sub> (°C)	T-T <sub>mean</sub>	T <sub>d</sub> -T <sub>d mean</sub>	P (mb)	P-P <sub>mean</sub>	Wind direction (degrees)	WS (m/sec)	WS-WS <sub>mean</sub>	SL	SL-SC <sub>mean</sub>	Type
B5B	-16.6	-18.9	+4.5	+5.0	1023.5	+3.7	220-130	4.1	+0.3	7.4	+2.4	1a
H63	-35.8	-39.9	-10.1	-9.9	1012.3	-2.4	70-340	3.9	+1.5	5.3	-1.1	
Dav8	-23.8	-27.7	-4.5	-5.7	1011.3	-9.7	60-70	7.2	+5.1	4.8	+0.2	1b
Dav10	-27.9	-31.1	-8.6	-9.1	1040.1	+19.1	60-90	5.0	+2.9	0	-4.6	
B205	-12.4	-17.2	-4.4	-7.1	993.7	-15.3	110-160	7.4	+4.9	5.3	-2.8	
B4	-10.6	-12.8	-0.4	0	1006.6	-6.4	240-290	5.9	+3.3	8.5	-0.9	11a
E13	-24.9	-29.3	0	0	1009.4	-9.6	250-310	5.6	+2.9	4.5	+1.3	
B18	-22.8	-25.2	+1.8	+2.6	1020.8	-2.2	60-70	6.7	+2.3	9.0	+4.1	11b
B20	-30.4	-34.0	-0.3	-0.7	1022.5	+4.1	340-50	3.7	+0.1	0.8	-2.9	
B68	-24.4	-30.3	-0.5	-3.4	1034.7	+11.7	360-10	5.6	+3.1	2.5	-2.2	
B69	-23.9	-28.5	0	-1.6	1023.2	-0.7	40-50	8.3	+5.5	3.3	-1.4	
B72	-30.1	-33.9	-6.2	-7.0	1028.3	+5.3	260-130	3.4	+0.9	3.0	-1.7	
Dav1	-26.8	-30.0	-9.9	-10.5	1027.6	+7.1	60-110	3.4	-1.2	1.0	-3.8	
B144	-35.4	-38.6	-5.6	-5.3	1038.8	+8.8	200-310	2.5	+1.4	1.0	-2.0	
B151	-28.5	-33.2	-0.9	-1.7	1030.6	+3.6	40-70	5.1	+1.9	0	-2.8	
F4	-28.4	-33.6	-2.5	-4.3	1031.9	+5.9	70-90	5.9	+5.3	4.5	-1.2	
E15	-26.4	-31.3	-1.5	-2.0	1024.1	+5.1	40-60	5.3	+2.6	0.8	-2.4	
B53	-24.4	-26.7	-1.6	-1.2	1007.3	-10.7	220-340	3.0	+2.3	7.0	+0.3	11c
B62	-27.1	-30.2	-6.0	-4.8	1028.6	+8.8	320-70	4.5	+0.1	1.7	-3.3	
B71	-24.6	-28.7	-1.0	-1.5	1020.5	-3.4	320-50	3.1	+0.3	4.0	-0.7	
E3	-29.2	-34.2	+4.2	-5.9	1002.1	-13.9	50	6.3	+5.7	-	-	
E6	-13.3	-16.7	+12.6	+12.6	1000.8	-18.0	80-90	6.3	+5.7	9.5	+3.8	
E8	-22.8	-27.8	+1.4	+0.3	1010.5	-6.5	230	5.1	+3.6	3.0	-1.4	
E9	-13.3	-18.9	+10.9	+8.6	1031.4	+14.4	280-360	4.5	+3.0	5.0	+0.6	
E10	-23.5	-26.7	+0.7	+0.8	1010.3	-6.7	60-140	5.2	+3.7	5.3	+0.9	
E12	-27.2	-31.5	-2.3	-2.2	1017.1	-1.9	20-40	4.1	+1.4	0	-3.2	

Table A2 continued

Sample	T (°C)	T <sub>d</sub> (°C)	T-T <sub>d</sub> mean	T <sub>d</sub> -T <sub>d</sub> mean	P (mb)	P-P mean	Wind direction (degrees)	WS (m/sec)	WS-WS mean	SC	SC-SC mean	Type	
B9	-17.8	-22.2	-0.9	-3.0	1017.1	+5.1	90	3.8	+2.3	2.0	-5.4	111a	
B13	-29.3	-33.3	-2.4	-2.7	1040.1	+16.6	70-100	3.5	+0.5	3.0	-0.9		
B54	-33.5	-36.5	-11.5	-12.1	1020.8	+2.4	90-120	3.4	+2.6	0	-6.7		
B122	-18.3	-21.7	-4.1	-5.0	999.8	-10.2	330	4.4	+2.4	10	+3.1		
B127	-23.1	-27.5	-8.9	-10.8	1032.0	+22.0	70	6.7	+4.7	0	-6.9		
B134	-31.4	-35.4	-5.7	-7.1	1017.4	+6.4	40-190	4.2	+1.2	-	-		
t1	-21.7	-28.3	+3.3	0	1009.3	-6.7	260-280	8.0	+7.4	-	-		
t2	-19.3	-24.8	+5.7	+3.5	1016.3	+0.3	50-300	4.9	+4.3	-	-		
B12	-28.3	-31.7	-1.4	-1.1	1021.1	-2.4	290-300	4.6	+1.6	2.0	-1.9		111b
B15	-22.2	-25.2	+4.7	+5.4	1007.3	-16.3	50	7.0	+1.0	9.0	+5.1		
B60	-23.2	-29.9	-2.1	-2.0	1014.4	-5.4	60	11.1	+6.7	6.0	+1.0		
B139	-18.9	-22.9	-0.6	-2.4	1003.9	-11.1	60-100	3.8	+1.2	3.3	-1.4		
B149	-26.9	-30.3	+2.9	+3.0	1031.3	+1.3	310-70	2.4	+1.5	4.0	+1.0		
B150	-28.3	-	-0.7	-	-	-	50-70	5.4	+2.2	2.0	-0.8		
E5	-29.2	-35.8	-3.3	-6.5	1031.0	+5.0	300	4.8	+4.2	4.5	-1.2		
L7	-26.4	-31.7	-0.5	-2.4	1024.1	-1.9	320	3.8	+3.2	5.1	-0.6		
B23	-36.7	-40.2	-9.8	-10.2	1029.6	+13.9	10-140	1.2	-2.7	2.0	-3.3	111c	
B25	-31.4	-35.0	-4.5	-5.0	1019.1	+3.4	60	5.2	+1.3	1.0	-4.3		
B26	-32.9	-37.1	-4.4	-5.4	1017.8	+0.7	130-350	2.7	-1.1	4.0	-0.5		
B143	-32.1	-35.4	-13.8	-14.9	1036.1	+21.1	300-320	2.1	-0.5	1.8	-2.9		
B6	-25.2	-28.9	-8.8	-10.0	1017.8	+6.4	70-160	2.4	-0.1	4.7	-2.7	111d	
B49	-23.1	-24.2	-2.6	-1.4	1022.8	+2.0	60-90	4.6	+1.9	7.5	-		
B52	-18.6	-21.1	+4.2	+4.4	1029.6	+11.6	240-300	6.3	+5.6	6.3	-		
B116	-7.5	-10.0	+5.9	+5.8	1017.4	+0.4	260-350	6.1	+2.8	9.5	+1.4		

Table A3: Meteorological characteristics of polluted air masses (850 mb data)

Sample	T (°C)	T <sub>d</sub> (°C)	T-T <sub>mean</sub>	T <sub>d</sub> -T <sub>d</sub> mean	Height (gpm)	H-H <sub>mean</sub>	Wind direction (degrees)	WS (m/sec)	WS-WS <sub>mean</sub>	T <sub>5fc</sub> -T <sub>850</sub>	Mean T <sub>5fc</sub> -T <sub>850</sub>	Type
B50	-10.7	-15.0	-1.2	+4.4	1434	+28	150-275	4.5	+1.5	-5.9	-11.9	1a
B63	-31.5	-35.2	-17.3	-14.5	1186	-149	245- 45	3.1	+1.3	-4.3	-11.0	
Dav8 Dav10 B205	no data available											1b
B4	-19.0	-22.2	-4.0	-4.6	1240	-107	70	2.1	+0.4	+8.4	+4.7	11a
E13	-21.1	-21.7	-4.9	-1.0	1296	-71	260-340	9.7	+6.1	-2.4	-8.7	
B18	-15.4	-19.3	+2.0	+4.9	1372	-15	85-95	5.0	-2.5	-7.4	-7.1	11b
B20	-21.6	-28.8	+0.4	-3.0	1388	+68	35-80	4.1	-2.8	-8.8	-8.6	
B68	-14.6	-19.4	+1.2	+3.6	1430	+29	300- 40	12.5	+7.8	-3.8	-8.1	
B69	-24.0	-31.2	-8.2	-8.2	1424	+23	55-75	7.6	+2.9	+0.1	-8.1	
B72	-18.5	-32.2	-2.7	-9.2	1383	-18	235-335	4.7	0	-6.9	-8.1	
Dav1	-20.0	-22.6	-8.8	-1.8	1437	+32	50-85	1.8	-3.3	-6.8	-7.5	
B144 B151	no data available											
E4	-19.7	-30.0	-0.4	-4.8	1480	+83	100-140	8.7	+6.4	-11.3	-6.6	
E15	-18.8	-24.9	-2.6	-2.2	1301	+14	60-80	10.8	+7.2	-6.4	-8.7	
B53	-20.8	-21.1	-3.4	-0.7	1282	-90	330	11.0	+8.9	-3.5	-5.4	11c
B62	-9.9	-22.8	-0.4	-3.4	1495	+88	120-200	3.1	+0.1	-17.2	-11.9	
B71	-16.2	-27.8	-0.4	-4.8	1331	-70	90-330	2.9	-1.8	-8.4	-8.1	
E3	-25.9	-31.2	+1.2	-7.0	1202	-114	80	13.9	+13.8	-5.2	-3.3	
E6	-6.0	-7.9	+13.3	+17.3	1312	-85	150-190	12.3	+10.0	-9.0	-6.6	
E8	-8.8	-8.8	+7.6	+13.6	1179	-176	120	7.2	+6.9	-10.1	-7.8	
E9	-2.4	-9.4	+14.0	+13.0	1508	+153	210-270	10.3	+10.0	-8.8	-7.8	
E10	-15.2	-25.0	+1.2	-2.6	1324	-31	50-250	13.6	+13.3	-9.6	-7.8	
E12	-17.1	-24.4	-0.9	-1.7	1351	-16	30-90	6.0	+2.4	-9.1	-8.7	

Table A3 continued

Sample	$T$ ( $^{\circ}\text{C}$ )	$T_d$ ( $^{\circ}\text{C}$ )	$T - T_{\text{mean}}$	$T_d - T_{d \text{ mean}}$	Height (gpm)	H-H mean	Wind direction (degrees)	WS (m/sec)	WS-WS mean	$T_{\text{Sfc}} - T_{\text{B50}}$	$T_{\text{Sfc}} - T_{\text{B50}}$ Mean	Type	
B9	-11.5	-25.6	+0.9	-7.3	1376	+43	110	10.0	+7.6	+0.6	-4.5	111a	
B13	-19.6	-29.3	+0.4	-1.7	1508	+130	90-170	3.4	-3.6	-9.7	-6.9		
B54	-20.5	-25.0	-3.1	-4.6	1317	-55	40-350	2.2	+0.1	-13.0	-5.4		
B122	-8.7	-9.2	+1.7	+6.6	1147	-199	220	5.0	+0.5	+1.0	-3.8		
B127	-15.0	-27.1	-4.6	-11.3	1491	+145	85-90	14.5	+10.0	+1.0	-3.8		
B134	-24.2	-29.2	-5.5	-6.1	1269	-30	70-190	12.3	+0.3	-6.8	-7.0		
E1	-26.9	-30.3	-5.2	-6.1	1259	-57	270-275	11.4	+11.3	+3.0	-3.3		
E2	-18.5	-21.3	+3.2	+2.9	1365	+49	275-50	10.4	+10.3	-1.5	-3.3		
B12	-23.3	-26.5	-3.2	+1.1	1333	-45	350	7.2	+0.2	-5.2	-6.9		111b
B15	-19.8	-25.0	+0.2	+2.6	1262	-116	85	8.9	+1.9	-2.4	-6.9		
B60	-12.8	-24.7	-3.3	-5.3	1358	-49	85-90	9.0	+6.0	-10.4	-11.9		
B139	no data available												
B149	no data available												
B150	no data available												
E5	-21.2	-26.5	-1.9	-1.3	1515	+118	340-350	10.8	+8.5	-8.3	-6.6		
E7	-17.0	-21.1	+2.3	+4.5	1456	+59	330-360	11.6	+9.3	-8.0	-6.6		
B23	-30.6	-33.3	-13.4	-12.4	1355	+43	20-265	6.5	+0.1	-6.1	-8.9	111c	
B25	-21.8	-35.1	-4.6	-14.2	1330	+18	75-80	7.2	+0.8	-9.6	-8.9		
B26	-23.4	-25.6	-6.2	-2.3	1317	+5	20-305	2.7	-4.0	-9.5	-8.8		
B143	no data available												
B6	-19.4	-23.8	-7.0	-5.5	1321	-12	50-70	2.8	+0.4	-9.5	-4.5	111d	
B49	-19.2	-20.7	-2.9	+1.9	1311	-75	80	6.2	+1.6	-3.9	-4.8		
B52	-18.9	-21.4	-1.5	-1.0	1517	+145	235-325	10.5	+8.4	-0.8	-5.4		
B116	-15.6	-16.2	-1.2	+5.4	1343	-28	345	3.0	-3.4	-0.6	+1.0		

Table A4: Transport pathway types and supporting evidence

Sample	Sampling period	Type	Quality	Vertical extent	700 mb 5 day mean	Trajectory conf.
358	Dec 31, '77-Jan 9, '78	1a	poor	surface only	no	no
363	Feb 6-9, '78		moderate	some support at 500 mb	yes	yes
David	Apr 3-6, '79	1b	good	supported at 500 mb	yes	no
David	Apr 11-14, '79		moderate	supported at 500 mb	no*	no
8275	Nov 23-25, '79		poor	some support at 500 mb	no	yes
84	Oct 8-12, '76	11a	good	supported at 500 mb	yes	yes
813	Mar 14-19, '80		good	supported at 500 mb	no*	yes**
813	Dec 27, '76-Jan 5, '77	11b	moderate	supported at 500 mb	yes	no
323	Mar 15-31, '77		good	supported at 500 mb	yes	yes
355	Mar 1-5, '78		moderate	little support at 500 mb	no	no
359	Mar 6-3, '78		moderate	little support at 500 mb	no	yes
872	Mar 20-22, '78		moderate	little support at 500 mb	no	yes
David	Apr 1-3, '78		poor	little support at 500 mb	yes	no
3144	Feb 1-4, '79		moderate	supported at 350 mb	yes	yes
9151	Mar 12-14, '79		good	supported at 500 mb	(yes)	yes
84	Jan 5-8, '80		good	supported at 500 mb	yes	yes
815	Mar 27-30, '80		poor	supported at 500 mb	no	no**
352	Dec 12-14, '77	11c	good	supported at 500 mb	no*	yes
362	Jan 30-Feb 5, '78		moderate	supported at 500 mb	yes	yes
371	Mar 14-19, '78		poor	no support at 500 mb	yes	no
83	Dec 24-25, '79		good	supported at 500 mb	maybe	yes
56	Jan 21-22, '80		moderate	supported at 500 mb	maybe*	no
58	Feb 3, '80		moderate	supported at 500 mb	yes	no
59	Feb 15-16, '80		good	supported at 500 mb	no	no
810	Feb 22-25, '80		good	supported at 500 mb	yes	yes
812	Mar 8-10, '80		poor	supported at 500 mb	yes	yes**
89	Nov 15-19, '76	111a	moderate	supported at 500 mb	no	no
813	Dec 3-5, '76		good	supported at 500 mb	yes	yes
354	Dec 15-18, '77		good	supported at 500 mb	yes	yes
8122	Nov 3-5, '78		moderate	supported at 500 mb	yes	yes
8127	Nov 24-27, '78		poor	supported at 500 mb	no*	no
8134	Dec 23-25, '78		moderate	no support at 500 mb	no	no
81	Dec 5-6, '79		moderate	supported at 500 mb	no	yes
82	Dec 14-18, '79		good	supported at 500 mb	yes	yes
812	Nov 30-Dec 2, '75	111b	moderate	supported at 500 mb	no	no
815	Dec 13-16, '76		moderate	little support at 300 mb	yes	no
860	Jan 16-20, '78		good	supported at 500 mb	no	yes
8139	Jan 12-15, '79		poor	no support at 500 mb	maybe*	no
2149	Feb 26-Mar 1, '79		poor	no support at 500 mb	yes	yes
3150	Mar 4-8, '79		good	supported at 500 mb	yes	yes
55	Jan 10-11, '80		good	supported at 500 mb	yes	no
57	Jan 30-31, '80		good	supported at 500 mb	yes	no
323	Feb 1-3, '77	111c	good	supported at 500 mb	yes	yes
825	Feb 16-25, '77		moderate	supported at 500 mb	yes	no
325	Feb 26-Mar 3, '77		poor	no support at 500 mb	yes	yes
3143	Jan 28-31, '79		moderate	little support at 500 mb	(yes)	no
36	Oct 25-Nov 4, '76	111d	good	supported at 500 mb	yes	yes
844	Nov 15-21, '77		good	supported at 500 mb	yes	yes
352	Dec 3-11, '77		moderate	supported at 500 mb	yes	yes
8116	Oct 9-12, '78		good	supported at 500 mb	yes	yes

\* because of averaging

\*\* GMCC

Table A5: Transport pathway types and conditions over the source area

Sample	transport pathway type	probable source region	XHn/KV	presence of anticyclonic conditions over source region	occurrence of surge
B58	1a	US east coast	0.3	Dec 11-16, '78	Dec 17-22, '78
B63		US east coast	0.7	Jan 22-25, '78	Jan 26, '78
Dav8	1b	US east coast	0.6	Apr 2, '79	Apr 3, '79
Dav10		US east coast	1.0	Apr 5, '79	Apr 6, '79
B205		US east coast	0.2	several days	Nov 21-26, '79
B4	11a	Western Europe	2.9	since Oct 1, '76	Oct 6, '76
E13		Western and Eastern Europe	0.8	Mar 9-13, '80, moving west	Mar 9-11, '80
B18	11b	Eastern Europe	0.8	since Dec 17, '76, moving east	Dec 24-28, '76
B28		Western Europe	1.0	since Mar 14, '77, moving east	Mar 16-19, '77
B68		Western Europe	0.6	since Feb 19, '78, moving east	Feb 23-27, '78
B69		Central and Eastern Europe	0.7	since Feb 19, '78, moving east	Feb 23-27, '78
B72		Western Europe	0.9	Mar 10-13, '78, indifferent	Mar 13-15, '78
Dav1		Eastern Europe	0.9	Mar 22-23, '78, indifferent	Mar 23-27, '78
B144		Western Europe	0.8	Jan 14-22, '79	Jan 23-24, '79
B151		Central Europe	0.9	Mar 4-7, '79, stationary	Mar 8, '79
E4		Central Europe	0.7	over E-Europe, moving east	Dec 24-31, '79
E15		Northeastern Europe	0.9	weak and stationary	Mar 21, '80

Table A5 continued

Sample	transport pathway type	probable source region	Xln/XV	presence of anticyclonic conditions over source region	occurrence of surge
B53	11c	Great Britain, then Eastern Europe	1.9	from Dec 1, '77 blocking high moving east	Dec 3-13, '77
B62		Western and Eastern Europe	0.8	Jan 15-23, '78, moving east	Jan 19, 22-24, '78
B71		Eastern Europe	0.9	indifferent	Mar 6, '78
E3		Eastern Europe	1.1	Dec 15-16, '79, moving east	Dec 17-18, '79
E6		Central Europe	1.0	Jan 7-18, '80	Jan 13-16, '80
E8		Central Europe	0.9	Jan 26-30, '80, stationary	Jan 31-Feb 1, '80
E9		Central Europe	1.3	Feb 6-8, '80, stationary	Feb 9-10, '80
E10		Central Europe	1.7	Feb 13-16, '80, stationary	Feb 18-22, '80
E12		Central Europe	0.6	Feb 26-27, '80, moving east rapidly	Feb 28-29, '80
B9	111a	Eastern Europe Western USSR	2.0	Nov 2, '76, moving east	Nov 6-8, '76
B13		East of Urals	1.5	no	Nov 21-28, '76
B54		Eastern Europe Northwestern USSR	1.5	from Dec 1, '77 blocking high over Great Britain moves east	Dec 11-15, '77
B122		East of Urals	14.9	indifferent	7 nov '78
B127		East of Urals	5.4	indifferent	Nov 6(7), '78
B134		Volga-Urals	1.1	Dec 13-16, '78, stationary	Dec 18-19, '78
E1		Volga-Urals Western USSR	2.7	stationary for weeks, retreating and weakening towards the end	Nov 26-30, '79
E2		many	1.0	Dec 9, '79, stationary	Dec 11, '79

Table A5 continued

Sample	transport pathway type	probable source region	XHn/XV	presence of anticyclonic conditions over source region	occurrence of surge
B12	IIIb	Volga-Urals	1.6	since Nov 3, '76, moving east	Nov 21-28, '76
B15		West of Urals Volga-Urals	1.9	blocking over Urals present for a long time	Dec 1-7, '76
B60		Western USSR	1.4	since Jan 5, '78, stationary	Jan 12-15, '78
B139		West of Urals	15.9	since Jan 2, '79, stationary	Jan 7-10, '79
B149		Eastern Europe	1.3	stationary for a long time	Feb 21-26, '79
B150		Northeastern Europe	1.3	since Feb 25, '79, moving south from Great Britain, dissipating	Feb 26-28, '79
E5		Eastern Europe Western USSR	1.4	Dec 25-27, '79, moving east	Dec 27, '79-Jan 4, '80
E7		Eastern Europe Western USSR	1.3	Jan 19-24, '80, moving east	Jan 25-Feb 2, '80
B23	IIIc	West of Urals	1.4	stationary	Jan 24-29, '77
B25		Southwestern USSR	1.1	stationary/eastward	Feb 8-14, '77
B26		Eastern Europe Western USSR	1.2	anticyclone from Europe moves east	Feb 16-19, '77
B143		Eastern Europe	1.2	Jan 22-25, '79, moving east	Jan 23-28, '79
B6	IIId	East of Urals	3.4	stationary, Asiatic anticyclone breaks into two cells	Oct 27, '76
B49		Western USSR Volga-Urals	10.1	since Nov 1, '77, moving east	Nov 3-9, '77
B52		Volga-Urals	2.2	stationary	Nov 27-29, '77
B116		Western USSR	21.0	since Oct 1, '78, moving east	Oct 5, '78

Table A6: Transport pathway types and estimated travel times

Sample	Type	Surge	Arrival	Travel time (days) min-max	Estimated travel time (days)
856	Ia	Dec 17-22	Dec 21-Jan 4	9 - 18	14 ± 4
963		Jan 26	Feb 7-9	12 - 14	13 ± 1
Dav8	Ia	Jan 3			
Dav10		Apr 5	no data		
8205		Nov 21-24			
84	IIa	Oct 5	Oct 11-12	5 - 6	5 ± 1
E13		Mar 9-11	Mar 14-19	3 - 10	8 ± 2
318	IIb	Dec 24-28	Dec 31-Jan 2	3 - 9	7 ± 2
328		Mar 16-19	Mar 21-23	2 - 7	5 ± 1
293		Feb 23-27	Mar 5	7 - 11	9 ± 2
869		Feb 23-27	Mar 6-9	8 - 14	11 ± 3
872		Mar 13-15	Mar 20-22	5 - 9	7 ± 2
Dav1		Mar 23-27	Apr 1-3	5 - 8	7 ± 1
8144		Jan 23-24	no data		
3151		Mar 8	Mar 12-14*	3 - 5	
E4		Dec 24-31	Jan 5-6	5 - 13	10 ± 3
E15		Mar 21	Mar 27-30	5 - 9	7 ± 2
853	IIc	Dec 3-13	Dec 12-14	0 - 11	3 ± 3
852		Jan 19,22-24	Jan 30-Feb 1	6 - 13	10 ± 3
871		Mar 6	Mar 14-16	8 - 10	9 ± 1
E3		Dec 17-18	Dec 24-25	6 - 8	7 ± 1
E6		Jan 13-14	Jan 21-22	7 - 9	8 ± 1
E8		Jan 31-Feb 1	Feb 8	7 - 8	7 ± 1
E9		Feb 9-10	Feb 15-16	5 - 7	5 ± 1
E10		Feb 18-22	Feb 22-25	0 - 7	6 ± 1
E12		Feb 28-29	Mar 3-10	8 - 11	10 ± 2
89	IIIa	Nov 5-8	Nov 19-20	11 - 14	12 ± 2
813		Nov 21-28	Dec 3-5	5 - 14	10 ± 4
954		Dec 11-15	Dec 15-18	0 - 7	6 ± 1
8122			Nov 7		
9127		Nov 6 (?)	Nov 25-25	19 - 20	19 ± 1
8134		Dec 18-19	Dec 23-25	5 - 8	7 ± 1
E1		Nov 26-30 (?)	Dec 5-6	5 - 10	8 ± 2
E2		Dec 11	Dec 14-18	3 - 7	6 ± 1
812	IIIb	Nov 21-28	Dec 1-2	3 - 11	9 ± 2
815		Dec 1-7	Dec 13-15	6 - 15	11 ± 4
860		Jan 12-16	Jan 21-22	5 - 10	8 ± 2
8139		Jan 7-10	no data		
8149		Feb 21-24	Mar 1-2*	5 - 9	7 ± 2
8150		Feb 26-28	Mar 5*	6 - 9	7 ± 1
E5		Dec 27-Jan 4	Jan 10-11	6 - 15	11 ± 4
E7		Jan 25-Feb 2	Jan 26-31	0 - 6	5 ± 1
823	IIIc	Jan 24-29	Feb 1-4	3 - 11	9 ± 2
825		Feb 8-14	Feb 24-25	10 - 17	13 ± 4
826		Feb 16-19	Feb 25-Mar 1	7 - 12	10 ± 3
8143		Jan 23-28	Jan 28-31*	0 - 9	7 ± 1
86	IIId	Oct 27	Nov 1-3	5 - 7	5 ± 1
849		Nov 3-9	Nov 15-15	6 - 13	10 ± 3
852		Nov 27-29	Dec 3-9	9 - 12	10 ± 2
2115		Oct 5	Oct 11-12	6 - 7	7 ± 1

\* according to trajectories